

THE UNIVERSITY OF HULL

From Water Soluble Mesogens to Liquid Crystal Gold Nanocomposites –  
Synthesis and Investigation of Flexible Chain Variation in Rod – Shaped  
Mesogens

being a Thesis submitted for the Degree of Ph.D.

in the University of Hull

by

Faleh Alqahtany, MSc

March, 2015

## Acknowledgements

Firstly, I want to thank my supervisor, Prof. G. H. Mehl, for his continuous support in both doing the experiments and writing the report.

Secondly, I want to thank especially my colleagues, Dr. Fabio Lodato, Dr. Chris Schubert and Ionut Ichim.

Thirdly, I would like to thank all my colleagues in both Labs C302 and C305.

Last, but not least, I thank my parents for supporting me whole-heartedly.

## Abstract

A number of new liquid crystalline systems were synthesized and the liquid crystal phase behaviour was investigated. The investigation of the liquid crystal properties involved the characterisation of the neat substances by optical polarizing microscopy (OPM), differential scanning calorimetry (DSC) and for selected samples by x-ray diffraction (XRD) of magnetically aligned sample. The molecular architectures explored are based on a number of rod shaped architectures functionalized with either alkyl groups or ethylenoxy groups, at both ends of the central aromatic core, or at one terminus. The number was increased to three ethylenoxy chains. Additionally, for selected mesogen the results of the LC behaviour on the attachment gold nanoparticles was investigated. For the materials bearing ethylenoxy chains the mesomorphic phase behaviour on mixing with water was investigated by OPM of a number of selected mixtures.

## Abbreviations

Chemical shift in parts per million	$\delta$
4-Dimethylaminopyridine	DMAP
Dichloromethane	DCM
Triethylamine	Et <sub>3</sub> N
Minute	Min
Methyl	Me
Gas chromatography	GC
Nuclear magnetic resonance	NMR
Deuteriochloroform	CDCl <sub>3</sub>
Tetramethylsilane	TMS
Mole	mol
Part per million	ppm
Tetrahydrofuran	THF
Thin layer chromatography	TLC
AuNPs	Gold Nanoparticles
HPLC	High Performance Liquid Chromatography
MALDI	Matrix-assisted laser desorption/ ionization
DPPF	(1,1'-Bis(diphenylphosphino) ferrocene) palladium (II) dichloride
DPPB	1,4-Bis(diphenylphosphino)butane

## List of Figures

Figure 1-1: The schematic representation of ordering; a) typical crystal with 3D positional order structure; b) liquid crystals molecular structure; c) isotropic structure. <sup>8, 9</sup> .....	2
Figure 1-2: Polymeric liquid crystals, main chain and side chain type. <sup>20</sup> .....	4
Figure 1-3: Anionic surfactants. <sup>18</sup> .....	5
Figure 1-4: Cationic surfactants. <sup>18</sup> .....	6
Figure 1-5: Structure of micelles formed by amphiphilic molecules. <sup>21-23</sup> .....	7
Figure 1-6: Nematic phase statistically parallel. <sup>27</sup> .....	8
Figure 1-7: Definition of the angle $\theta$ in nematic phase molecule axis.....	9
Figure 1-8: Schematic representation of molecule fluctuations resulting a local smectic arrangements within a nematic phase; depicted a SmC like clustering. ....	10
Figure 1-9: Schematic representation of smectic A, B and C phase. <sup>44</sup> .....	11
Figure 1-10 : Schematic representation of a cholesteric liquid crystal helicoidal. <sup>47</sup> .....	12
Figure 1-11: Structure of hexagonal lyotropic liquid crystal phases. <sup>49</sup> .....	13
Figure 1-12: Structure of the reversed hexagonal lyotropic liquid crystal phase. <sup>52</sup> .....	14
Figure 1-13 : Structure of the cubic lyotropic liquid crystals. <sup>54</sup> .....	14
Figure 1-14 : Lamellar lyotropic crystals phase. <sup>55</sup> .....	15
Figure 1-15 : Phase diagram for a typical soap in water. <sup>56</sup> .....	16
Figure 1-16: Three examples of aromatic polyamides with lyotropic liquid crystal phase behaviour, C is known as Kevlar (dissolved in high concentrations of sulphuric acid). <sup>18</sup> .....	17
Figure 2-1: The Structures of Chromonic N and M phases. <sup>69</sup> .....	19
Figure 2-2: N, M and P phases viewed down the column axes. <sup>74</sup> .....	19
Figure 2-3: The chromonic M and O phase structures. <sup>77</sup> .....	20
Figure 2-4: The molecular structure of C.I. Direct Blue 67. <sup>95</sup> .....	23
Figure 2-5: a) The preparation of an aligned dye coated polymer film via ‘command plate’ produced by the Weigert effect; b) the epitaxial alignment of a chromonic N phase by a photoaligned command plate. <sup>97, 98</sup> .....	24
Figure 2-6: The packing within the columns. a; simple, molecules stacking on top of each other within a column, with end-to-end and side-to-side disorder. b; an alternating head-to-tail assembly, showing a structure close to a crystallographic two-fold rotation axis. c; showing columns with a helical envelope. d; a half-and-half overlap, looking like a wall. e; A type of (d). <sup>108</sup> .....	25

Figure 3-1: The Lycurgus Cup in reflected and transmitted light. <sup>155</sup> .....	29
Figure 5-1: X-ray diffraction shows beams from continuous cones and a crystal powdered sample. <sup>161</sup> .....	35
Figure 5-2: Schematic representation of the operation of a DSC and a sample thermogram. <sup>162 163</sup> .....	37
Figure 5-3: A schematic representation of a TEM. <sup>164</sup> .....	38
Figure 5-4: A schematic representation of the different transitions between the bonding and anti-bonding electronic states when light energy is absorbed in UV-Visible Spectroscopy. <sup>165</sup> .....	41
Figure 5-5: A schematic illustration of a transmitted light polarizing microscope. <sup>166</sup> ..	43
Figure 5-6: Description of OPM operation principles. <sup>167</sup> .....	44
Figure 6-1: Scheme for the synthesis of compounds 6-4 and 6-5.....	47
Figure 6-2: Scheme showing the chemical shifts in an <sup>1</sup> H NMR spectrum.....	49
Figure 6-3: Different textures of compound 6-4 (A, B heating) (C, D cooling) with magnification of 100x (OPM).....	50
Figure 6-4 : a) X-ray diffractograms at 155 °C for compound 6-4, in the nematic phase, b) NcybC phase aligned in a magnetic field. ....	50
Figure 6-5 : Red line: $\chi$ scan at $2\theta$ values 2-4°; black line 15-25° $2\theta$ without division of the scattering in the isotropic phase. ....	51
Figure 6-6 : Textures of compound 6-5 (water contact) with magnification of 100x (OPM). ....	52
Figure 6-7: Scheme shows the absence of hydroquinone in the chemical shifts in an <sup>1</sup> H NMR spectrum. ....	52
Figure 6-8 : DSC trace for compound 6-5. ....	53
Figure 6-9: Red line: $\chi$ scan at $2\theta$ values 2-5°; black line 15-25° $2\theta$ without division of the scattering in the isotropic phase. ....	54
Figure 6-10: X-ray diffractograms at 60 °C for compound 5, in the nematic phase. ....	54
Figure 6-11: Textures of compounds 6-15 (a) and 6-16 (b, c) with magnification of 100x (OPM). ....	55
Figure 6-12 : DSC trace of compound 6-17.....	56
Figure 6-13: These spectrum of compound 6-15; the main peak 479.2168 represents the [M+ H <sub>2</sub> O]. ....	57
Figure 6-14: These spectrum of compound 6-16 the main peak 465.2378 which represent the [M+ H <sub>2</sub> O]. ....	57
Figure 6-15: The main peak 665.66 which represent the [M+ Na] <sup>+</sup> .....	61

Figure 6-16: The spectrum for the crude product of compound 6-5.....	61
Figure 6-17: The <sup>1</sup> H NMR spectrum for hydroquinone.....	62
Figure 6-18: The <sup>1</sup> H NMR spectrum for the monoreacted product of compound 6-5....	62
Figure 7-1: Scheme for the synthesis of compound 7-12. ....	83
Figure 7-2: DSC heating and cooling trace for material 7-12.....	88
Figure 7-3: The spectrum of compound 7-12; the main peak 1066.57 represents the [M+ H <sub>2</sub> O] .....	89
Figure 7-4: The spectrum of compound 7-12; the main peak 4.24 showing 100% purity. .....	89
Figure 7-5: Micrographs of the crystalline phase of compound 7-12.....	90
Figure 7-6: Micrographs of compound 7-12 with water, contact sample.....	90
Figure 7-7: Schematic of compound 7-12 and water preparation used for detection and study of lyotropic behaviour. ....	91
Figure 7-8: Microphotographs of the contact sample at different temperature, (a),(b),(c),(d),(e) and (f) were mixtures of 5 wt % compound 7-12 and 95 wt % water.	92
Figure 7-9: Optical images of 16 wt % compound 7-12 and 84 wt % water with magnification of 400x (POM).....	93
Figure 7-10: Optical image of 20 wt % compound 7-12 and 80 wt % water on cooling. .....	94
Figure 7-11: Sketched provisional phase diagram of compound 7-12 and water.....	94
Figure 8-1: Scheme of the strategy used to synthesise compounds 8-9, 8-12 and 8-13. .....	106
Figure 8-2: <sup>1</sup> H NMR spectra of methyl 4-((11-(methylsulfinyl)undecyl)oxy) (spectrum A) and methyl 4-((11-mercaptoundecyl)oxy) benzoate (spectrum B).....	109
Figure 8-3 : Preparation scheme for < 2 nm coated AuNPs. <sup>171, 172</sup> .....	112
Figure 8-4: Scheme of facile synthesis of gold monodisperse (3 - 6 nm coated AuNPs). <sup>171, 172</sup> .....	113
Figure 8-5: Scheme of the procedure used to synthesise compounds 8-14, 8-15, 8-15 and 8-17.....	115
Figure 8-6: <sup>1</sup> H NMR spectra of compound 8-14 (spectrum A) and compound 8-15 (spectrum B).....	117
Figure 8-7: <sup>1</sup> H NMR spectra of compound 8-16 (spectrum A) and compound 8-17 (spectrum B).....	117
Figure 8-8: Schematic representation of AuNPs coated with target mesogen.....	118
Figure 8-9: DSC curves of compound 8-9. Heating / cooling rate is 10°C /min. ....	119

Figure 8-10: Textures obtained by OPM for compound 8-9. a) SmA at 157 °C, b) and c) nematic at 177 °C and 178 °C.....	119
Figure 8-11: <sup>1</sup> H NMR spectra comparison of the free ligand (compound 8-11) (spectrum A) and mesogen covered gold NPs (compound 8-12) (spectrum B). ....	120
Figure 8-12: UV spectra of compound 8-12. ....	121
Figure 8-13: TGA spectrum of compound 8-12. ....	122
Figure 8-14: TEM images of material 8-12. ....	123
Figure 8-15: OPM of compound 8-12 with analyser offset by 10 degrees and maximum gain settings of the camera; images a, b and c were taken with magnification of (x100); image d was taken with magnification of (x500).....	124
Figure 8-16: DSC curves for compound 8-13.....	125
Figure 8-17 : DSC curves for compound 8-13.....	126

## Contents

1	Introduction.....	1
1.1	History of liquid crystals .....	1
1.2	The definition of liquid crystals .....	1
1.3	Classifications of liquid crystals.....	2
1.3.1	Thermotropic liquid crystals .....	2
1.3.2	Lyotropic liquid crystals .....	5
2	Chromonics.....	18
2.1	Chromonic phases .....	19
2.2	Chromonic phase structure and properties .....	22
2.3	New chromonic materials.....	23
2.4	The preparation of patterned dye films .....	24
2.5	Molecular stacking patterns in chromonic systems.....	25
3	Nanoparticles .....	26
3.1	Gold nanoparticles.....	28
3.2	Preparation methods for AuNPs.....	29
4	Aims.....	31
5	Materials .....	32
5.1	Instrumentation.....	32
5.1.1	Vacuum pump .....	32
5.1.2	<sup>1</sup> H Nuclear Magnetic Resonance (NMR) Spectrometry .....	32
5.1.3	Gas chromatography- mass spectrometry (GC –MS).....	32
5.2	General Process .....	33
5.2.1	Thin Layer Chromatography (TLC) .....	33
5.2.2	Column Chromatography.....	33
5.2.3	Elemental Analysis.....	33
5.2.4	X-Ray Diffraction (XRD). .....	34
5.2.5	Differential Scanning Calorimetry (DSC). .....	36
5.2.6	Transmission electron microscopy (TEM) .....	38
5.2.7	UV-Vis spectroscopy .....	40
5.2.8	Optical Polarising Microscopy (OPM) .....	43
5.2.9	Thermal Gravimetric Analysis (TGA).....	45
6	Chromonic .....	46
6.1	Results and discussion.....	47

6.1.1	Challenge in the synthesis of rod shaped LC difunctionalized ethyleneoxy chains	58
6.1.2	Problems in the synthesis of target 3	63
6.2	Summary	65
6.3	Experimental procedures	66
6.3.1	Synthesis of 1-bromo-2-(2-(2-methoxyethoxy)ethoxy)ethane	66
6.3.2	Synthesis of methyl 4-(2-(2-(2-methoxyethoxy) ethoxy) ethoxy) benzoate	67
6.3.3	Synthesis of 4-(2-(2-(2-methoxyethoxy)ethoxy)ethoxy)benzoic acid	68
6.3.4	Synthesis of [1,1'-biphenyl]-4,4'-diyl bis(4-(2-(2-(2-methoxyethoxy) ethoxy) ethoxy) benzoate).	69
6.3.5	Synthesis of 1,4-phenylene bis(4-(2-(2-(2-methoxyethoxy) ethoxy) ethoxy) benzoate).	70
6.3.6	Synthesis of 1-bromo-4-methoxybenzene.	71
6.3.7	Synthesis of (4-methoxyphenyl) boronic acid.	72
6.3.8	Synthesis of 1, 4-phenylene dibenzoate	73
6.3.9	Synthesis of 4-(2-(2-(2-methoxyethoxy) ethoxy) ethoxy) benzoyl chloride	74
6.3.10	Synthesis of 4-hydroxyphenyl 4-(2-(2-(2-methoxyethoxy) ethoxy) ethoxy) benzoate.	75
6.3.11	Synthesis of 4-(2-(2-(2-methoxyethoxy) ethoxy) ethoxy) benzaldehyde.	76
6.3.12	Synthesis of (4-(2-(2-(2-methoxyethoxy) ethoxy) ethoxy) phenyl) methanol.	77
6.3.13	Synthesis of 1-(chloromethyl)-4-(2-(2-(2-methoxyethoxy) ethoxy) ethoxy) benzene.	78
6.3.14	Synthesis of 4'-cyano-[1,1'-biphenyl]-4-yl 4-(2-(2-(2-methoxyethoxy) ethoxy) ethoxy) benzoate	79
6.3.15	Synthesis of 4'-((4-(2-(2-(2-methoxyethoxy) ethoxy) ethoxy) benzyl) oxy)-[1,1'-biphenyl]-4-carbonitrile.	80
6.3.16	Synthesis of 1,4-bis((4- (2- (2- (2-methoxyethoxy) ethoxy) ethoxy) benzyl) oxy) benzene.	81
7	Hemiphasmidics	82
7.1	Synthesis discussion	83
7.2	Discussion of properties	87
7.2.1	Liquid crystal and thermal properties	88
7.2.2	MALDI and HPLC	89

7.3	Summary .....	96
7.4	Experimental procedures .....	97
7.4.1	Synthesis of methyl 3,4,5 tris(2(2(2methoxyethoxy) ethoxy)ethoxy) benzoate	97
7.4.2	Synthesis of 3,4,5-tris(2-(2-(2-methoxyethoxy) ethoxy) ethoxy) benzoic acid	98
7.4.3	Synthesis of 3,4,5-tris(2-(2-(2-methoxyethoxy)ethoxy) ethoxy) benzoyl chloride	99
7.4.4	Synthesis of methyl 4-(undec-10-en-1-yloxy) benzoate .....	100
7.4.5	Synthesis of 4-(undec-10-en-1-yloxy) benzoic acid .....	101
7.4.6	Synthesis of 4'-hydroxy-[1,1'-biphenyl]-4-yl 4-(undec-10-en-1-yloxy)benzoate.....	102
7.4.7	Synthesis of 4'-((4-(undec-10-en-1-yloxy)benzoyl)oxy)-[1,1'-biphenyl]-4-yl 3,4,5-tris(2-(2-(2-methoxyethoxy)ethoxy) ethoxy) benzoate .....	103
8	Liquid crystals attached to pentamethyldisiloxane and AuNPs with alkyl various chain length .....	105
8.1	Synthesis Discussion .....	106
8.2	Discussion of Properties .....	118
8.2.1	Liquid crystal and thermal properties of compound 8-9.....	119
8.2.2	Liquid crystal attached to AuNPs and thermal properties of compound 8-12.....	120
8.2.3	Liquid crystal and thermal properties of compound 8-13, 8-14, 8-15, 8-16 and 8-17.....	126
9	Summary.....	127
9.1	Experimental procedures .....	128
9.1.1	Synthesis of 4'-(benzyloxy)-[1,1'-biphenyl]-4-ol.....	128
9.1.2	Synthesis of 4'-(benzyloxy)-[1,1'-biphenyl]-4-yl 4-(undec-10-en-1-yloxy)benzoate.....	129
9.1.3	Synthesis of 4'-(benzyloxy)-[1,1'-biphenyl]-4-yl 4-((11 (methylsulfinyl) undecyl)oxy)benzoate .....	130
9.1.4	Synthesis of 4'-(benzyloxy)-[1,1'-biphenyl]-4-yl 4-((11-mercaptoundecyl)oxy) benzoate .....	131
9.1.5	Synthesis of ((11-(4-(((4'-(benzyloxy)-[1,1'-biphenyl]-4-yl)oxy)carbonyl)phenoxy) undecyl)thio)gold.....	132
9.1.6	Synthesis of 4'-(benzyloxy)-[1,1'-biphenyl]-4-yl 4-((11-(1,1,3,3,3-pentamethyldisiloxanyl) undecyl)oxy)benzoate .....	133
10	Overall summary.....	134
11	Outlook .....	136

12 References..... 137

# 1 Introduction

## 1.1 History of liquid crystals

In 1888, Austrian botanist Friedrich Reinitzer discovered that a material based on benzoyl cholesterol had two melting points. At 145°C the crystalline solid melted to an opaque (milky) liquid, upon further heating (170 °C) the sample became transparent.<sup>1,2</sup> Reinitzer wrote to the German crystallographer (physicist) Otto Lehmann, who was then working in Karlsruhe. Lehmann discovered that the opaque liquid possessed a unique kind of order, between that of a solid and liquid. Lehman coined the term liquid crystals, triggering significant interest within the scientific community.<sup>3,4</sup>

The German chemical industry began to explore the properties of liquid crystals. The company "Merck" which is based in Darmstadt became a leader in the field, as it developed what it called the liquid-crystal and fluid market since 1904. Eight years after O. Lehmann published his first work on liquid crystals "Merck" started to commercialize these materials and has since then been in the forefront of applications of liquid crystals research.<sup>5,6</sup>

## 1.2 The definition of liquid crystals

The difference between a liquid and a crystal is that in a liquid the molecules lack molecular order, while crystals are highly ordered. In a crystalline material the molecules have both positional and orientational order. Moreover, they are constrained both to fill specific sites in a lattice and orientate their molecular axes in a specific direction.<sup>7</sup>

The molecules in liquid crystals (Figure 1-1 b) are more ordered than in an isotropic liquid, where they are normally oriented randomly (Figure 1-1 c), but less ordered than typical crystals (Figure 1-1 a).

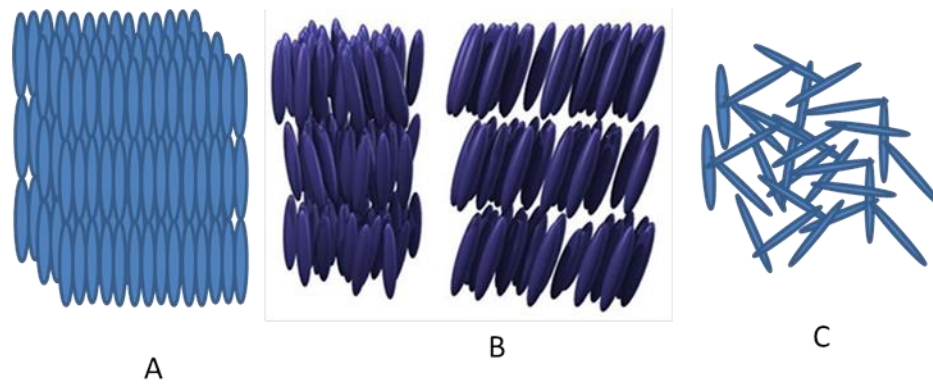


Figure 1-1: The schematic representation of ordering; a) typical crystal with 3D positional order structure; b) liquid crystals molecular structure; c) isotropic structure.<sup>8, 9</sup>

Order here means that the molecules in a crystalline phase have long-range positional and orientational order. 1D or 2D positional ordered liquid crystals are shown in figure 1-1 a, b<sup>10,11</sup> and 0D in isotropic liquid (Figure 1-1).

The term ‘mesophase’ originates from the Greek word, *meso* meaning between, as the molecular ordering in the intermediate phase lies between that of a perfect solid and an isotropic liquid.

Most liquid crystals are organic substances which can be encouraged to show liquid crystal phase behaviour by two different approaches, either by changing the temperature or the concentration of a solvent. Those obtained by changing the temperature are known as thermotropic liquid crystals, and those resulting from a concentration change in solvent are called lyotropic liquid crystals.<sup>12</sup>

### 1.3 Classifications of liquid crystals

Liquid crystals are divided into two main classes; thermotropic and lyotropic liquid crystals. Both of them are very important for very different industrial uses such as electro-optic displays, industrial or detergent soap manufacture.

#### 1.3.1 Thermotropic liquid crystals

The term ‘thermotropic’ liquid crystals is used because the transition involving the mesophases is most impacted by a change in temperature. It can be considered as the most common type of liquid crystals.<sup>13,14</sup> Additionally, thermotropic liquid crystals

can be classified into two sub-classes; high molar mass compounds such as polymers and dendrimers and low molar mass molecules. The field of low molar mass thermotropic crystals is distinguished between calamitic and discotic molecules.

- i. The term calamitic is used if the shape of the mesogens has a rod-like structure.

A common feature in calamitic liquid crystals is that they have a rigid core unit ensuring the anisotropic character, together with flexible terminal chains and it is very common that they include very polar groups, such as alkoxy or ester groups.

- ii. Discotic molecules: the mesogens have a disc-like shaped structure.

Usually, a discotic system consists of a rigid, flat core unit and flexible side groups which are around this disc-like core. The core unit is mostly aromatic; an example is the triphenylene group.

The physical properties and the transition temperature of the calamitic and discotic systems can be influenced by the length and molecular side chains or the nature and size of the central core.

Moreover, the field of high molar mass liquid crystals has been divided into several categories, such as dendritic liquid crystals and polymer liquid crystals. Dendritic molecules are usually symmetrical and the core functional group tends to adopt a spherical, three-dimensional shape. The liquid crystal groups tend to surround this central group. Polymer liquid crystals consist of repeating monomer units which form a chain.<sup>7</sup> Mesogenic (liquid crystalline) units are separated by flexible spacers and the most common are alkyl chains.<sup>15,16</sup>

The use of polymer materials is very common. Many of them occur naturally, such as proteins (wool) and cellulose (cotton). The majority of polymer materials are synthesised each year for a very wide variety of applications for daily use including plastic bags, clothing and building.<sup>7,17</sup>

The LC polymers are classified in accordance with the molecular architectural attachment of the mesogenic monomers. Main-chain polymers are constructed through joining the rigid mesogenic units together by linking units (figure 1-2 b).

Side-chain polymers are formed by a polymer backbone and the mesogenic are parallel. The nature of the polymer backbone is generally variable (Figure 1-2 a).<sup>18,19</sup>

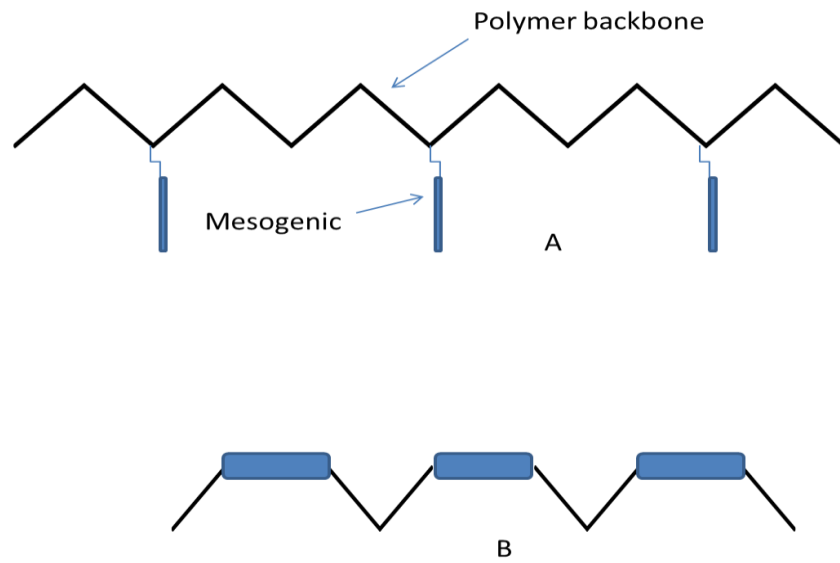


**Figure 1-2:** Polymeric liquid crystals, main chain and side chain type.<sup>20</sup>

### 1.3.2 Lyotropic liquid crystals

The most commonly encountered type of liquid crystals is related to a different class of material called lyotropic liquid crystals. They were discovered before thermotropic LCs but their significance was overlooked. Lyotropic liquid crystal phases are generated by the solution of amphiphilic molecules in a solvent which is normally water. There are many different types of lyotropic liquid crystal phase structures, each of which has a varied range of molecular ordering in the solvent. The type of lyotropic phases is dependent on the concentration of the material in the solvent. It has also proven possible to change the type of lyotropic phase exhibited at each concentration by altering the temperature.

Lyotropic liquid crystal phases are often found in everyday life. Examples are surfactants in water, such as detergents and soaps. In addition, foam that forms in a soap dish is a liquid crystal phase that has been generated by dissolution of soap in water. Another example is cake batter which often contains materials forming lyotropic liquid crystals phases. The molecular structures that form lyotropic liquid crystals phases are amphiphilic in nature. This refers to molecules that have both polar (head group) and non-polar (tail group) regions in the same molecule. Soaps such as sodium stearate have a polar head group made up of a carboxylate group and a non-polar group, such as an alkyl chain. These are known as anionic surfactants because the polar head groups are anionic in nature (Figure 1-3).

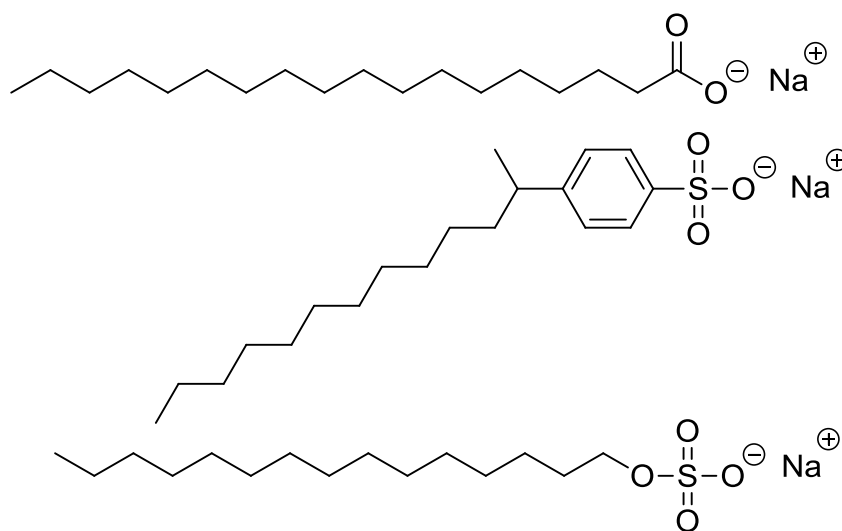


**Figure 1-3: Anionic surfactants.**<sup>18</sup>

Surfactants possessing positively charged head groups are known as cationic surfactants. Examples include ammonium chloride surfactant molecules. Ammonium chloride as a common cation constitutes the polar head group and the alkyl chain is the hydrophobic unit (Figure 1-4 in 1). Molecules 2 and 3 in figure 1-4 are examples of more elaborate cationic surfactants.

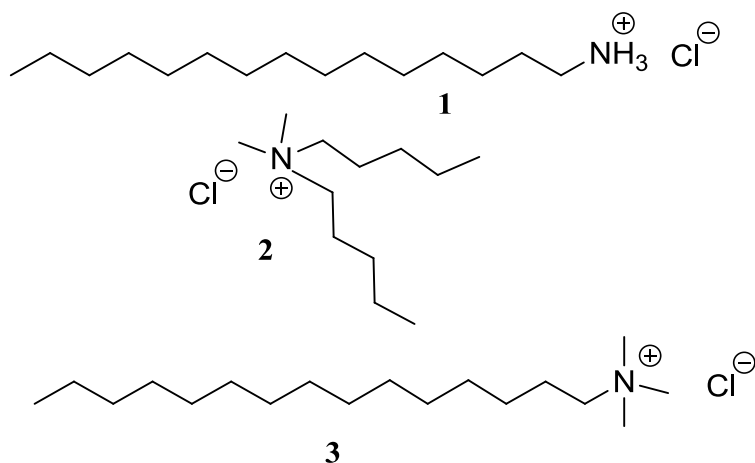


**Figure 1-4: Cationic surfactants.**<sup>18</sup>

Amphiphilic molecules are usually symbolized as circles (polar head) with an attached chain (non-polar) as shown in Fig 1-5, and usually have more than one non-polar unit. These amphiphilic materials are either dissolved to form a micellar solution or are insoluble. Micelles are aggregates of molecules that form for instance when the non-polar chains aggregate with each other and are removed from water solvent by the surrounding polar head groups. Micelles are stable in water as long as the concentration of surfactants is above the critical micelle concentration.

Individual micelles can in certain concentration ranges aggregate into lyotropic phases. Surfactants dissolved in water are characterized by a parameter known as the Krafft point, which is defined as the temperature ( $T_k$ ) above which micelles are soluble, generating lyotropic liquid crystal phases. Below this temperature micelles are insoluble and no LC phase is observed.

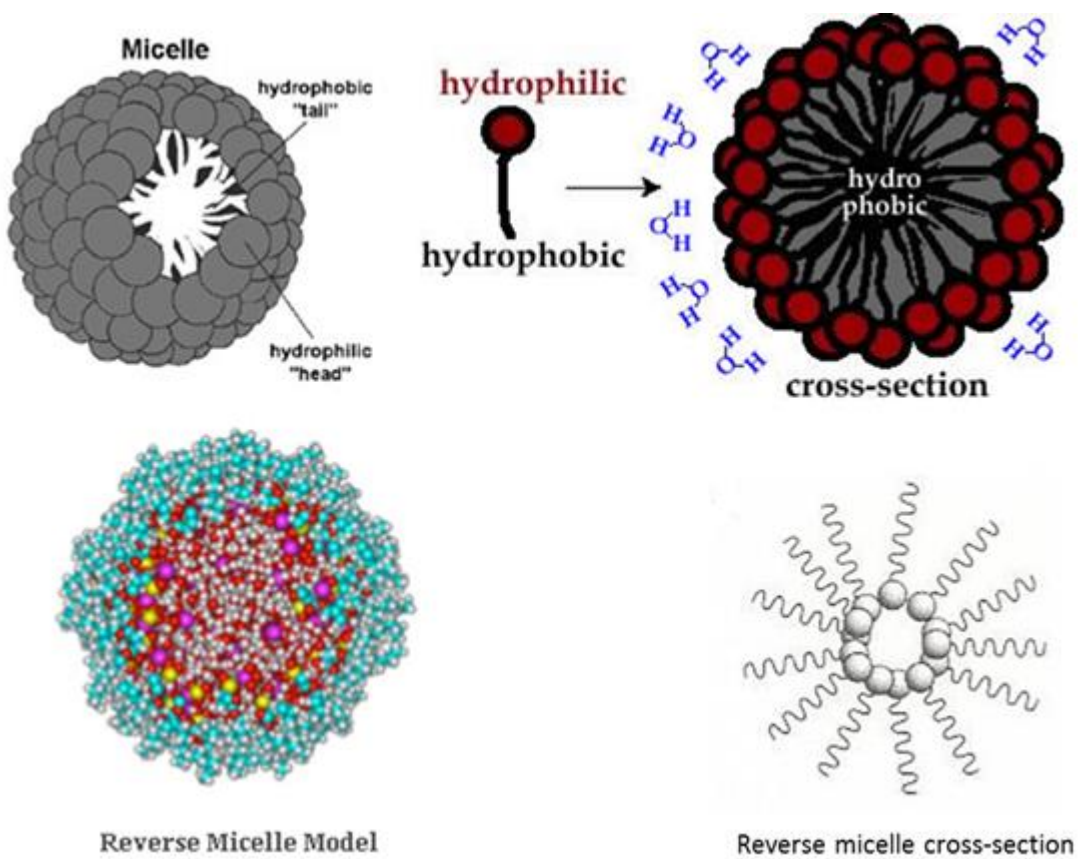


Figure 1-5: Structure of micelles formed by amphiphilic molecules.<sup>21-23</sup>

### 1.3.2.1 Mesophases

There are three main type of mesophases which can be distinguished, as follows:

i. Nematic phase

The nematic phase has the simplest structure of all liquid crystal mesophases, and is more fluid than the smectic phases. The nematic phase is one of the most investigated and best understood of all LC phases, as it is technologically the most important of all the thermotropic liquid crystal phases; the vast majority of all LC devices use molecules in the nematic phase as the core of their technology. In the nematic phase molecules do not have any positional order and are characterized by one dimensional orientational order (figure 1-6). There is only one uniaxial nematic phase and on heating this phase turns to an isotropic liquid. A LC material that displays only a nematic phase is called a Nematogen (individual molecules).<sup>24</sup> The long molecular axes orientate in a preferred direction called the director ( $\mathbf{n}$ ). The nematic phase is characterised generally by a well-defined degree of order, typically termed the order parameter,  $S$ . This order parameter describes the fluctuation of the molecular long axis of a given molecule from the preferential orientation direction of the molecule from the overall direction of the molecular long axes of the nematic mesogens and  $h$  is termed the nematic *director* ( $\mathbf{n}$ ).<sup>25</sup>  $S$  is described by Formula 1,

Formula 1: 
$$\langle S = \frac{1}{2}(3\cos\theta^2 - 1) \rangle$$

Where  $\theta$ , is the angle between the long axis of the molecules and the director  $\mathbf{n}$  (figure 1-7).<sup>7, 26</sup>

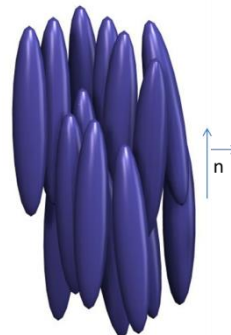


**Figure 1-6:** Nematic phase statistically parallel.<sup>27</sup>

When molecules are parallel to the director  $\mathbf{n}$  as would be the case for an idealized crystal, the order parameter is  $S = 1$  which represents the highest possible degree of order, whereas for a completely disordered state,  $S = 0$ , there is no long range ordering present; hence the material is an isotropic liquid. This concept is valid too for disc shaped molecules which form a nematic phase. However as these systems are far from the subject matter of this thesis, this will not be discussed further.

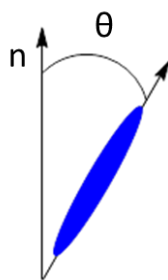


**Figure 1-7:** Definition of the angle  $\theta$  in nematic phase molecule axis.

The existence of biaxial nematic phase systems is also actively reported both in theory and by experiments and is still controversially discussed. Although known for lyotropic systems, nematic biaxial phase behaviour has been reported for only a few organic thermotropic compounds. The most often used description for a biaxial nematic is that of rotationally symmetric, board shaped molecules with two axes of rotation; or in other words nematic ordering can occur in two directions at the same time with an along a molecular long axis, the main nematic director and ordering along a short molecular axis, which is often called the biaxial nematic director short. The first biaxial nematic to be observed experimentally was lyotropic.<sup>28</sup> Biaxial nematic phase behaviour has been realized for side-chain liquid crystal polymers.<sup>29-32</sup> Systems based on organosiloxane tetrapodes<sup>33</sup> were found to exhibit a stable biaxial nematic phase; it has been discussed for bent core molecules, mainly for those based on an oxadiazole core, although other structures have been proposed, such as mixtures of rod and disc shaped molecules.<sup>34</sup>

In recent years the observation that smectic like fluctuations can occur in nematics has been discussed very actively. These fluctuations are typically called smectic cybotactic clusters. These clusters may exist close to the transitions between smectic and N phases (figure 1-8) or sometimes over the full width of the nematic phase.<sup>35</sup> Cybotactic clusters have been observed in polymeric systems<sup>36</sup>, bent core liquid crystals<sup>37</sup> and disc-shaped dimers.<sup>38</sup>

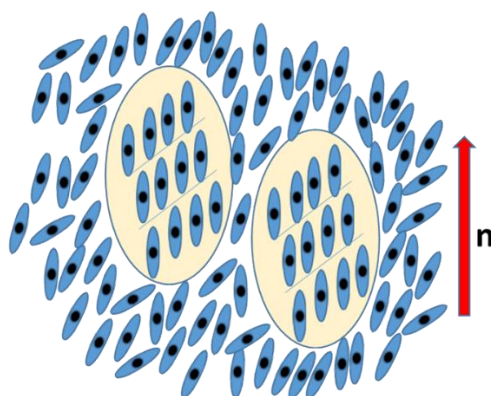


**Figure 1-8:** Schematic representation of molecule fluctuations resulting in local smectic arrangements within a nematic phase; depicted as SmC-like clustering.

The smectic clusters can be understood as smectic-like nano-metric assemblies which fluctuate, which means that they assemble and disassemble continuously over time, making them thus different from smectic phases.

The quite recent discovery of a new nematic phase or potentially even a set of nematic phases attracted considerable interest. The first report of an additional nematic phase, in temperature below the conventional nematic phase and termed  $N_x$ , was by Ungar et al in 1992 who reported for polymeric systems sharp transitions on DSC in the nematic region but the absence of any evidence for smectic phase behaviour.<sup>39</sup> Schroeder et al. observed in 2003 for hockey stick shaped systems a nematic-nematic transition at temperatures above the formation of a columnar phase.<sup>40</sup> Sepelj, et al. reported in 2006 on a symmetric dimeric system containing imine groups an additional nematic phase.<sup>41</sup> More recently Panov et al discussed in 2010 and in a number of follow-on reports in more detail the observation of a second nematic phase in very simple dimeric cyanobiphenyl based compounds, where the mesogenic groups are separated by an odd spacer hydrocarbon group.<sup>42, 43</sup> Since the observation of nematic-nematic transitions in such simple systems interest in this field has increased rapidly and a number of models for this phase have been discussed, based on a wide array of experimental methods and reports. As this field is outside the scope of this thesis, the phase structure of this second nematic will not be discussed further.

## ii. The Smectic /Crystal phases

The smectic phases are layered structures which possess a well-defined interlayer distance. Smectics are more ordered than nematics. In many materials the smectic

phases will occur at a lower temperature and often at higher temperature a nematic phase will occur. The smectic mesophases have a lamellar structure. There are many types of smectic phases such as SmA, SmB, SmC and up to SmK; only the three most common smectic phases SmA, SmB and SmC will be discussed. The smectic phases SmA, SmB and SmC are characterized by short range positional correlations between layers. In other words the behaviour of molecules in one layer is almost independent of the molecules in the next layers. The difference between the smectic phases is due to variety of molecular arrangements within the layers as shown schematically in Fig 1-9.

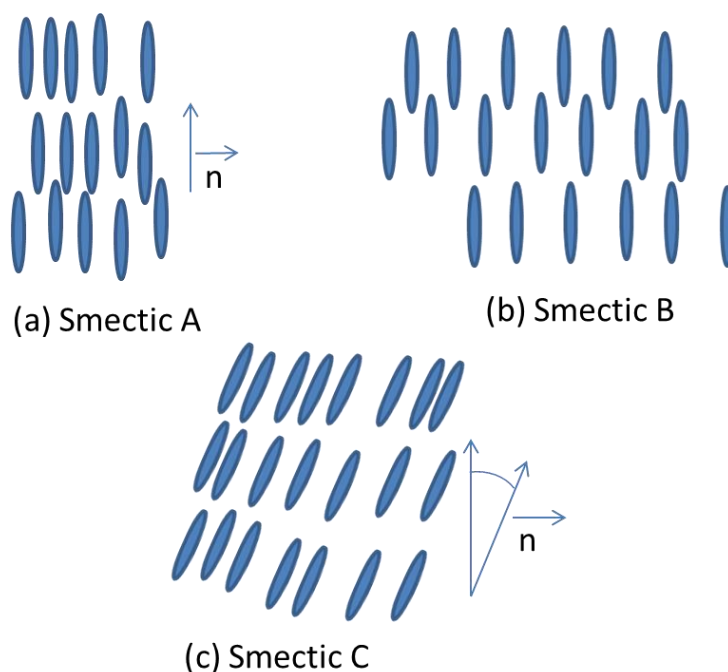


Figure 1-9: Schematic representation of smectic A, B and C phase.<sup>44</sup>

In the SmA phase there is no positional correlation from layer to the next and no ordering of the molecules within the layer. The layer structure can be weak. The molecules are on average positional orthogonal to the layer normal. The SmB phase is more ordered than the SmA phase, and it shows a regular hexagonal ordering of the molecules within the layer but still no positional correlation from one layer to the next exists. In SmC phase the molecules within the layer are tilted with respect to the layer. There is no correlation from one layer to the next.

iii. Chiral nematic ( Cholesteric) phase

This is termed *Cholesteric phase* as the first compound that has given this type of phase were derivatives of cholesterol. The most important feature of the molecules that give the chiral nematic / cholesteric phase is that they are optically active. The chiral nematic phase is similar to the nematic phase except the molecular orientation shows as a helicoidal superstructure Fig 1-10. The molecules rotate along the axis of the helicoidal and  $P$  is the pitch length which is the distance along the optic axes to observe  $360^\circ$ .<sup>45,46</sup>

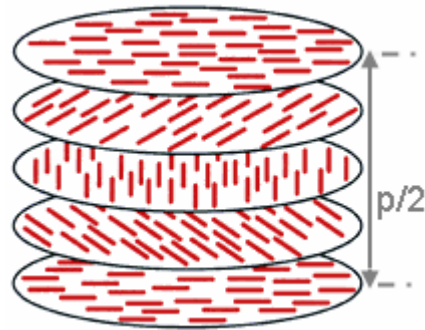


Figure 1-10 : Schematic representation of a cholesteric liquid crystal helicoidal.<sup>47</sup>

### 1.3.2.2 The structures of lyotropic liquid crystals phase

There are several different types of lyotropic liquid crystal phases, exhibited by surfactant systems which have been studied at range concentrations. Three different classes of lyotropic liquid crystal phases are commonly found. These are the hexagonal, cubic and lamellar phases, all of which have been characterised by x-ray diffraction techniques and many other methods.<sup>48</sup>

i. The hexagonal lyotropic liquid crystals phases

The hexagonal lyotropic liquid crystals phases have a molecular ordering which results in a hexagonal cylindrical arrangement, shown schematically in Fig 1-11.

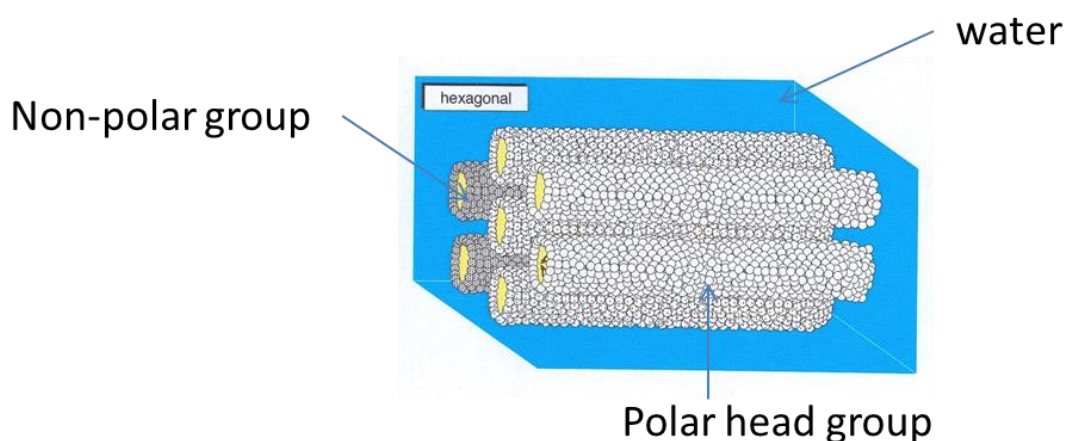


Figure 1-11: Structure of hexagonal lyotropic liquid crystal phases.<sup>49</sup>

The hexagonal lyotropic liquid crystals have water around the cylindrical pack as shown in Fig 1-11. The cylinders are made up of a hydrocarbon group pointing towards the centre and the polar group to the outside. The hexagonal phases are further classified into the normal hexagonal phase  $H_I$  (figure 1-11) and reverse hexagonal phase  $H_2$  (figure 1-12).<sup>50</sup>

The reversed hexagonal phase is conceptually similar to the hexagonal phase except that the structure is reversed inside out (the non-polar chain appears to the outside of the cylinders and the polar head group is in the centre).<sup>51</sup>

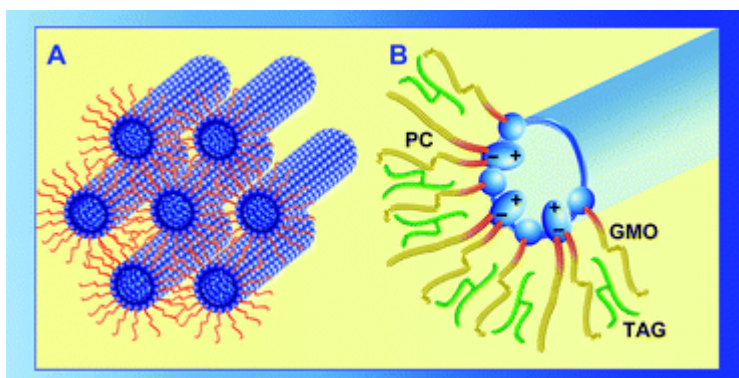


Figure 1-12: Structure of the reversed hexagonal lyotropic liquid crystal phase.<sup>52</sup>

ii. The cubic lyotropic liquid crystal phases

Cubic lyotropic liquid crystal phases are not as commonly found as hexagonal columnar systems and are characterised with similar methods as the lamellar or hexagonal phase. It has been suggested that the cubic phase is an intermediate phase in transition between hexagonal H<sub>2</sub> and the lamellar phase, which is stabilized at a critical temperature.<sup>53,7</sup>

The phase diagram shows that the exact structure relates to cubic phase position, and there are at least two types of cubic phases. Each can be generated in the ‘normal’ and ‘reversed’ form, which makes four different phase types in total. The cubic lyotropic liquid crystal phases are very viscous and more viscous than the hexagonal (Fig 1-13).

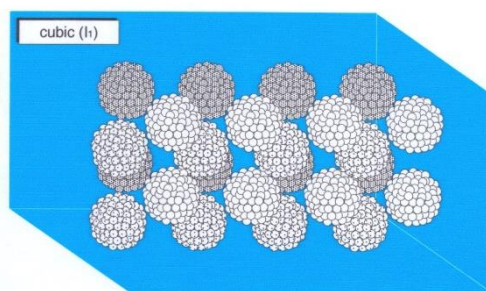


Figure 1-13 : Structure of the cubic lyotropic liquid crystals.<sup>54</sup>

iii. The lamellar lyotropic liquid crystals phase

For the lamellar lyotropic liquid crystal phase structure it can be seen that a particular phase consists of a layered arrangement of amphiphilic molecules as shown in Fig 1-14. Two antiparallel oriented hydrocarbon groups point towards each other forming a hydrocarbon mid area of the lamellar packing and the polar groups interact with the water. The lamellar phase is formed from a minimum concentration of 50% surfactant.

At higher concentrations of solvent hexagonal or isotropic micellar phases are observed. Despite the decreased water content of the lamellar phases compared to the hexagonal phase, they tend to be less viscous than the cubic or hexagonal lyotropic phases.<sup>18</sup>

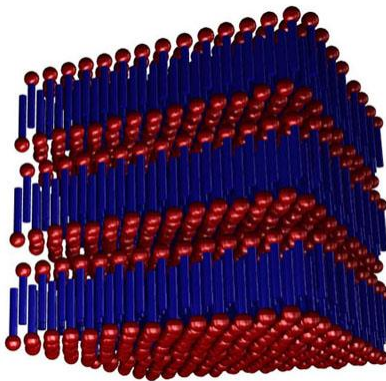


Figure 1-14 : Lamellar lyotropic crystals phase.<sup>55</sup>

### 1.3.2.3 Phase diagrams

Phase diagrams are used to describe the phase behaviour of liquid crystal materials. This is particularly important in the study of lyotropic LCs. An example is shown in Fig 1-15. The X-axis represents the amphiphilic concentration and temperature is parallel along the Y-axis. The diagram often shows liquid crystal behaviour of a mixture of lyotropic and thermotropic liquid crystals. This phase diagram shows the range of concentration and temperature with each phase.<sup>18</sup>

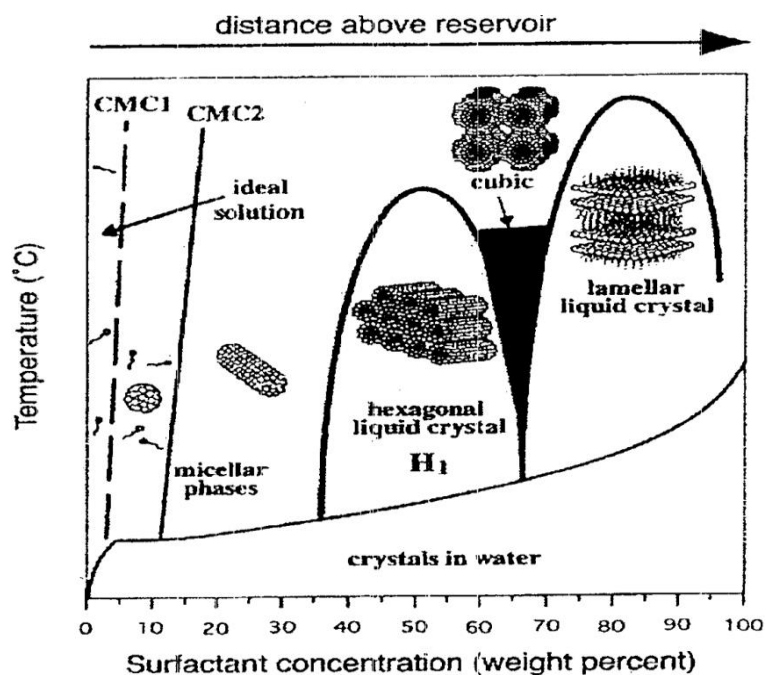


Figure 1-15 : Phase diagram for a typical soap in water.<sup>56</sup>

The concentration at which micelles form in solution is called the critical micelle concentration (CMC) and  $T_k$  is the Krafft temperature. This is the temperature above which lyotropic liquid crystal phase behaviour can be found.

#### 1.3.2.4 Lyotropic liquid crystals polymers.

There are two main conditions required for a polymer to exhibit lyotropic liquid crystal phase behaviour, which can be fairly rigid. It should dissolve in a solvent and the concentration in a solvent must be high enough to form a liquid crystalline phase so that these macromolecules constantly interact with one another. This cannot to be achieved if the macromolecules do not dissolve in the solvent.

One example of a class of synthetic polymer liquid crystals is the polyamides, shown in figure 1-16. The majority of large molecules that form liquid crystal phases are biologically important; for instance, cellulose derivatives are polymer liquid crystals.

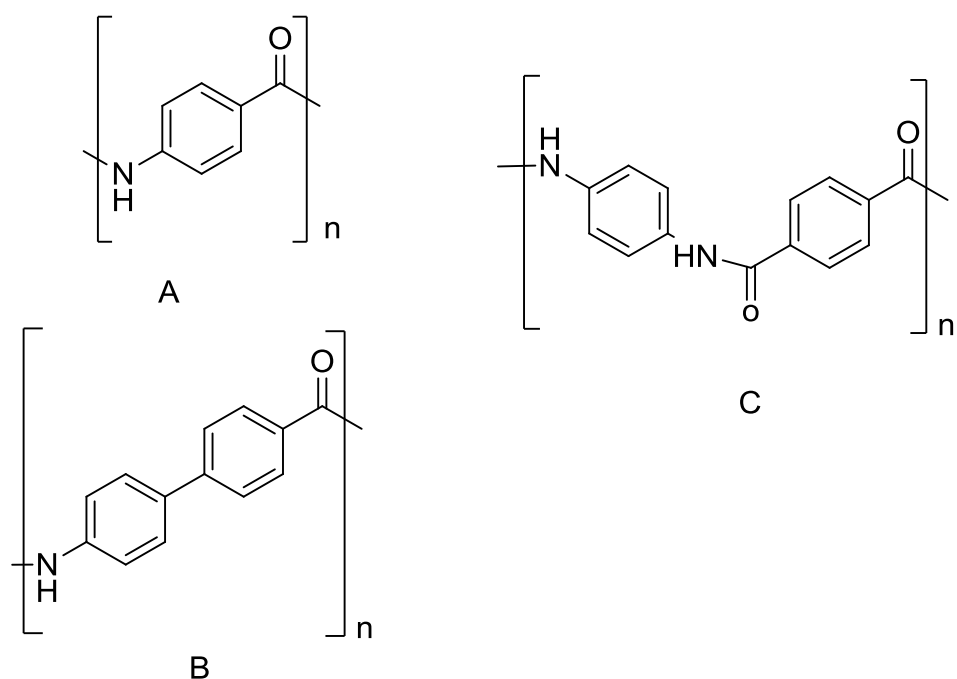


Figure 1-16: Three examples of aromatic polyamides with lyotropic liquid crystal phase behaviour, C is known as Kevlar (dissolved in high concentrations of sulphuric acid).<sup>18</sup>

### 1.3.2.5 Biological liquid crystals

Biological membranes and cell membranes are a form of liquid crystal. Their constituent molecules (phospholipids) are oriented perpendicular to the membrane surface, and the membrane is flexible. As in lyotropic lamellar systems, the biological structure is all water-based as a solvent and the lyotropic liquid crystals phase require water as well to form. The chemical reactions in water can produce a product that does not dissolve in water which forms a precipitate. In certain conditions the precipitate forms a rigid structure. Such processes are biologically important.<sup>18</sup> However, this is not the subject matter of this thesis, so it will not be discussed further.

## 2 Chromonics

About twenty years ago, it was becoming clear that there is a widely and well-known family of lyotropic liquid crystals with properties which are very different from those of conventional amphiphiles. This family consists of different kinds of dyes, drugs, nucleic acids, carcinogens, antibiotics, and anticancer agents. The majority, with respect to the properties, differ from ordinary lyotropic liquid crystals of the detergent/ soap/ phospholipid type. The molecules have aromatic structures rather than aliphatic. In addition they are rigid and not flexible and planar disc-like or plank-like, rather than rod-like. The hydrophilic groups are positioned around the periphery of the molecules instead of at one end and the molecules aggregate in solution into columns, not into micelles.

## 2.1 Chromonic phases

The name *chromonic* comes from the bis-chromone structure of the commonly marketed anti-asthmatic known in the UK as INTAL and in the USA as Chromolyn.<sup>57-64</sup>

Chromonic mesophases are lyotropic isotopes of the discotic mesophases and there are some parallels in their history. All chromonic phases are composed of columns of  $\pi$ -stacked aromatic molecules. Chromonic systems forming both N and M phases are well-documented and there are hundreds of examples. The classic chromonic phases are the nematic phase. Figure 2-1 shows the general structure of the N and M phases. In both phases, the molecules are packed in columns. In the N phase, the columns are almost parallel, but there is no positional and orientational order of the columns. In the M phase, the columns are ordered in a hexagonal symmetry and have long-range order (figure 2-1).<sup>65-68</sup>

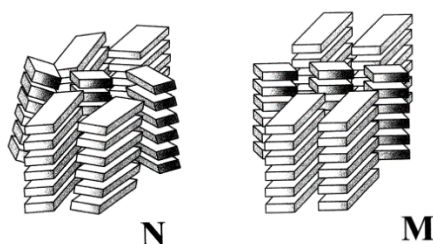


Figure 2-1: The Structures of Chromonic N and M Phases.<sup>69</sup>

However, there are other further phases such as the P phase and the rectangular O phase. The P phase shows that a single mesophase is formed which has optical textures which change simply from some properties of an N phase to those of an M phase as the temperature is raised (figure 2-2).<sup>70-73</sup> In a N/M system, where the columns have a plank-like or elliptical cross section, the change from M to N includes a quite change in the system of rotational motion of columns about the column axis. In the N phase, the columns are somewhat shorter, more fluid and can rotate independently, whereas in the more closely packed M phase, there is not sufficient room to do this.

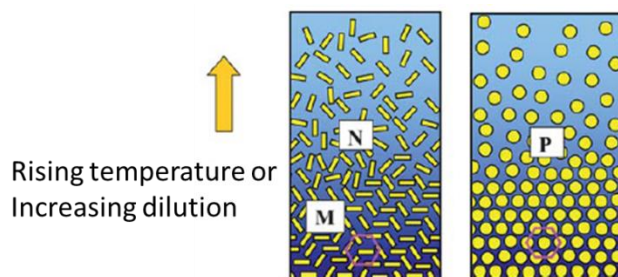


Figure 2-2: N, M and P phases viewed down the column axes.<sup>74</sup>

The rectangular O phase has been predicted. John Lydon has mentioned that ‘There have been some indications of its existence but as far as I am aware, no well-authenticated examples have been reported’.<sup>74</sup> The O phase was found to exist at lower temperatures and at higher concentrations. The structure in this phase is characterized by a transient cybotactic herringbone packing. There have been expectations of a low temperature phase which might well be a rectangular phase formed from the M phase when the thermal motion is decreased. The low temperature, phase for the commercial dye disodium cromoglycate (DSCG) observed at sub-zero temperatures, by adding an antifreeze to prevent the temperature of ice formation, may well be of this type (Figure 2-3).<sup>75, 76</sup>

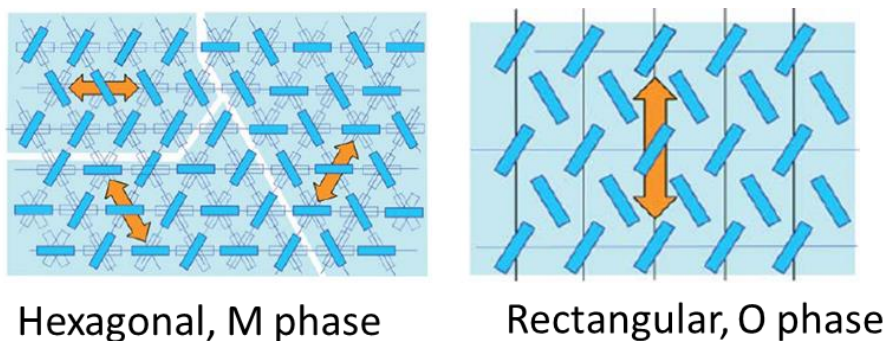


Figure 2-3: The chromonic M and O phase structures.<sup>77</sup>

To sum up, the chromonic phases have different symmetry and structure. Table (1) below summarizes the various phases for the chromonic crystalline state.

Table 1: table below shows chromonic phase type and structure which they are composed of columns of  $\pi$ -stacked aromatic molecules.<sup>78</sup>

Chromonic phase type	The structure
<b>N</b>	The columns in N are more or less parallel, but there is no positional order ordering with only orientational long-range order of stacking columns.
<b>M</b>	The M phase has an array of parallel columns with orientational and positional long-range order of column long axes. The columns are stacking on a lattice with statistical hexagonal symmetry.
<b>P</b>	An array of parallel columns lying on hexagonal symmetry with positional and orientational long range order of column long axes.
<b>O</b>	The O phase has parallel columns lying on a rectangular lattice with orientational and positional long range order of columns long axes.

## 2.2 Chromonic phase structure and properties

The ‘carbonaceous phases’ had been known and characterised by the coking industry for a long time and ‘negative nematic’ liquid crystalline phases years before Chandrasekhar’s classic work on columnar liquid crystals. They are aggregations of dye molecules which look like coins on top of each other or packs of cards. In many cases, chromonic systems are more close to thermotropic systems than to normal amphiphiles. In both cases, the driving force forming the liquid crystalline phase and the aggregation (face-to-face) of molecules forming columns is the same. The geometrical aspects of the column packing are almost the same in both cases, the difference being that in one case the columns are in a matrix of alkyl chains and in the other, they are formed in water. However, so far chromonic counterparts of all of the thermotropic discotic phases have not yet been found. Until now no well-authenticated tilted chromonic systems have been reported.

In general, the chromonic molecules prefer to aggregate into columns, even in very dilute solutions, somewhat similar to lyotropic mesogens which form micelles before a mesophase is formed.<sup>79, 80</sup> However there is a difference; no specific optimum column lengths are favoured, thus there is no analogue of the cmc of normal amphiphiles. The term ‘isodesmic’ (it has been used in the aggregation of nucleic acids in solution) has been applied to the stable build-up of chromonic aggregates where the addition or removal of one molecule from a pile is always related to the same increment of free energy.<sup>81, 82</sup>

There are fundamental differences between normal amphiphiles and chromonic systems, concerning what happens at the lower temperature limit of forming mesophase. In normal amphiphiles, there are two regions of micro-phase; the hydrophilic (aqueous) and the hydrophobic, aliphatic parts. As the temperature is lowered, the alkyl chains usually move in the hydrophobic region and freeze out to form a gel phase. This kind of segregation is too weak to be able to fulfil the requirement of micelles forming mesophase. This results in a lower temperature limit characterised by its Krafft point. In chromonic systems the opposite occurs; due to the absence of alkyl chains in chromonic systems (or the absence of the right lengths of alkyl chains), chromonic systems do not show a Krafft point. In addition the lower temperature is limited and marked by the appearance of water ice, normally a few degrees below 0°C.<sup>61, 63</sup>

The chromonic materials are different in other aspects in their self-assembly behaviour as well. Often a tendency to form ABAB stacks is observed. Nothing similar is known for lyotropic liquid crystals. The alternating column should be regarded as the structural unit of the phase.<sup>83, 84</sup>

## 2.3 New chromonic materials

In the last few years the reports of new chromonic mesophases have increased; these include as well a report on a new metallo-mesogen and excitingly, a non-aqueous chromonic system.<sup>85, 86</sup> There are important new chromonic materials such as the azo dye, (C.I Direct Blue 67)<sup>87, 88</sup> as shown in figure 2-4, xanthone derivatives,<sup>89</sup> benzopurpurin 4B,<sup>90</sup> phthalocyanines, porphyrin derivatives,<sup>91</sup> Levafix Goldgelb,<sup>92</sup> Violet 20<sup>93</sup> and Blue 27.<sup>94</sup> C.I Direct Blue 67 exhibits a typical behaviour of a N/M phase. This can be counted as a useful new chromonic compound. The aqueous solutions of this dye form chromonic phases identified by the use of temperature-controlled X-ray diffraction, UV-visible spectroscopy and polarised light microscopy. However, at low concentrations the dye molecules form columnar aggregates.<sup>87</sup>

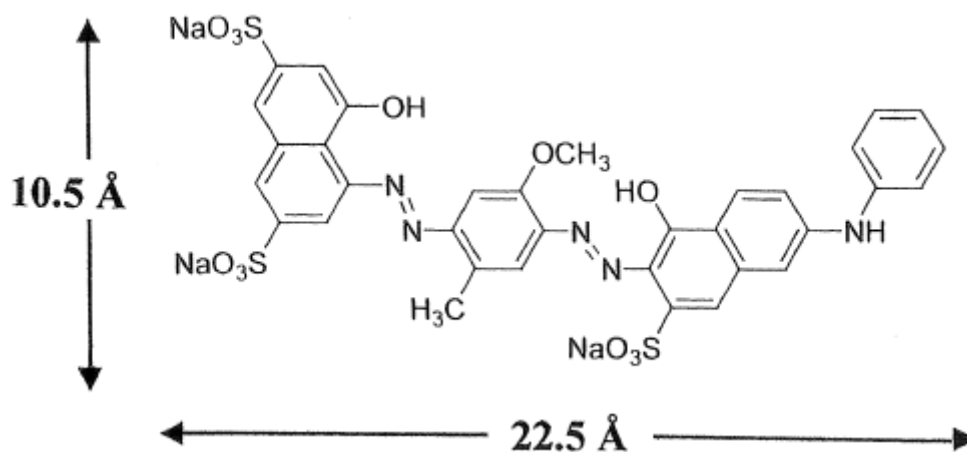


Figure 2-4: The molecular structure of C.I. Direct Blue 67.<sup>95</sup>

The packing repeat length is 3.4 Å and the diameter of the column and the length of the molecule were found to be comparable, suggesting that the column is a unimolecular stack. One of the most interesting features found is that the addition of a small amount of anionic surfactant (0.01% by wt.) was found to increase the stability of the nematic phase. In this concentration there is no indication of the added amphiphile having a

direct structural impact on the mesophase, for example coating the columns and the impact should be subtle.

## 2.4 The preparation of patterned dye films

About ten years ago it was becoming clear that a photoalignment approach has been developed. The Weigert effect (dichroism introduced in a silver-silver chloride photographic emulsion by a beam of linearly polarized light) technique depends on the effect of some photochemical reactions to the orientation of the plane of polarised light striking the molecule deposited on a surface. Reactions for which the Weigert effect has been explored include photodimerization, photobleaching and photoisomerism. In the photoalignment of photoisomerisable molecules, the sample at the final state has the molecular director aligned normal to the electric vector of the incident light (Figure 2-5 a).<sup>96</sup>

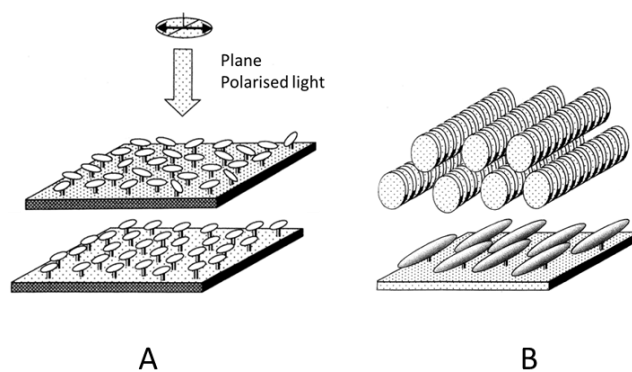


Figure 2-5: a) The preparation of an aligned dye coated polymer film via ‘command plate’ produced by the Weigert effect; b) the epitaxial alignment of a chromonic N phase by a photoaligned command plate.<sup>97, 98</sup>

The favourite compound for making aligned films using the Weigert effect is azobenzene. However, the azobenzene in the visible wavelengths range is weakly absorbed and it is, therefore, by no means ideal. A potential solution for this problem is the use of a film of photoaligned azobenzene molecules which are able to align epitaxially molecules in liquid crystalline phases (figure 2-5 b). The photoaligned substrate can be used as a ‘command surface’, which is in turn able to direct the alignment of the mesophase. Photoinduced alignment of this type was demonstrated with thermotropic mesophases (the films should be an azodoped polymer, polymers with side groups of azobenzene or polymers with side groups of cinnamic acid) and it has also been shown that it works for the lyotropic phase, so it is expected that it could be used to align the chromonic N phase.<sup>92, 99-107</sup>

## 2.5 Molecular stacking patterns in chromonic systems

The few X-ray diffraction studies of chromonic systems show that most of the molecules stack on top of each other, in columns with cross-sectional areas of dimensions more or less close to that of a single molecule. In this type of packing there are a large number of different variants with different geometrical relationships between adjacent molecules and with varying degrees of randomness possible (figure 2-6).

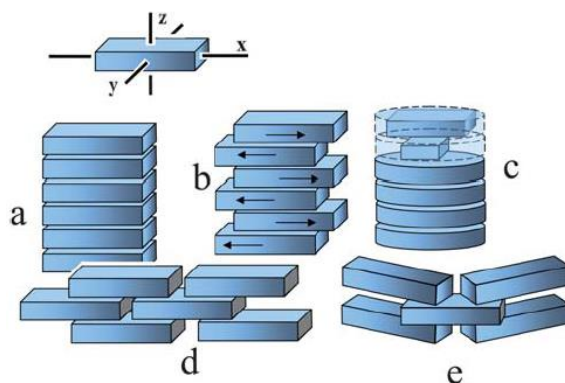


Figure 2-6: The packing within the columns. a; simple, molecules stacking on top of each other within a column, with end-to-end and side-to-side disorder. b; an alternating head-to-tail assembly, showing a structure close to a crystallographic two-fold rotation axis. c; showing columns with a helical envelope. d; a half-and-half overlap, looking like a wall. e; A type of (d).<sup>108</sup>

Chiral chromonic molecules have been investigated. They stack in a twisted manner as shown in Fig. 2-6 (c) showing columns with a helical envelope. (a) Simple, molecules stacking on top of each other within a column, with end-to-end and side-to-side disorder. (b) An alternating head-to-tail assembly, showing a structure close to a crystallographic two-fold rotation axis. (d) A half-and-half overlap, look like a wall. (e) A type of (d) giving a curved sheet which can form a chimney structure.

### 3 Nanoparticles

Over the last two decades, extensive attention of scientists has been drawn to a number of different research areas, for instance physics, chemistry and biology.<sup>109</sup> In nanomaterials research, development has attempted to create materials with novel chemical and physical properties. These have unique properties when compared to the same material at micro and macro scale.<sup>110</sup> Researchers have progressed in learning the importance of understanding the fundamental size- and shape-dependent properties. Basically, nanoparticles have a diameter range of  $\sim 1 - 100$  nanometers<sup>111</sup>, depending on inter-particle distance (1nm is  $\sim 4.5$  times the atomic spacing), particle size (1 nm is  $\sim 6$  times the atom size of gold), the nature of the organic coating shell and the shape of the nanoparticles.<sup>112</sup> There is a great interest regarding the future of various metal nanoparticles such as platinum<sup>113, 114</sup>, copper<sup>115-117</sup>, CdSe<sup>115, 118</sup>, tin<sup>119</sup>, silver<sup>112, 120</sup>, iron<sup>121</sup>, gold and others.

Nanoparticles (NPs) can be classified into two main groups: organic NPs (micelles, polymer based NPs, carbon nanotubes (CNT)) and inorganic NPs (quantum dots, magnetic NPs, gold NPs). Nanoparticles applications are a result of two major factors: organisation and size. As different sizes of nanoparticles give different properties, researchers around the world are taking on the challenge to explaining this behaviour of these materials. The purity and polydispersity of these materials are decisive, in terms of properties but very hard to control. These defects are miniscule compared to the NPs' final applications. It was predicted that as NP's size is decreased which the diameter ranges from 1-10 nm (intermediate between the size of small molecules and that of bulk metal), the number of free electrons is reduced and their properties are owned mainly by quantum-mechanical rules.<sup>122-127</sup> Gold or silver nanoparticles smaller than 3 nm are no longer considered noble metals, as their reactivity is significantly increased and they have high potential to be used in catalysis. Overall, the properties of small nanoparticles differ from the ones in bulk materials. This influences the physical and chemical properties, which is why the synthesis of size-controlled nanoparticles is very important and an ongoing challenge.

Related to the size, the shape of nanoparticles is another important factor. The properties can vary as a function of the packing complexity if the parameter can be controlled. For instance, for the synthesis of one-dimensional (1-D) structures such as nanoribbons, nanowires or nanotubes, there are various and well-established techniques.

This field has attracted widespread interest over the past decade due to their many potential applications. Especially, research on the nanoribbons structure can help to investigate the basic issues about the effects of dimensionally and the transport phenomena in a confined space,<sup>128</sup> as only one single direction is available for charge transport; the other two are considered poor. The 3-D nanostructures offer countless potential applications as the final nanostructure is a result of a synergetic effect of the size, shape and contrast of the NPs plus their functionality, brought by the layer(s) that cover(s) the nanoparticles. There are a wide variety of methods which have been used and are under continuing development, such as “bottom-up” and “top-down” approaches. In the “bottom-up” methods, a small components, such as atoms and molecules, are assembled in a very controlled process.<sup>129</sup> The “top-down” approach starts from an assembly, a bulk material and via different techniques, like lithographic techniques, the formation of smaller moieties and other properties. However, these is a size limit which can be achieved to form the necessary resolution and the ability to form a three-dimensional structure with specific characteristics. Therefore, the “bottom-up” molecular self-assembly is the preferred method for preparing most nanostructures, because of its diversity.

Several methodologies have been developed to synthesize nanoparticles which will be prepared by using either physical or chemical methods. Physical methods depend on using the mechanical subdivision of the metallic aggregates and evaporation of a metal in a vacuum by resistive heating or laser ablation. However, the reduction of metal salts in solution is involved in chemical methods. This is considered the most suitable way for size-control of the particles and modification of the surface chemical composition.<sup>130</sup> In the majority of NPs synthetic procedures, organic compounds have been used in most reactions to protect the NPs, to control their size, for better chemical reactivity and for modification of their physical properties as well. Coordinative ligands, polymer micelles have been explored to stabilize the NPs. The preparation of NPs of the right shape and size is improving their applicability, as well as the possibility of ligand exchange after the nanoparticles using an appropriate compound, in terms of shape, size and functionality.

A basic problem with non metallic noble NPs is that they tend to oxidize, so metal atoms not oxides are required. In the synthesis the organic layer is needed as well in order to protect metal nanoparticles from deprecation. For instance, iron NPs can oxidize quickly; however, if they are protected by an organic layer, this improves stability. On the other hand, the “core-shell” method is based on encapsulating a

nanoparticle inside a bigger particle in order to achieve the nanoparticle coating. In these materials a layer of atoms or molecules covers a smaller nanoparticle. This configuration of the nanoparticle complexes can make excellent candidates for a number of potential applications and a synergy of properties. For example, the internal particle can be magnetic and the outer one could exhibit interesting optical behaviour due to their sensitivity to the surface structure of the material. A number of nanoparticles have been synthesised to have this core-shell structure.<sup>131, 132</sup>

Nanoparticles can form the basis of an important category of liquid crystalline materials. The degree of organisation in liquid crystal nanoparticles' (LCNPs) is based on the fluidity and order which influence the physical and chemical behaviour. They provide the chance to create a large number of complex structures, and with it, unique properties. The nanoparticle's metallic core and the organic layer(s) play an important role in its features. Example are gold nanoparticles (Au NPs) and iron based nanoparticles, like iron platinum nanoparticles such as (Fe/Pt NPs); the first for their optical properties and the latter for their intrinsic magnetic properties.<sup>133, 134</sup> Considering these NPs covered with liquid crystals, properties and potential applications can be increased and developed.

### **3.1 Gold nanoparticles**

Researchers have focused on a wide range NPs in the past decades and it is very likely that research on AuNPs will continue for the foreseeable future. Gold has always been valuable to humans and efforts go back thousands of years. One of the most famous examples of aesthetic use in ancient time is the Lycurgus Cup, in which gold NPs in ruby glass are used to generate different colours (Figure 3-1). Gold nanoparticles are generally considered one of the best researched in modern science. Past decades have witnessed in science, and the rise of developed technology for the facile synthesis of thermally- and air-stable gold nanoparticles of polydispersity in size and controlled size. These developments led to a huge interest among researchers due to the vast range of applications. One of the most important reasons for the interest of gold to researchers is its elemental stability. Stable materials such as gold are used as contrast agents in electron microscopy due to their electron-density. Gold nanoparticles exhibit fascinating properties in different fields of materials science. The absorption band of AuNPs in the visible region is very strong, this is a particles effect since it is absent from the individual atom and also in the bulk.

The synthesis of gold nanoparticles have been developed in different methods. Turkevich explored method to obtain gold nanoparticles (AuNPs) in the size range of 10-20 nm by stabilising them in water by citrate in 1951.<sup>135, 136</sup> However, 1994 Brust and co-worker published a biphasic method that allowed one to obtain 2 nm size particles.<sup>137</sup> In most syntheses of the gold nanoparticles salts are transferred to the organic phase by a quaternary ammonium and are then reduced by a borohydride in the presence of thiols. Brust also extended this synthesis in 1995 to *p*-mercaptophenol AuNPs in a single phase.<sup>135</sup> These methods had a large impact on the field, because it helps the facile synthesis of thermally- and air-stable AuNPs with reduced dispersity and controlled size by Brust. The fabrication of nano-devices with novel structures and functionalities<sup>138-141</sup> were explored and increased the number of publications by scientists. Astruc<sup>127</sup> published a general review on AuNPs and their applications few years ago and was followed with many other publications,<sup>126, 142-144</sup> reviews,<sup>125, 145, 146</sup> and a book<sup>147</sup> on NPs and their applications.<sup>148-154</sup>



Figure 3-1: The Lycurgus Cup in reflected and transmitted light.<sup>155</sup>

### 3.2 Preparation methods for AuNPs

The preparation and synthesis of AuNPs have their advantages and disadvantages. The most current successfully techniques and methods which have been used will be discussed. Preparation of stable dispersions of gold nanoparticles in water is very useful for some applications.<sup>156</sup> Despite the importance of the synthesis of gold nanoparticles using water, it has a number of obstacles. For instance, removing the residue of

stabilizers is very difficult, ionic interactions is problematic and low content of gold nanoparticles in the reactions leads to low yields. Preparation of gold nanoparticles in an organic solvent eliminates the inherent problems when using water. AuNPs in high concentrations can be prepared with controlled size and shape and developed monodispersity. Chemical reduction of gold salt is a general way to prepare AuNPs. For this method typically four components are used: solvent, reducing agent, metal salt and a stabilizing agent. For a few years two methods for preparing AuNPs: these were the citrate method<sup>157, 158</sup> and the two-phase method<sup>130, 159</sup>.

In recent years, Brust and coworkers reported the preparation of gold nanoparticles by protecting the nanoparticles with a monolayer of dodecanethiolate. It is a simpler method; the NPs synthesis is carried out in a one-phase system and the requirements are the metal precursor, the reducing agent and the functional organic capping agent (thiol). This method avoids the necessity of the ligand exchange step, which is why the Brust method has been chosen for use in this project. This method resulted in highly monodisperse NPs, of good quality and shape, and they can be delivered many times without aggregation and losing their potential properties. The size of NPs can be controlled and the procedure conditions in terms of desired ratio of gold to ligand can be prepared with reproducible results.<sup>130, 160</sup>

## 4 Aims

It is the aim of the project to explore a series of organic liquid crystals based on rod shaped mesogenic groups. It is the overall aim to gain additional understanding of the correlations between chemical structure and physical properties. The length of the aromatic core is to be varied. The number and type of flanking chains is to be varied between one hydrocarbon chain and two ethylenoxy chains at both terminus of the rod shaped molecule and one alkyl chain at one terminus and three ethylenoxy chain at the other end of the molecule. For material containing ethylenoxy chains the phase behaviour in mixtures with water is to be investigated. Additionally, the synthesis of AuNP in the range of 2-3 nm and the attachment of LC groups is to be investigated.

## 5 Materials

All products used in the laboratory were purchased from Sigma Aldrich, Fluorochem, Acros, Alfa Aesar and Fisher Scientific company.

### 5.1 Instrumentation

#### 5.1.1 Vacuum pump

Volatile solvent was removed with a Buchi RE111 rotary evaporator. The Pumps mechanism was used to evaporate the solvent to allow the gases to flow and be intensified, then the compound would remain.

#### 5.1.2 $^1\text{H}$ Nuclear Magnetic Resonance (NMR) Spectrometry

NMR spectra were recorded at room temperature as solution in deuteriochloroform ( $\text{CDCl}_3$ ). Tetramethylsilane (TMS) was used as internal standard. The spectra were recorded on a Joel ECP 400 spectrometer and the chemical shifts ( $\delta$ ) are given in parts per million (ppm) with coupling constants in Hertz (Hz), at a frequency of 400 MHz for  $^1\text{H}$  and 100 MHz for  $^{13}\text{C}$  spectra.

s - singlet

d - doublet

t – triplet

quat – quartet

quint – quintet

sext – sextet

dd – double doublet

dt – double triplet

tt – triple triplet

m – multiplet

br – broad peak

#### 5.1.3 Gas chromatography- mass spectrometry (GC –MS)

Method: Injector temperature  $300\text{ }^\circ\text{C}$ , helium flow rate 1.0 ml/min, oven temperature  $50\text{ }^\circ\text{C}$  for 4 min ramped at  $26.0\text{ }^\circ\text{C}/\text{min}$  to  $250\text{ }^\circ\text{C}$ , held for 0.00 min and programme temperature  $100\text{ }^\circ\text{C}$  for 2.00 min.

## 5.2 General Process

### 5.2.1 Thin Layer Chromatography (TLC)

Chromatography was used to separate mixtures of substances into their components. All worked on the same principle. The mobile phase carries the components of the mixture at different rates through the stationary phase. Silica gel was the stationary phase. TLC has a substance which fluoresces in UV light. A pencil line is drawn close to the bottom of the plate and a small drop of the product and starting materials added. The length distance of compound moving measured against the solvent point yields the  $R_f$  value.

### 5.2.2 Column Chromatography

Column chromatography is a method used to purify individual compounds from mixtures of other compounds. Separations was carried out using BDH silica gel, 33-70  $\mu\text{m}$ . The silica gel was eluted in appropriate solvents which were prepared. The wanted product was filtered through Schleicher & Schuell filter papers.

### 5.2.3 Elemental Analysis

Elemental analysis is used to determine the elements and relative ratios of hydrogen and carbon present in the sample. The sample is burned in order to remove the excess of oxygen. The expected values for the sample are compared and the error should not be more than 0.3%. The analysis was carried out using a Fisons EA1108 CHN analyser.

#### 5.2.4 X-Ray Diffraction (XRD).

X-ray diffraction is a technique for determining crystal structure and revealing physical properties of materials. The X-ray beam passes through a crystal which causes the beam to scatter and spread into particular directions, enabling measurement of the average space within crystal layers. Moreover, X-ray finds unknown materials and measures the shape and size of crystals regions, as well as the position of atoms, chemical bond, crystalline phases and other information. Figure 5-1 shows that  $2\theta$  is the incident angle and  $r$  is the path difference between two waves. The materials were placed in glass capillary (number 14 Hilgenberg), with outside diameter of glass capillary 1.00 mm and measurements were conducted on cooling from 190 °C to 40 °C, every 5 K. All the values of the layer spacing  $d$ -value are in nm.

Bragg's law explained the interference pattern of X-rays scattered by crystals and helps to measure the intensity of scattered waves and angle.

$$2d\sin\theta = n\lambda$$

where  $d$  is the spacing between diffracting planes,  $n$  is any integer,  $\theta$  is the incident beam angle and  $\lambda$  is the wavelength of the incident beam (1–100 angstroms).

X-rays were generated using a copper tube (Cu K $\alpha$  radiation, graphite monochromator,  $\lambda = 1.54 \text{ \AA}$ ) and detected on a 2-D image plate MAR345 detector with diameter 345 mm, distance from the detector was 300 mm. The data were analysed by using “Datasqueeze” software and the OriginPro 8.6 software package from OriginLab.

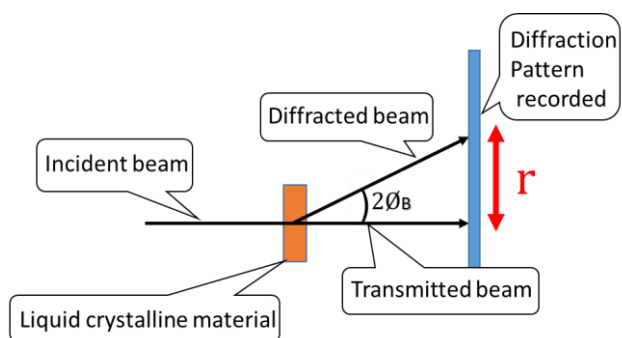


**Figure 5-1:** X-ray diffraction shows beams from continuous cones and a crystal powdered sample.<sup>161</sup>

### 5.2.5 Differential Scanning Calorimetry (DSC).

This is a thermoanalytical technique in which a curve of heat fluxes versus time or versus temperature and confirms liquid crystal transitions. The DSC instrument shows the number of enthalpy of transition (the enthalpy of melting to estimate both purity and degree of crystallinity), the ranges of temperature and the transitions between the phases. In addition, DSC shows melting for organics and clearing points exhibited by LCs. Phase transitions occur when there are changes in the molecular ordering. Changes in molecular ordering have associated changes in enthalpy. An endothermic process is when a material passes from a more ordered to a less ordered state (e.g. from a crystal to a mesomorphic state). However, when material passes from a less ordered to a more ordered state, it is exothermic. One of the best features of the DSC instrument is the repetition of heating and cooling cycles. The second or third heating and cooling cycles were taken to calculate the transition and enthalpy values in order to get the same thermal for each sample. The measurements and heating flows are carried out in a controlled atmosphere. For the DSC work analysis consists of the sample and the reference material. The sample and the reference were heated at the same rate over a known temperature range in the whole experiment. When a solid organic sample melts to a liquid, it requires more heat flux to the sample to increase its temperature at the same rate as the reference. The DSC is designed in such a way that the temperature of both samples are raised linearly with time. The reference material must be well characterized and have well-known heat capacity over the temperature range of the experiment. For the reference the sample was gold and both samples were prepared in an aluminium pan (in a separate furnace).

These experiments give quality and quantity of information on physical and chemical properties and changes in a materials during or after exothermic or endothermic processes.

The DSC instrument provides useful information and can be used to give an indication of liquid crystal materials, such as melting and boiling points, crystallization time, glass transitions, specific heat capacity, oxidative/thermal stability, reaction kinetics, percentage of crystallinity and purity.

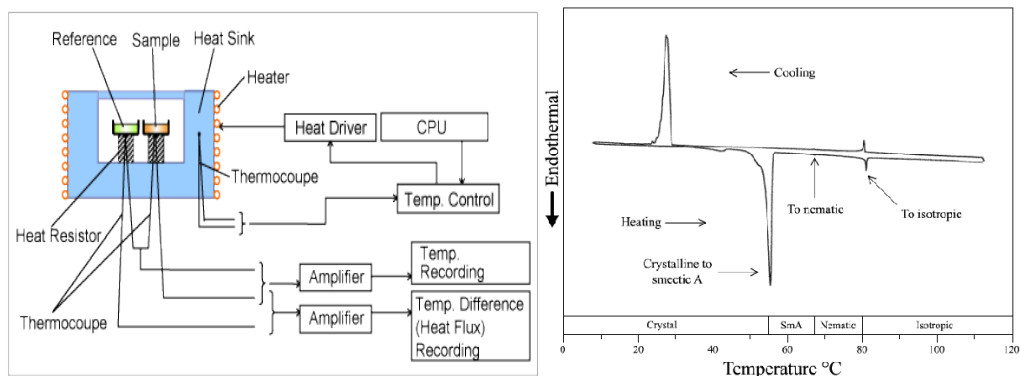


**Figure 5-2:** Schematic representation of the operation of a DSC and a sample thermogram.<sup>162 163</sup>

The technique was developed by E.S. Watson and M.J. O'Neill in 1962. The DSC instrument used was Mettler DSC822e with STAR<sup>e</sup> software, DSC calibrated using indium (melting point onset 156.6 °C, 28.45 J/g). The calibration of the DSC was checked daily using the indium standard allowing  $\pm 0.3$  °C and  $\pm 0.3$  J/g experimental error, and using an aluminium reference pan.

The following terms are used for phase identification:

Mp = melting point

Tg = glass transition

C = crystal transition

N = nematic

SmA = smectic A

SmC = smectic C

Iso = isotropic liquid

## 5.2.6 Transmission electron microscopy (TEM)

TEM was performed with a sufficient level of magnification in the range of x1,500 to x1,200,000 with a JEOL 2010 instrument, running at 200kV with a lanthanum hexaboride (LaB6). Resolution: 2nm (with LaB6 emitter) and images were taken with a Gatan Ultrascan 4000, 64 megapixel digital camera operated using Digital Micrograph.

A TEM runs on the same basic principle as the optical microscope. The difference is that the TEM works using electrons instead of light. What can be observed through a microscope is limited to the wavelength of the light source, which is around 600 nm. Electrons have a lower wavelength (in the order of pm). Short wavelengths make it possible to obtain images with a good resolution, thousands of times better than that of an optical microscope. The possibility for high magnification makes the TEM a valuable tool for researchers.

The light source emitted at the top of the TEM travels through a vacuum inside the column of the microscope, which is about 2 meters in length. Instead of light being focused through a glass lense, it is focused in a very thin beam of electrons using electromagnetics. Then the electrons are transmitted through the specimen to be analysed. Depending on the density, scattered electrons hit more of the present material and disappear from the beam. At the bottom of the microscope unscattered electrons reach the fluorescent screen, resulting in a 'shadow image' of the material. This image is white and black with different parts displayed in varied darkness (grey) depending on the density of the part hit by the electrons beam. These images can be captured directly by the TEM operator or photographed with a camera (figure 5-3).

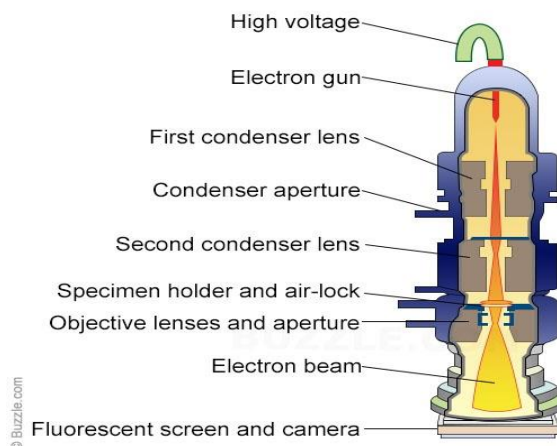


**Figure 5-3:** A schematic representation of a TEM.<sup>164</sup>

Due to the use of electron microscopy small objects can be magnified 1,000,000 times, down to three to 10 angstroms (1 angstrom is  $1 \times 10^{-7}$  mm). TEM provides an opportunity to identify small details in biological cells and other materials in depth. This ability to analyse and achieve a high level of magnification by TEM can be used in many research areas, for example materials science, nanotechnology, medical, biological, forensic analysis, gemmology and semiconductor research. In addition, it can be used to help the interpretation of life sciences, such as in the study of viruses and cancer research, as well as in industry and education.

Transmission Electron Microscope instrumentation is a very advanced tool for researchers with a number of advantages. For example, images are detailed with high-quality; it can provide information on element and compound structure; it can yield information on surface features, size, shape and structure; TEMs can be used in a wide range of applications and in a variety of different scientific, educational and industrial fields; it shows the most powerful magnification, potentially over one million times or more and TEMs are easy to operate with proper training.

High-resolution transmission electron microscopy (HRTEM) is an imaging tool which shows directly a two-dimensional projection of the crystal with defects. HRTEM allows imaging of atoms and channels in the lattice structures of a material, so it can show atoms exactly on top of each other. HRTEM enables study and analysis of properties of materials in nanoscale, due to its high magnification and resolution.

Preparation of TEM samples can be complex because of the film thickness of the materials to be analysed, which should not be more than hundreds of nanometres. Samples are dissolved in a solution and put onto the TEM grids or films.

### 5.2.7 UV-Vis spectroscopy

The optical properties of targets were investigated with a Varian Cary 50 BIO UV/VIS spectrophotometer equipped with a Varian Cary single cell peltier accessory (to control temperature measurements) and a Thermo Oriel Illuminator with Xenon and/or Mercury lamps and Oriel Instruments power supply and controller. The wavelength of the instruments used was roughly in the range of 200-900 nm.

UV-vis Vis spectrophotometer consists of the following components: a light source (UV and visible), sample containers for the quartz cell, a wavelength selector (monochromator) for splitting the beam into its component wavelengths by the grating, detector, signal processor and readout.

Ultraviolet-visible spectroscopy (UV-Vis) refers to reflectance or absorption spectroscopy in the ultraviolet-visible spectral region to determine solutions to transit metal ions and organic compounds. It uses light in the visible and adjacent (near-UV and near-infrared (NIR)) ranges. Absorption spectroscopy measures the transitions and excitation of electrons from the ground state to the excited state. UV-Vis spectroscopy compare the intensity of light before (reference) and after passing through a sample.

Most of the absorption of molecules containing  $\pi$ -electrons (double bond) or n-electrons (non-bonding electrons) occurs with a particular energy level for the  $\pi$ -electrons, which is when a specific amount of energy is absorbed. This would get excited to a higher energy ( $\pi^*$  energy) level for the electrons.

As a result of this, the highest energy (smaller energy gap) occupied molecular orbital (HOMO) and lowest energy (bigger energy gap) unoccupied molecular orbital (LUMO). The absorption depends on how easily the electrons get excited and the wavelength of the light.

Atoms and molecules can absorb electromagnetic radiation but it will be at different wavelengths. Absorption bands corresponding to structural groups and functions within the molecule. Chemical groups (which contain electrons) must exist to absorb ultraviolet or visible light.

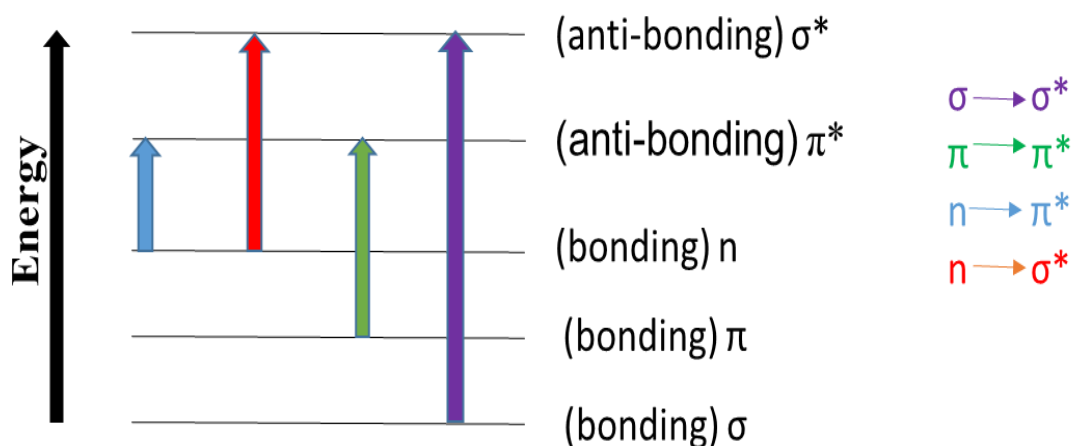


Figure 5-4: A schematic representation of the different transitions between the bonding and anti-bonding electronic states when light energy is absorbed in UV-Visible Spectroscopy.<sup>165</sup>

There are types of electron transition (figure 5-4) which are:

- $\sigma$  to  $\sigma^*$  transitions

An electron in a bonding sigma orbital of a molecule is excited to the corresponding antibonding orbital sigma star. The energy required for  $\sigma$  to  $\sigma^*$  transition is large. For instance, methane which has a single bond (C-H), can only undergo this transition. It shows an absorbance maximum at 125 nm. The wavelength of this transition is very short, so absorptions would not be seen in a UV-Vis spectrum.

- $n$  to  $\sigma^*$  transitions

Saturated organic compounds containing atoms with lone pairs (unshared electrons) undergo  $n$  to  $\sigma^*$  transitions. This type of transition requires a great deal of energy (but less energy than  $\sigma$  to  $\sigma^*$  transitions) and therefore occurs in the far ultraviolet region. Most  $n$  to  $\sigma^*$  absorption peaks appear below 200nm, for example, water and ethanol. Peaks in the UV region are relatively small.

- $n$  to  $\pi^*$  transitions and  $\pi$  to  $\pi^*$  transitions

Most organic materials undergo  $n$  to  $\pi^*$  or  $\pi$  to  $\pi^*$  transitions (excited state). The peaks appear in the spectral region (200 - 700 nm) because of the energy required for absorption is less. It occurs at longer wavelengths than transitions to  $\sigma^*$  antibonding orbitals. These transitions to  $\pi^*$  require the presence of an unsaturated functional group in their molecules to provide the  $\pi$  electrons.

UV-Vis spectroscopy is usually used for the analysis of samples of organic materials in solution, so sample is offered in the form of homogenised liquid. On the other hand, it can analyse solids and gases.

Transition metal ions are coloured when they are in solution, absorbing the visible light. This is due to the *d* electrons from the metal which can be excited from an energy state to another light energy state. The colour of the metal solution can be affected by other species, for example, anions or ligands.

## 5.2.8 Optical Polarising Microscopy (OPM)

Optical polarised microscopy (OPM) is used for identification and determination of materials melting points. In addition it is used in Photomicrographs and film phase transitions in LCs materials. It was undertaken using an Olympus BX51TF microscope connected with to Olympus InfinityX camera. Hot-stage microscopy was undertaken with a Linkam LTS350 hot stage and a Linkam LNP to control temperature or a Mettler Toledo FP82 hot stage and Mettler Toledo FP90 Central Processor control unit. A Leica VMHB was used for materials which needed to be melted for an easier manipulation or a controlled melt. Solid and powdered materials were sandwiched between a microscopy slide and a cover glass slip and heated under control to the desired temperature and phase transitions.

An optical polarising microscope uses polarised light in order to investigate optical properties of LCs materials, particularly, in the investigation of new and less familiar materials. There are many application areas for OPM instrument, such as liquid crystals, biology, and medicinal chemistry.

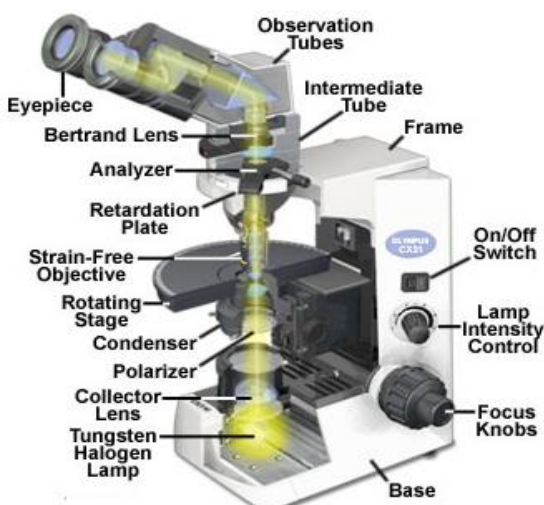


**Figure 5-5:** A schematic illustration of a transmitted light polarizing microscope. <sup>166</sup>

As described in Fig.5-5 and 5-6, the OPM, compared to a typical optical microscope, has a number of differences in terms of equipment and resolution, more complex construction and some additional components for example, a rotating stage, a polarizing condenser with a polarizer, an objective for polarized light, a Bertrand lens and an analyser.

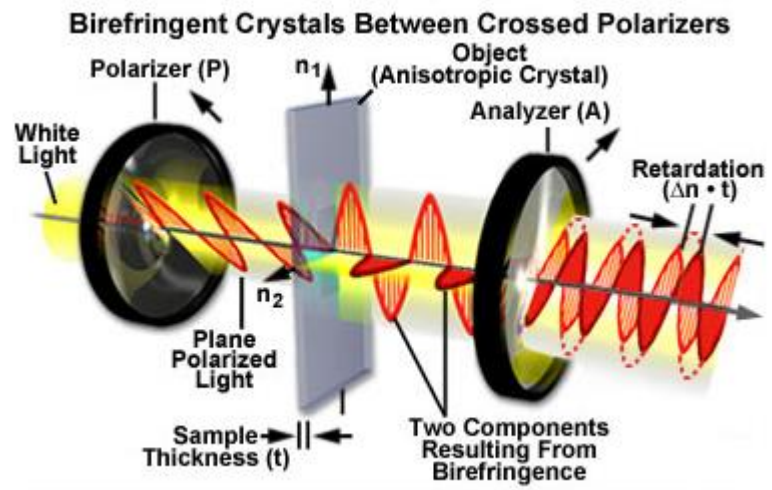


Figure 5-6: Description of OPM operation principles.<sup>167</sup>

### 5.2.9 Thermal Gravimetric Analysis (TGA)

Thermal Gravimetric Analysis (TGA) was used to determine the percentage of gold nanoparticles by burning the organic parts in an inert atmosphere at high temperature. It was carried out on a Mettler Toledo TGA/DSC1 controlled with a GC100 gas controller (gas delivery flow rate system). Samples were run and analysed in air and nitrogen environment. Samples of about 2-15 mg, were used in Alumina crucibles of 17  $\mu$ L. Sample were burned in nitrogen first then continued burning in air (flow rate of 100 ml/min) and the data were treated with STAR<sup>e</sup> system software, version 11.

TGA is generally used to determine specific characteristics and features of materials that exhibit either mass loss of volatile compounds for instance moisture or gain due to decomposition and oxidation. Some common applications of TGA are: materials which contain moisture or volatiles, analysis of decomposition patterns, studies of degradation and thermal stability of materials, mechanisms and reaction kinetics, determination of organic sample content and detection of inorganic impurity (such as ash) content in a sample. A TGA consists of a high precision balance with a pan loaded with the sample and a programmable furnace. The sample pan supported by high accuracy balance measures change in mass and change in temperature. The mass of the sample will be monitored during the experiment. Purge gas controls (this gas may be inert or a reactive gas) is passed over the sample to prevent oxidation or other undesirable side reactions.

The operational program for the TGA furnace was set for a constant heating flow to the sample and a constant loss of mass registered as a function of time.

The fundamental principle of TGA involves heating a sample at a constant rate (up to 2000°C), whilst continuously weighing of the sample, depending on the analysis method and the type of instrument used. As the temperature of the sample increases, some components are evaporated or decompose (oxidise) and their mass loss can be calculated in weight percentage. The results are shown by the STAR<sup>e</sup> system software as a graph with the temperature on the X-axis and the mass loss on the Y-axis.

In addition, the data can be adjusted through curve smoothing and first derivatives of sample components used to determine inflection points to help with more interpretation. TGA is used as a technique to characterize various materials such as LCs coated with NP and with pharmaceutical and petrochemical applications.

## 6 Chromonic

Liquid crystalline phase behaviour of ethylenoxy group functionalized molecules has in the main been associated with lyotropic liquid crystalline phase behaviour. For thermotropic systems it has been connected to investigations of LC crown-ethers and for the investigation of complex perforated lamellar super-structures. Not much work has been reported on the investigation of calamitic mesogens consisting of benzoic acid aromatic esters with the terminal chains bearing oligo-ethylenoxy groups. Thus such systems were explored, especially as these materials can combine thermotropic phase behaviour with some solubility in water, giving rise to the potential of chromonic properties.

In this report we will describe the results of our synthetic efforts and of the chemical characterisation of the materials and the investigation of the liquid crystal properties using optical polarizing microscopy (OPM), Nuclear magnetic resonance ( $^1\text{H}$  NMR) and differential scanning calorimetry (DSC). Additionally we report our results on the qualitative miscibility studies of these molecules with water, based on OPM experiments.

## 6.1 Results and discussion

The synthesis and characterization of the liquid crystals (compounds **6-4** and **6-5**) will be discussed and the properties will be presented. The synthetic route is shown in Fig 6-1.

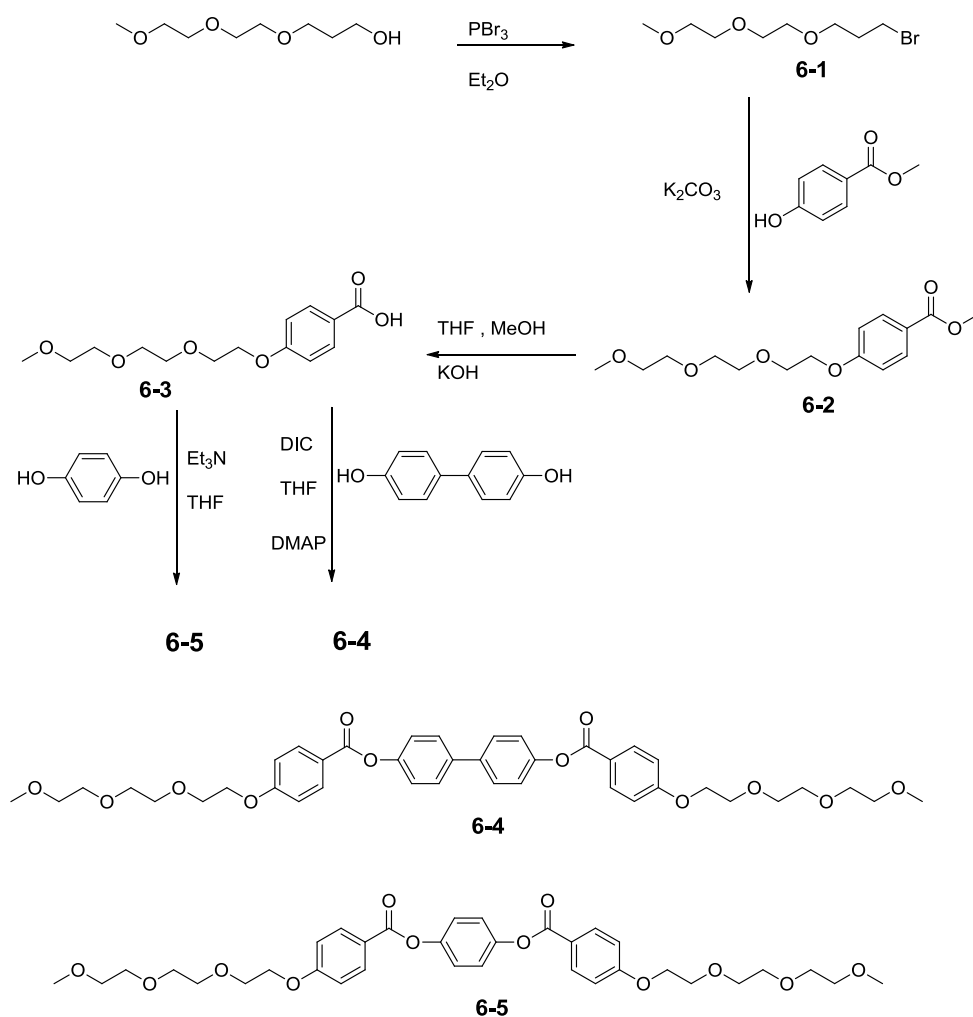
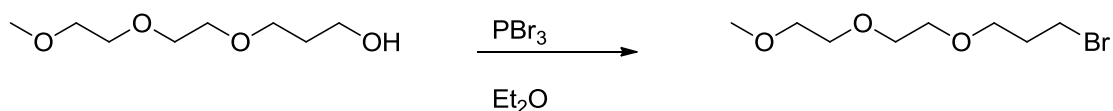


**Figure 6-1:** Scheme for the synthesis of compounds **6-4** and **6-5**.

The first step of this synthesis was a bromination. This was a very straightforward reaction which produced a good yield (61.2%).

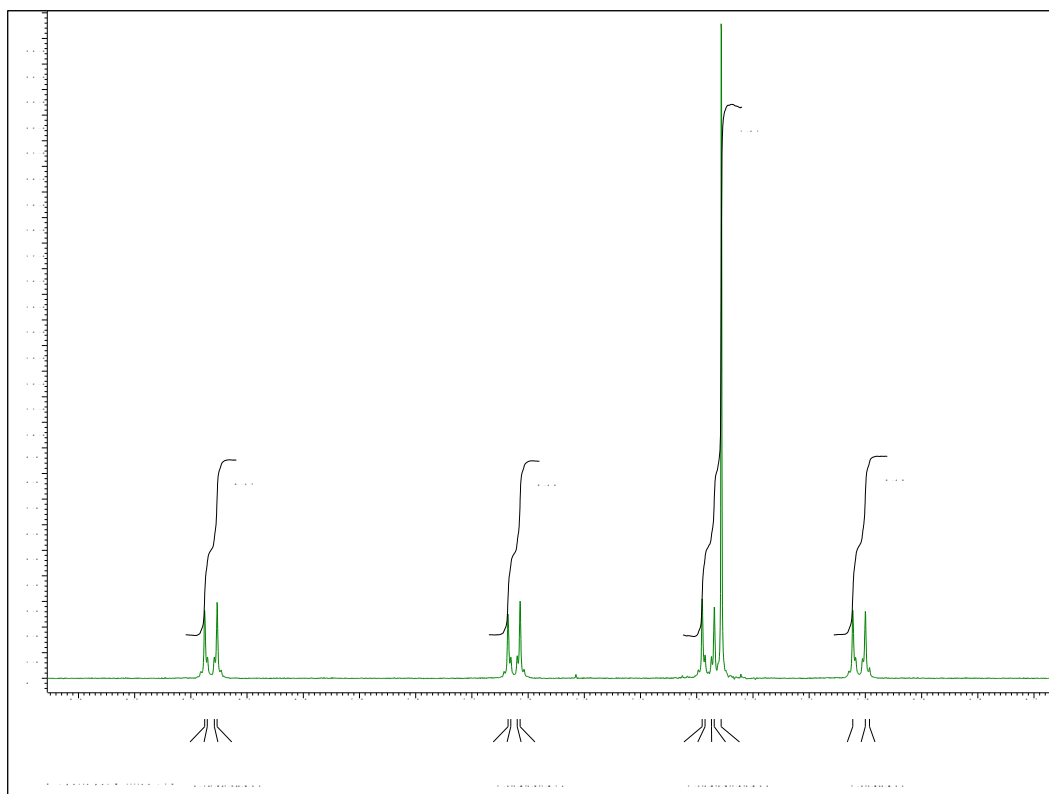


The second step was a Williamson etherification (compound **6-2**). A considerable amount of material is lost through purification, due to a high solubility in water. This explains why the yield for the reaction was not very high (48%). The following step was the hydrolysis of the methyl ester (compound **6-3**) which produced in a good yield (75.5%).

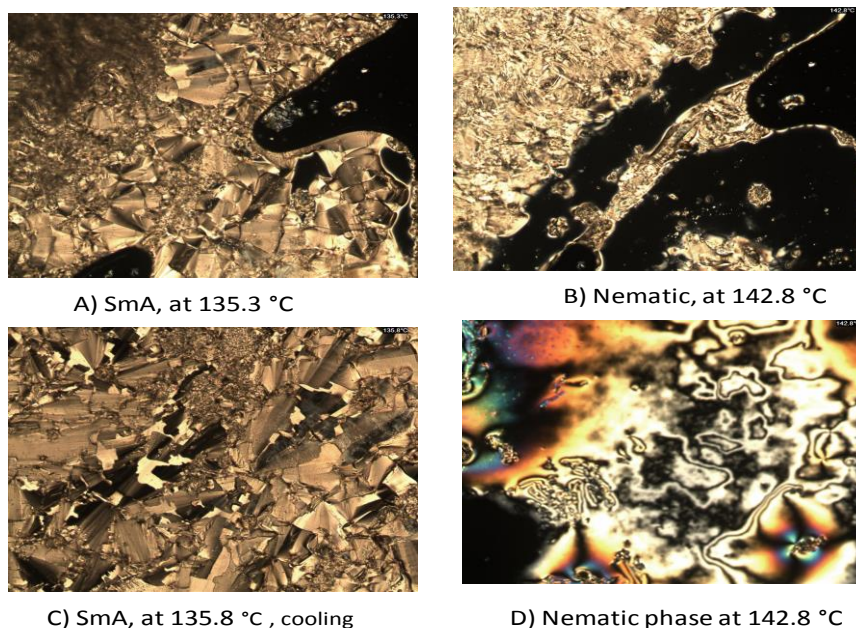
The final step of the synthesis was to employ a Steglich esterification. Initial attempts using dicyclohexylcarbodiimide (DCC) failed to produce the target molecule. Further attempts using diisopropylcarbodiimide (DIC) afforded the final product (compound **6-4**) in moderate to average yields (32%). The DIC reaction was monitored by thin layer chromatography (TLC). The reaction was terminated after 18 hours. Purification of compound **6-4** by silica gel column chromatography proved to be difficult. As a mobile phase, ethyl acetate/ hexane (1:1) was used, but some impurities remained. After several crystallizations (ethyl acetate and hexane) and further purification by silica gel column chromatography, substantial progress in removing impurities was made. The progress of impurities removal was checked by TLC. For the sake of economy of both time and solvents, an attempt was made to extract the compound by washing it with basic solution (KOH (aq)). The compound was checked by <sup>1</sup>H NMR, which indicated the absence of impurities. However, HPLC peaks showed that 30% impurities were present. The spectra peaks for 4,4'-dihydroxybiphenyl appeared at  $\delta=7.02$  and  $\delta=7.63$ . It was considered that the 4,4'-dihydroxybiphenyl signals overlap with the target compound in TLC and NMR. After chromatographic separation over 6 days in order to remove all the impurities, NMR and TLC confirmed that successful purification of compound **6-4** was achieved (figure 6-2).

<sup>1</sup>H NMR, elemental analysis (EA), differential scanning calorimeter (DSC) and X-ray diffraction (XRD) were performed to make sure that the desired product was isolated. In addition, the spectrum showed the peaks of the aromatic group (target) with the expected chemical shifts as shown in Fig 6-2. The liquid crystalline phase behaviour of compound **6-4** was investigated by OPM, where a SmA phase at 135.3°C was identified as shown in Fig 6-3 (a). Increasing temperature the material was transformed to a

nematic phase at 142.8°C as shown in Fig 6-3 (b). Increasing the temperature to 220 °C the nematic phase turned to an isotropic liquid. However, cooling the isotropic sample showed the formation of a nematic phase at 142.8 °C and the formation of a SmA phase at 135.8°C (Figure 6-3 c).

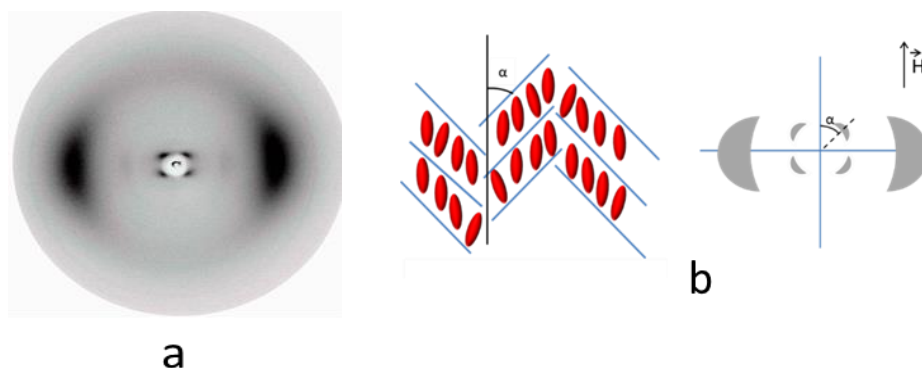


**Figure 6-2:** Scheme showing the chemical shifts in an  $^1\text{H}$  NMR spectrum.

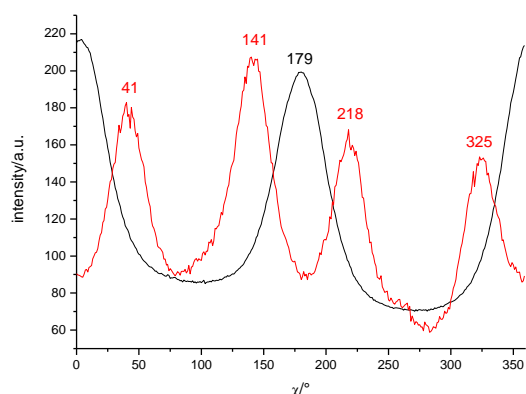


**Figure 6-3:** Different textures of compound **6-4** (A, B heating) (C, D cooling) with magnification of 100x (OPM).

X-ray data were collected at cooling in the range from 190°C to 40 °C every 5°C for compound **6-4**. Unfortunately data for the isotropic state could not be collected at high isotropization, as this high temperature is beyond the operating temperature of the oven for the diffractometer. It is noted that the sample was aligned with a magnet (0.5 T) in the vertical direction. Fig 6-4 a shows a typical diffractogram collected for the nematic phase at 155 °C. Fig 6-4 b is a schematic representation of XRD patterns and molecular arrangements. The diffractogram is characterized by strong arc like wide angle equatorial reflections and four reflections in the small angle region.



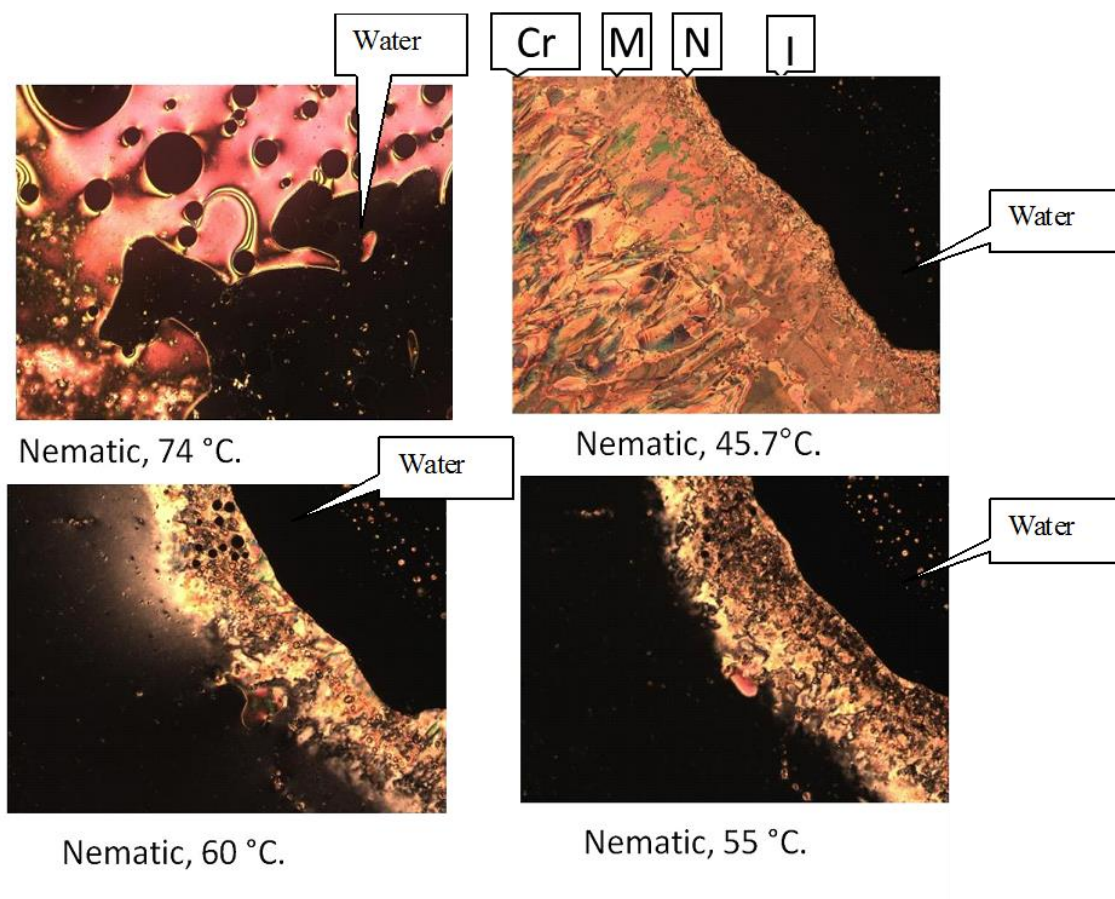
**Figure 6-4 :** a) X-ray diffractograms at 155 °C for compound **6-4**, in the nematic phase, b) NcybC phase aligned in a magnetic field.



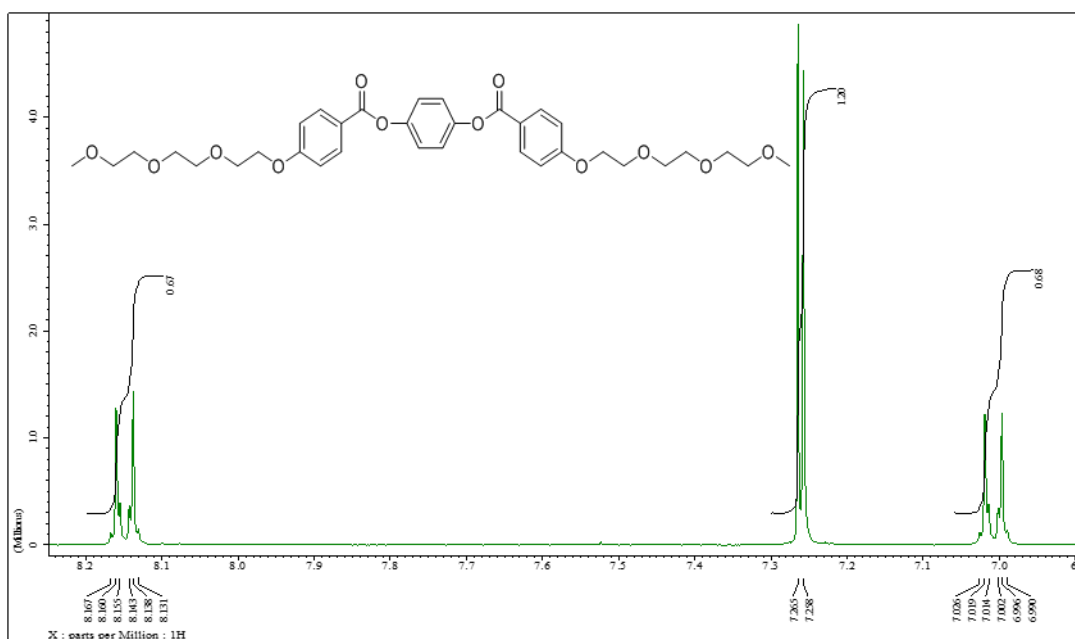
**Figure 6-5** : Red line:  $\chi$  scan at  $2\theta$  values 2-4°; black line 15-25°  $2\theta$  without division of the scattering in the isotropic phase.

Fig 6-5 shows a  $\chi$  scan of the wide angle region and small angle region. The black line shows a maximum of 179° close to the value of 180° for a full equatorial maximum. The red line is the  $\chi$  scan for the small angle region.

The results obtained for compound **6-5** indicate that it has quite different properties. When compared to **6-4** mesogen, compound **6-5** appears to be water soluble and more solid-like (figure 6-6). Thus low transition temperature and a relatively small nematic range from 48 °C to 78 °C was achieved. The material, containing a hydroquinone core, is suitable for further investigation due to the observed liquid crystal range (clearing point) being lower than the boiling point of water. However, the properties of these liquid crystals are still not fully understood because of the amount of water contained. The spectra peak for hydroquinone appears in the aromatic region at  $\delta=7.22$ . The purity of the final mesogen was checked by  $^1\text{H}$  NMR (figure 6-7), elemental analysis (EA) and the liquid crystal properties were investigated by optical polarised microscopy (OPM), differential scanning calorimeter (DSC) (figure 6-8), Mass Spectrometry and x-ray diffraction (XRD).



**Figure 6-6 :** Textures of compound 6-5 (water contact) with magnification of 100x (OPM).



**Figure 6-7:** Scheme shows the absence of hydroquinone in the chemical shifts in an <sup>1</sup>H NMR spectrum.



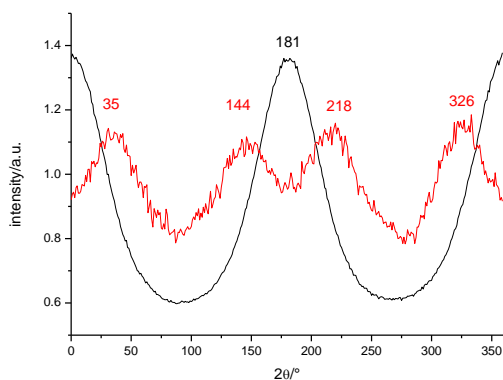


**Figure 6-9:** Red line:  $\chi$  scan at  $2\theta$  values  $2-5^\circ$ ; black line  $15-25^\circ$   $2\theta$  without division of the scattering in the isotropic phase.

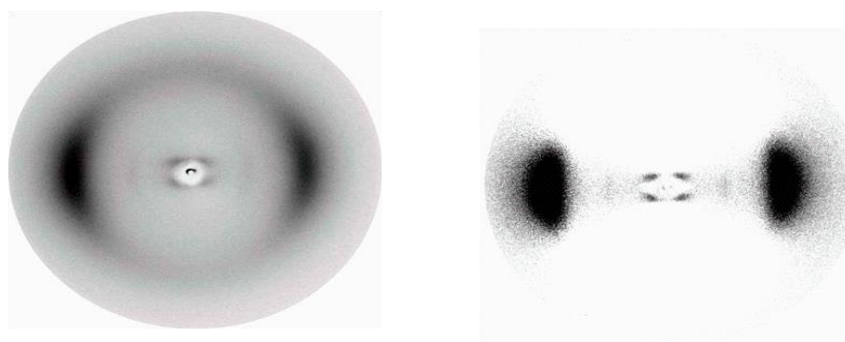
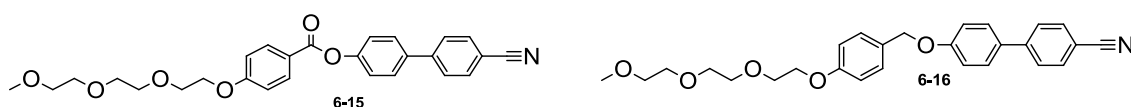


**Figure 6-10:** X-ray diffractograms at  $60^\circ\text{C}$  for compound 5, in the nematic phase.

From the maxima of the scattering in the small angle region the tilt angle  $\beta$  of the molecules in the cybotactic cluster can be estimated according to the following equation:  $\beta = (144^\circ - 35^\circ)/2 = 54.5^\circ$  or  $\beta = (326^\circ - 218^\circ)/2 = 54^\circ$ . These are very similar values, the XRD (figure 6-10) shows a nematic phase with a cybotactic cluster of the SmC-type and a tilt angle of about  $54^\circ$  is formed.



The structure of compounds **6-15** and **6-16** (experimental part) were confirmed by  $^1\text{H}$  NMR, elemental analysis (EA), results from Optical Polarizing Microscope (OPM) (figure 6-11), differential scanning calorimetry (DSC), mass Spectrometry as shown in figures 6-13 and 6-14 respectively. Compounds **6-15** and **6-16** have a liquid crystal range between Cr (64 N 130) 216 Iso, Cr 76 N 100 Iso respectively. For compound **16** the crystallisation temperature was reduced by  $30^\circ\text{C}$ .

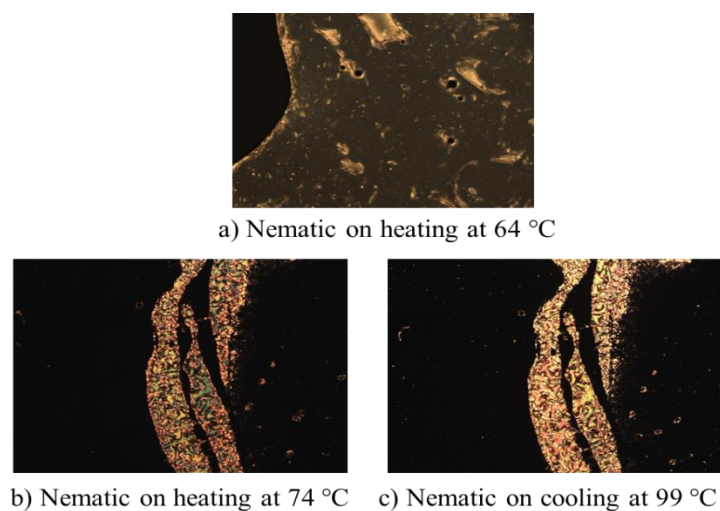


**Figure 6-11:** Textures of compounds **6-15** (a) and **6-16** (b, c) with magnification of 100x (OPM).

The chemical structure of compound **6-17** was confirmed by  $H^1$ NMR spectroscopy and the properties by DSC. The change of the ester linkages between the aromatic rings to ether groups resulted in a depression in the transition temperature of around 70 °C. It was noted that compound **6-17** decomposes partly during the purification process when using a silica gel filled column and the amount of one of the starting materials (hydroquinone) was increased. Moreover, the separation was difficult and time consuming. The reason for that could be that the stationary material is slightly acidic being responsible the degradation reaction. The DSC of the material showed that a phase transition at 6 °C occurs on cooling and broad isotropization occurs at about 20 °C (figure 6-12). However, it was not possible to obtain microscopy pictures due to the transition temperature being lower than room temperature (no birefringence detected).

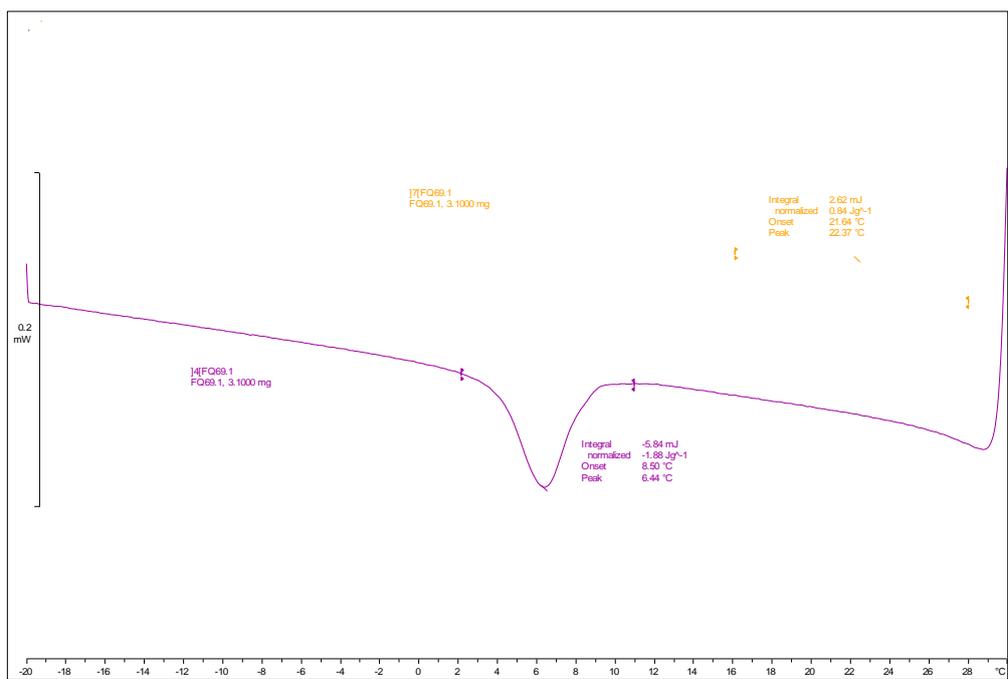


**Figure 6-12** : DSC trace of compound **6-17**.

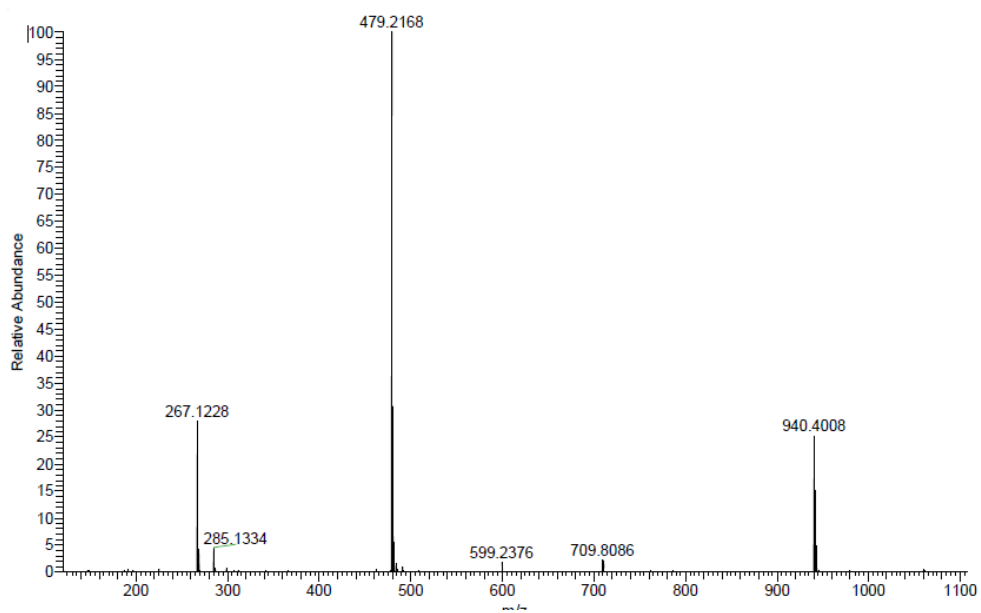


**Figure 6-13:** These spectrum of compound **6-15**; the main peak 479.2168 represents the  $[M+ H_2O]$ .

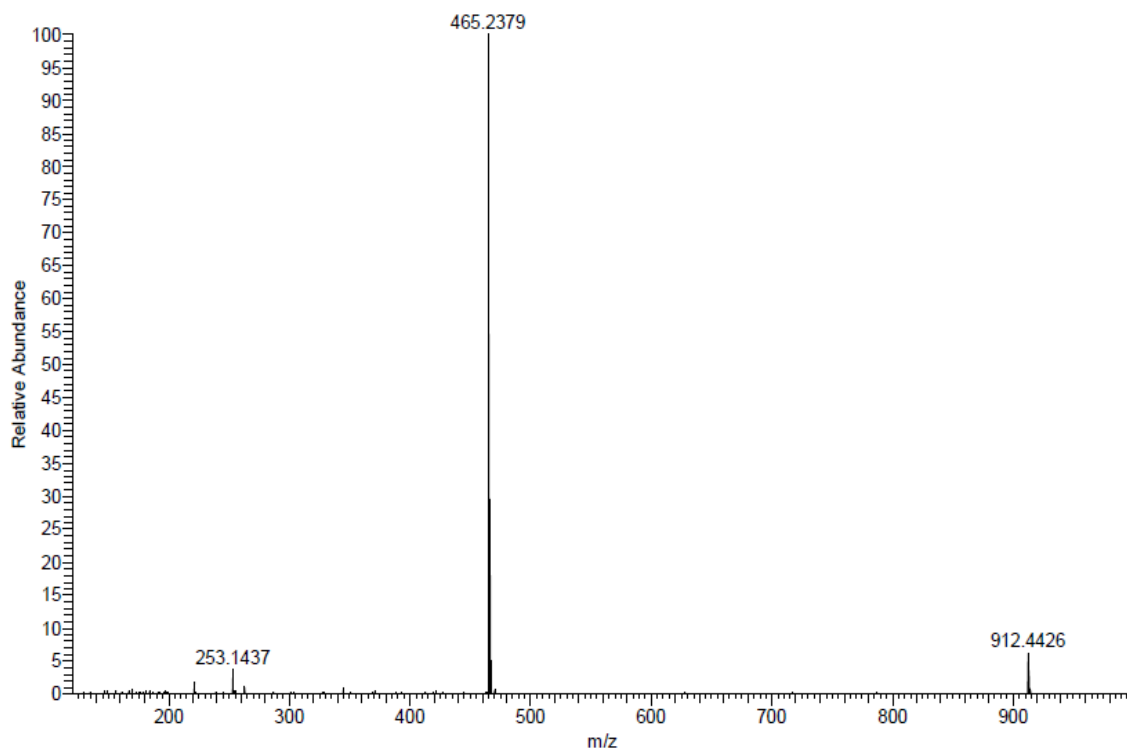


**Figure 6-14:** These spectrum of compound **6-16** the main peak 465.2378 which represent the  $[M+ H_2O]$ .

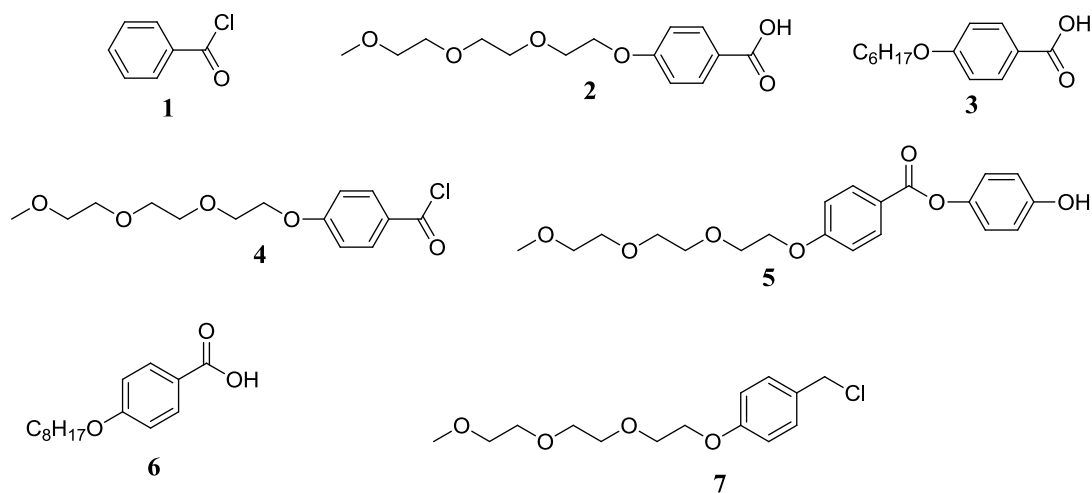
### 6.1.1 Challenge in the synthesis of rod shaped LC difunctionalized ethyleneoxy chains

One of the common problems faced was a Steglich esterification which did not work for the target compound. In addition, the amount of hydroquinone needed to be 2.5 mol less than the acid in order to get the disubstituted products. The syntheses of compounds **6-15** and **6-16** confirmed that hydroquinone is a difficult compound to remove from the target material. Table 2 summarised the reactions that were tried in order to obtain the target.

The general structure of the materials is:



The acids were used in order to prepare the product.



The targets.

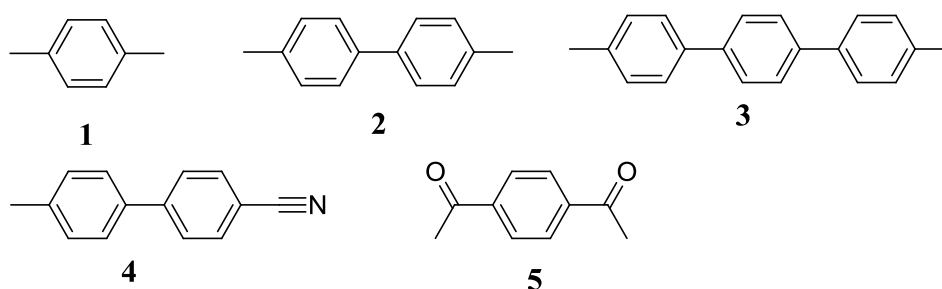


Table 2: The investigation of target 1

Entry	Acid	Carbodiimide	Time /hours	Target	Solvent	Product
i	2	DCC	18	2	THF	Monomer <b>5</b> , 45%
ii	2	DIC	18	2	THF	32%
iii	2	DCC/DIC	18	1	THF	Monomer <b>5</b> , 30% - 40%
iv	3	DIC	18	1	THF	Monomer <b>5</b> , 35%
v	4	Pyridine	18	1	Toluene	unidentified
vi	1	H <sub>2</sub> SO <sub>4</sub>	12	1	Toluene	unidentified
vii	1	Et <sub>3</sub> N	18	1	THF	20%
viii	4	Et <sub>3</sub> N	18	1	THF	Monomer <b>5</b> , 30%

The starting material (hydroquinone) might have degraded and this could explain some of the variation of the product. Therefore a new starting materials was ordered. However, the reaction did not show any improvement. Different acids were tried in order to find where the obstacle was. The same conditions as the Steglich esterification were applied. Table 2 (entry **vii**) shows that the desired product was formed, but in the same conditions other acids did not work.

The reaction discussed is very widely used and problems should not be expected. A number of avenues were explored to understand why the double esterification reaction did not proceed as anticipated. The starting materials (compound **6-9**) were resynthesized and the esterification reaction carried out using DCC, DIC, pyridine, Sulfuric acid triethylamine. As all the conventional methods were tried in order to yield the targeted product, an NMR spectrum was collected before purification. It was found that all peaks for the starting materials and additional peaks, in line with product formation were present. However, following column chromatography the peaks relating to the anticipated product were no longer detectable, indicating that deformation of the product, likely through cleavage of the ester groups had occurred.

Finally, an NMR spectrum of the products of an esterification was collected. Mass spectroscopy shows that the desired product was formed (figure 6-15). The NMR spectrum shown in Fig 6-16 shows clearly a singlet at  $\delta = 7.35$  which is the value expected for the central aromatic system. This value is different to that of the starting material hydroquinone where a singlet occurs at  $\delta = 6.69$  ppm (Fig 6-17) and is also different to that of the monoreacted material.

However, following purification by column chromatography the target material could not be detected. The monoreacted product (Fig 6-18) was however found, which was not present in the initial reaction mixture. This suggests that the target material degrades during the purification process using a silica gel filled column.

A reason for that could be that the stationary material is slightly acidic leading to an ester cleavage. A small amount of triethylamine was added to the mobile phase (eluent) in order to ensure that the pH of the eluent is slightly basic.

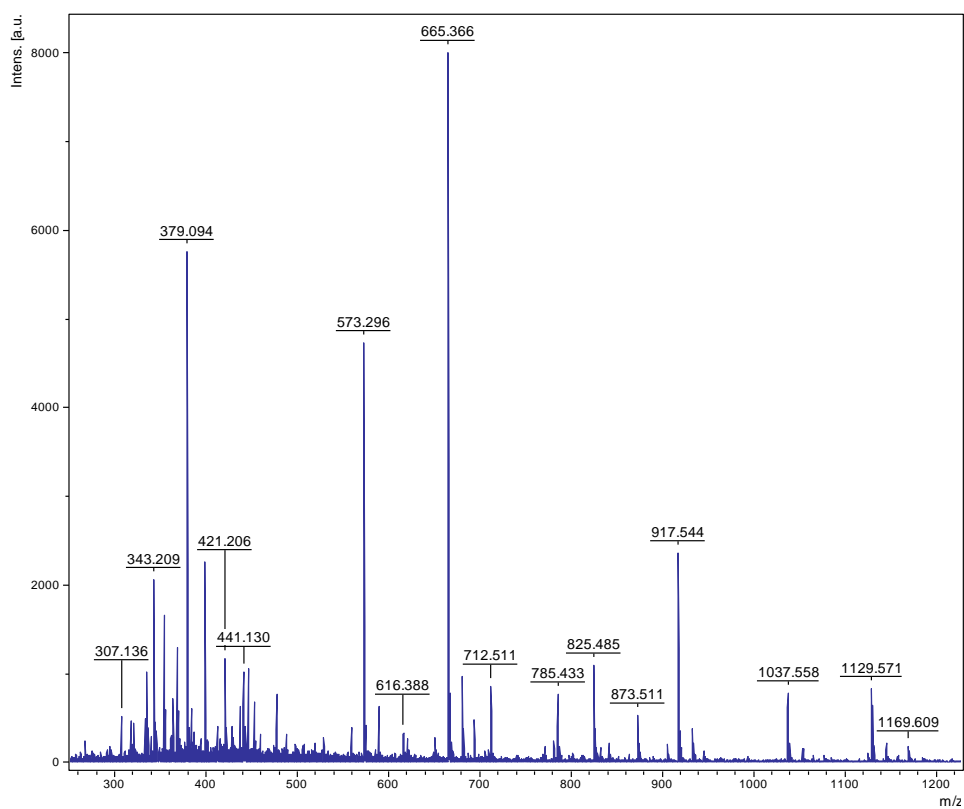


Figure 6-15: The main peak 665.66 which represent the  $[M+ Na]^+$

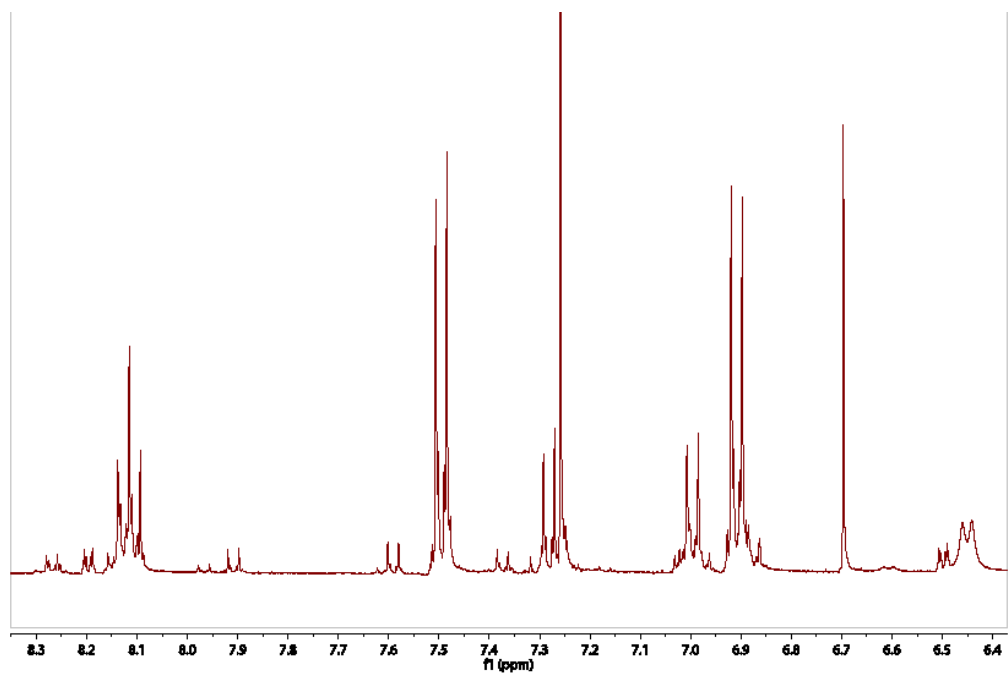
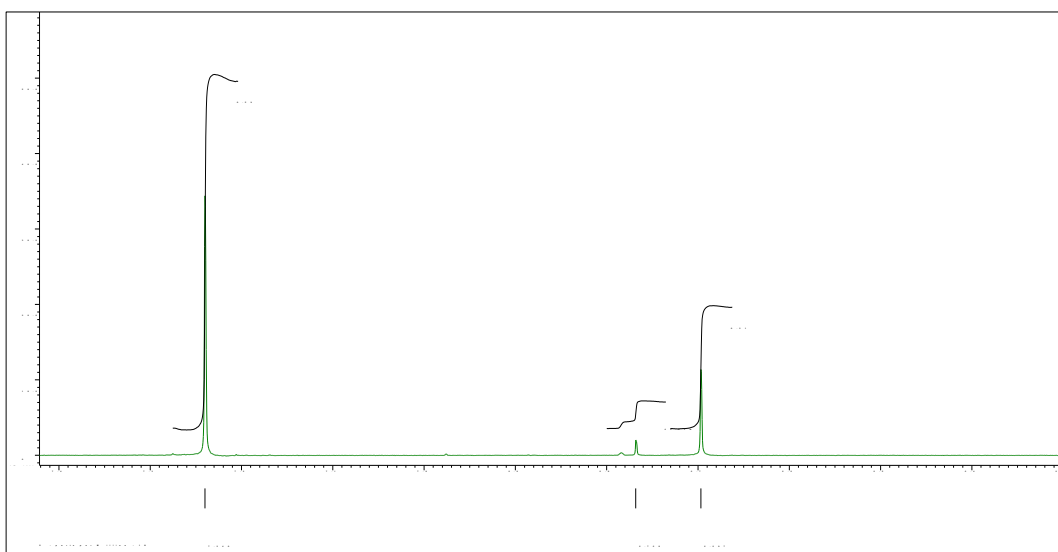
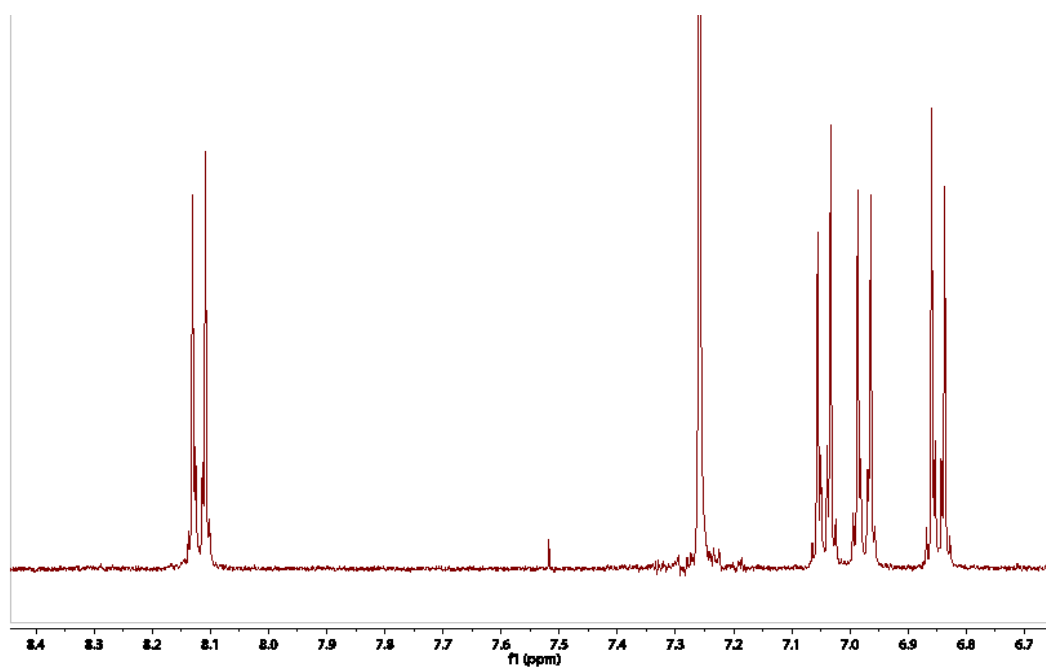


Figure 6-16: The spectrum for the crude product of compound 6-5.



**Figure 6-17:** The spectrum for hydroquinone.



**Figure 6-18:**  $^1\text{H}$  NMR spectrum for the monoreacted product of compound 6-5.

### 6.1.2 Problems in the synthesis of target 3

The first step to get the target was preparing the boronic acid which is the starting point of the synthesis. The preparation of 1-bromo-4-methoxybenzene acid was from 4-bromophenol in the presence of methyl iodide, butanone and potassium carbonate. A Grignard reaction was used in order to obtain 4-methoxyphenyl boronic. The result of the synthesis of target 3 the expected chemical shifts. Table 3 summarizes the experiments used to obtain the target 3.

Starting materials and acid were used.

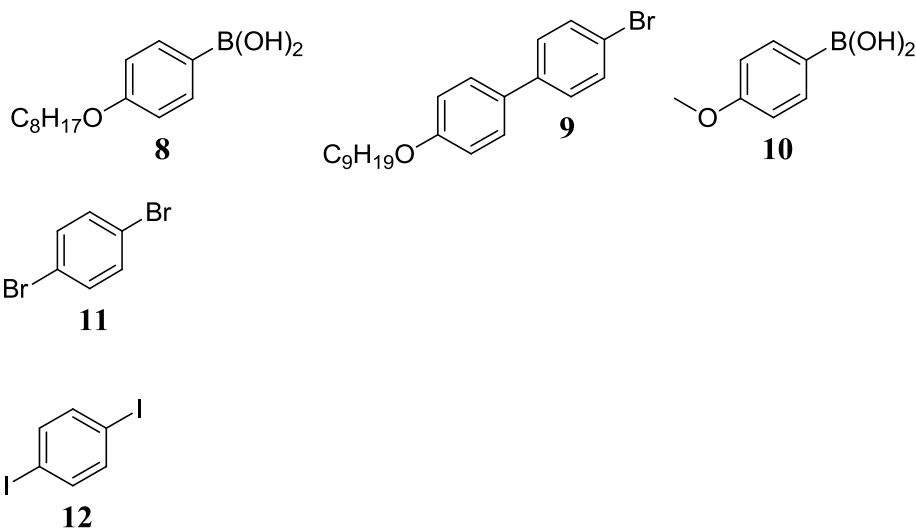


Table 3: The investigation of target 3

Entry	Starting Materials	solvent	acid	Time /h	conditions	Product
i	12	DMF	10	72	DPPB, CsF, Pd(OAc) <sub>2</sub>	unidentified
ii	11	Et <sub>2</sub> O	10	18	DPPF PdCl <sub>2</sub>	unidentified
iii	11	Toluene	10	72	CsF, PdCl <sub>2</sub>	unidentified
iv	9	THF	8	24	Pd(PPh <sub>3</sub> ) <sub>4</sub>	unidentified

## 6.2 Summary

Overall, synthesizing all intermediate compounds was straightforward. The preparation of compounds **6-4** and **6-5** in high purity was quite time consuming. This is due to the difficulty in separation of the target material (disubstituted) from the starting materials.

Moreover the product formed in the reaction has quite similar  $R_f$  values in most solvents, thus adduct and target material are quite difficult to separate. Thus an increase in yield and an improvement in the purification method is needed to improve and to simplify this procedure.

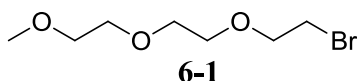
One of the aims for the future is to develop and optimize the synthetic methodology, addressing parameters such as a change in solvent, catalysts and the reaction conditions.

The synthetic route and the purification of compounds **6-15** and **6-16** (mesogen) needs to be improved to increase the reaction yield. Therefore, it is important to purify the final step to make this reaction more effective and efficient. A purification technique also needs to be developed in order to isolate the final product much easier more efficient despite having a very simple method to synthesize compounds **6-15** and **6-16** (mesogen), with methoxy side chain and all other intermediate compounds, a new method is required to increase the yield of mesogens with methoxy lateral side chain synthesis. A number of this type of mesogens with methoxy lateral side chain need to be tested and synthesized to establish a full characterization.

The most interesting of the investigated systems is compound **6-5**, which shows a nematic phase above room temperature, as confirmed by OPM and DSC experiments. XRD studies of magnetically aligned samples show that this nematic phase is of the NcybC type, with an apparent tilt of  $54^\circ$ . This indicates that the next neighbours in the clusters are strongly offset from each other. This material with two ethylenoxy chains at the termini of the mesogenic group form in water at temperatures above  $45.7^\circ\text{C}$  a nematic phase.

## 6.3 Experimental procedures

### 6.3.1 Synthesis of 1-bromo-2-(2-(2-methoxyethoxy)ethoxy)ethane<sup>168</sup>

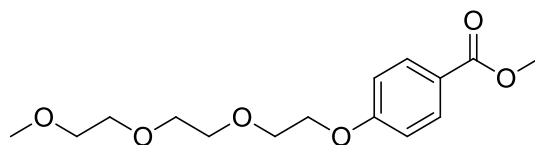


A dry, nitrogen-purged flask was charged with diethyl ether (100 ml) and tris (ethylene glycol) monomethyl ether (8.0 ml, 0.05 mol). The mixture was cooled to 0 °C and phosphorous tribromide (2.4 ml, 0.025 mol) was added dropwise to the solution. After the addition was complete, the reaction was allowed to stir at 0 °C for 15 min. Methanol (7.0 ml) was then added to the reaction mixture, the reaction mixture was allowed to warm at room temperature and stirred for 30 min. The reaction mixture was washed with water (10 ml) and the organic layer was washed with 5% sodium hydrogen carbonate (1x) and saturated sodium chloride (1x). The combined aqueous layer was extracted with ethyl acetate (4x) and the combined organic layer was dried over sodium sulphate. The remaining solvent was removed initially under reduced pressure then using an oil pump vacuum, which yielded a light yellow oily product (6.67 g).

**Yield:** 61.2%

**<sup>1</sup>H NMR, 400 MHz (CDCl<sub>3</sub>):**  $\delta$  [ppm] = 3.37 (s, 3 H), 3.55-3.76 (m, 10 H), 3.89 (t, 2 H).

### 6.3.2 Synthesis of methyl 4-(2-(2-(2-methoxyethoxy) ethoxy) ethoxy) benzoate



**6-2**

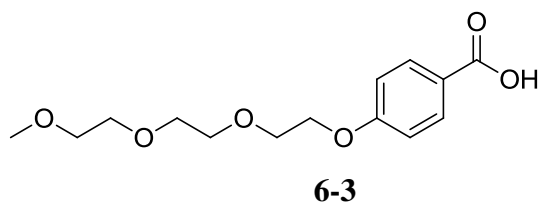
A mixture of methyl 4-hydroxy benzoate (2.73 g, 0.018 mol),  $K_2CO_3$  (13.8 g, 0.1 mol) and powdered 4 Å molecular sieves (10 g) in dry butanone (20 ml) was stirred over a 4-7 hour period. A solution of compound **6-1** (4.0 g) was added and the reaction mixture was heated under reflux at 120°C for an additional 18 hours until the reaction was complete (TLC). After filtration of the reaction mixture, the solvent butanone was distilled off and the residue was recrystallized from dichloromethane (10 ml) and ethyl acetate (10 ml) to yield white crystals (2.51 g).

**Mp:** 71 °C

**Yield:** 48%

**$^1H$  NMR, 400 MHz ( $CDCl_3$ ):**  $\delta$  [ppm] = 3.37 (s, 3 H), 3.55-3.76 (m, 8 H), 3.86 (s, 3H), 3.89 (t, 2 H), 4.14 (t, 2H), 6.89 (d, 2H), 7.94 (d, 2H).

### 6.3.3 Synthesis of 4-(2-(2-(2-methoxyethoxy)ethoxy)ethoxy)benzoic acid<sup>169</sup>



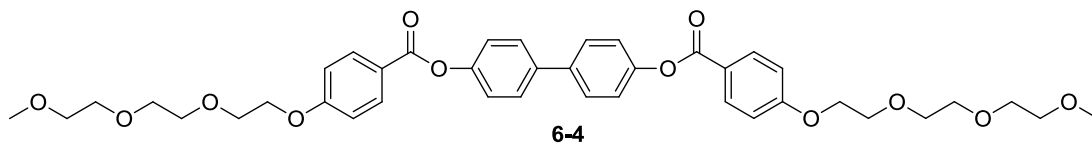
Compound **6-2** (47.66 g, 0.22 mol) was dissolved in THF (160 ml) and methanol (891 ml). A solution of KOH (42.4 g, 0.22 mol) in water (128 ml) was added. After stirring for 2 days at room temperature. The reaction was completed by heating at reflux for 2 h, the solvents were distilled off and ice/water (450 ml) added. After acidification with concentrated HCl (70 ml) the mixture was extracted with CH<sub>2</sub>Cl<sub>2</sub> (6 x 100 ml). After drying the CH<sub>2</sub>Cl<sub>2</sub> phase with MgSO<sub>4</sub>, the solvent was distilled off. Recrystallization from dichloromethane and ethyl acetate yielded off white crystals (4.0 g).

**Mp:** 71 °C

**Yield:** 75.5%

**<sup>1</sup>H NMR, 400 MHz (CDCl<sub>3</sub>):** δ [ppm] = 3.37 (s, 3 H), 3.55-3.76 (m, 8 H), 3.89 (t, 2 H), 4.14 (t, 2H), 6.89 (d, 2H), 8.00 (d, 2H).

### 6.3.4 Synthesis of [1,1'-biphenyl]-4,4'-diyl bis(4-(2-(2-(2-methoxyethoxy) ethoxy) ethoxy) benzoate).



Compound **6-3** (1.8 g) (7.0 mmol), 4, 4- dihydroxybiphenyl (0.4 g) (2.0 mmol) and 4-Dimethylaminopyridine (DMAP) (0.9 g) (7.0 mmol) was dissolved in anhydrous THF (40 ml) and diisopropylcarbodiimide (DIC) (1.5 g) (7.0 mmol) was added. After stirring for 18 h at room temperature, the reaction mixture was filtered and washed with CH<sub>2</sub>Cl<sub>2</sub>. After removal of the solvent, compound **6-4** was purified by column chromatography (pure ethyl acetate). Repeating the column chromatography with ethyl acetate and hexane (1:1) yielded a white product (1.38g).

**Mp:** 110 °C

**Yield:** 32 %

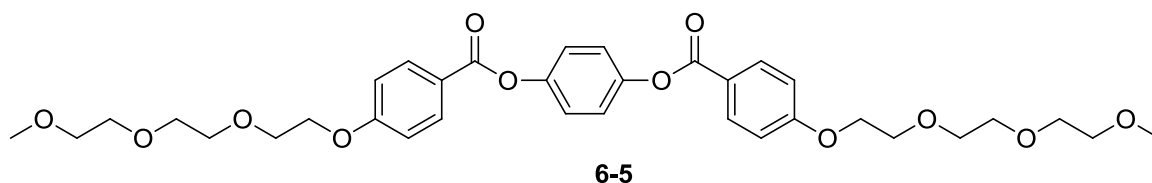
**<sup>1</sup>H NMR, 400 MHz (CDCl<sub>3</sub>):** δ [ppm] = 3.37 (s, 6 H), 3.55-3.76 (m, 16 H), 3.89 (t, 4 H), 4.22 (t, 4H), 6.99 (d, 4H), 7.27 (d, 4H), 7.61 (d, 4H), 8.14 (d, 4H).

**<sup>13</sup>C NMR, 100 MHz (CDCl<sub>3</sub>):** 167.7, 167.7, 165.2, 165.2, 148.3, 148.3, 137.6, 137.6, 130.9, 130.9, 130.9, 130.9, 129.5, 129.5, 129.5, 129.5, 122.1, 122.1, 122.1, 122.1, 121.8, 121.8, 71.6, 71.6, 70.4, 70.4, 70.4, 70.4, 70.1, 70.1, 69.3, 69.3, 59.3, 59.3.

**Experimental:** C, 65.86%, H: 6.45%

**Calculated:** C, 66.84; H, 6.45% (the product + 1 molecule of H<sub>2</sub>O)

### 6.3.5 Synthesis of 1,4-phenylene bis(4-(2-(2-(2-methoxyethoxy)ethoxy)ethoxy)benzoate).



Compound **6-3** (1.5 g) (5.0 mmol) was dissolved in dry toluene (20 ml) under nitrogen; thionyl chloride (0.6 ml, 5.0 mol) was added and the solution heated to 80 °C for 2 h, the reaction being completed after heating for 45 min at reflux. The thionyl chloride and toluene were distilled off under nitrogen atmosphere and the remaining product was dried further under vacuum. Triethylamine (0.7ml, 5.0 mmol) and a small amount of THF (5.0 ml) were added. A solution of hydroquinone (0.22 g) (2.0 mmol) in anhydrous THF (10 ml) was added to the residue dropwise. This reaction mixture was kept stirring at 80 °C for 18 h.

The reaction mixture was filtered and washed with CH<sub>2</sub>Cl<sub>2</sub>. After removal of the solvent, compound **6-5** was purified by column chromatography (hexane, acetone and diethyl ether) (2:1:1) and triethylamine (1.0 ml) was added to the solvent mixture in order to make it more basic. Recrystallization from ethanol yielded a white product (0.76 g).

**Mp:** 39 °C

**Yield:** 62 %

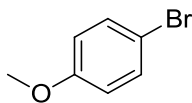
**<sup>1</sup>H NMR, 400 MHz (CDCl<sub>3</sub>):** δ [ppm] = 3.37 (s, 6 H), 3.55-3.76 (m, 16 H), 3.89 (t, 4 H), 4.22 (t, 4H), 7.10 (d, 4H), 7.28 (s, 4H), 8.14 (d, 4H).

**<sup>13</sup>C NMR, 100 MHz (CDCl<sub>3</sub>):** 167.6, 167.6, 165.2, 165.2, 146.2, 146.2, 130.9, 130.9, 130.9, 130.9, 122.0, 122.0, 122.0, 122.0, 121.8, 121.8, 114.3, 114.3, 114.3, 114.3, 71.6, 71.6, 70.4, 70.4, 70.4, 70.4, 70.1, 70.1, 69.3, 69.3, 59.3, 59.3.

**Experimental:** C: 63.54 %, H: 6.59 %.

**Calculated:** C: 63.36 %, H: 6.72 %.

### 6.3.6 Synthesis of 1-bromo-4-methoxybenzene.<sup>170</sup>



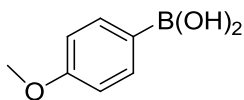
**6-6**

To a solution of 4-bromophenol (5.0 g, 0.02 mol) in butanone (70 ml, 0.02 mol) was added  $K_2CO_3$  (2.8 g, 0.02 mol) and methyl iodide (2.5 ml, 0.002 mol). The mixture was heated to reflux for 48 h. The reaction was followed by TLC. The mixture was filtered, washed with acetone and the solvent removed under reduced pressure. The product was dissolved in dichloromethane (150 ml) and the organic layer washed with water (75 ml), brine (75 ml) and dried over  $Na_2SO_4$ , which yielded a light red product (4.19 g).

**Yield:** 80%

**$^1H$  NMR, 400 MHz ( $CDCl_3$ ):**  $\delta$  [ppm] = 3.79 (s, 3H), 6.96 (d, 2H), 7.45 (d, 2H).

### 6.3.7 Synthesis of (4-methoxyphenyl) boronic acid.<sup>171</sup>



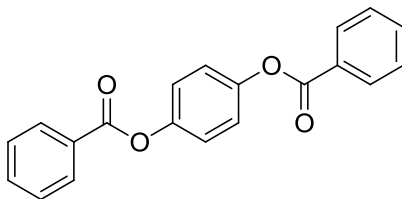
#### 6.1

To dry diethylether (60 ml) magnesium turnings (0.4 g, 0.017 mol) were added, compound **6-6** (4.0 g, 0.015 mol) was added dropwise at low temperature. After addition the reaction mixture was heated to reflux for 2 h. This yielded a white product (1.99 g).

**Yield:** 60%

**<sup>1</sup>H NMR, 400 MHz (CDCl<sub>3</sub>):**  $\delta$  [ppm] = 3.80 (s, 3H), 6.97 (d, 2H), 7.65 (d, 2H).

### 6.3.8 Synthesis of 1, 4-phenylene dibenzoate<sup>172</sup>



**7-7**

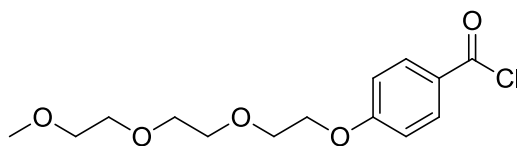
Benzoyl chloride (1.6 g, 0.01 mol) and triethylamine (1.0 g, 0.01 mol) (1.4 ml) were dissolved in a small amount of THF (1.0 ml). A solution of hydroquinone (0.5 g, 4.5 mmol) in anhydrous THF (10 ml) was added to the residue. This reaction mixture was kept stirring at room temperature for 18 h. Water (30 ml) and dichloromethane (30 ml) was then added; the phases were separated and the aqueous layer was washed with CH<sub>2</sub>Cl<sub>2</sub> (3 x 25 ml). The combined organic layers were dried over MgSO<sub>4</sub> and the solvents distilled off. Recrystallization from dichloromethane and methanol yielded a white product (0.41 g).

**Mp:** 196-198 °C

**Yield:** 13 %

**<sup>1</sup>H NMR, 400 MHz (CDCl<sub>3</sub>):**  $\delta$  [ppm] = 7.18 (s, 4H), 7.42 (dd, 4H), 7.53 (tt, 2H), 8.12 (dd, 4H).

### 6.3.9 Synthesis of 4-(2-(2-(2-methoxyethoxy) ethoxy) ethoxy) benzoyl chloride



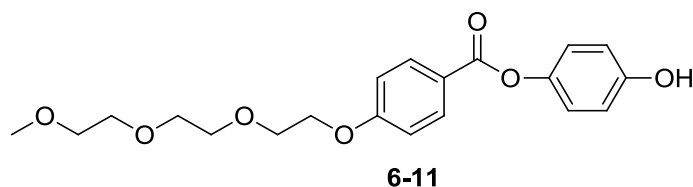
**6-8**

Compound **6-3** (1.8 g) (6.3 mmol) was dissolved in dry toluene (30 ml) under nitrogen; thionyl chloride (10 ml, 6.3 mol) was added and the solution heated to 80 °C for 2 h. The thionyl chloride and toluene were distilled off under nitrogen atmosphere and the remaining product was dried further under vacuum, which yielded a light red product (1.2 g) (a considerable amount of material was lost during the purification process).

**Yield:** 75 %

**<sup>1</sup>H NMR, 400 MHz (CDCl<sub>3</sub>):** δ [ppm] = 3.32 (s, 3 H), 3.54-3.76 (m, 8 H), 3.79 (t, 2 H), 4.31 (t, 2H), 7.17 (d, 2H), 8.03 (d, 2H).

### 6.3.10 Synthesis of 4-(2-(2-(2-methoxyethoxy)ethoxy)ethoxy)benzoate.



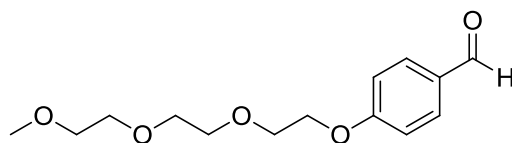
Compound **6-3** (2.46 g) (8.65 mmol) was dissolved in dry toluene (50 ml) under nitrogen; thionyl chloride (1.0 ml, 8.65 mol) was added and the solution heated to 80 °C for 2 h. The thionyl chloride and toluene were distilled off under nitrogen atmosphere and the remaining product was dried further under vacuum. Triethylamine (1.5 ml, 8.65 mmol) and a small amount of THF (10 ml) were added. A solution of hydroquinone (3.85 g) (35.0 mol) in anhydrous THF (10 ml) was added to the residue dropwise. This reaction mixture was kept stirring at 80 °C for 18 h. The reaction mixture was filtered and washed with CH<sub>2</sub>Cl<sub>2</sub>. After removal of the solvent, compound **11** was purified by column (pure ethyl acetate). Recrystallization from acetone and hexane yielded a white product (0.3 g).

**Mp:** 77 °C

**Yield:** 8 %

**<sup>1</sup>H NMR, 400 MHz (CDCl<sub>3</sub>):** δ [ppm] = 3.37 (s, 3 H), 3.55-3.76 (m, 8 H), 3.89 (t, 2 H), 4.14 (t, 2H), 7.13-7.31 (m, 6H), 8.00 (d, 2H).

### 6.3.11 Synthesis of 4-(2-(2-(2-methoxyethoxy) ethoxy) ethoxy) benzaldehyde.<sup>173</sup>



**6-12**

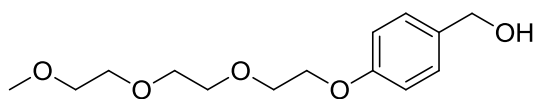
A mixture of 4-hydroxybenzaldehyde (7.0 g, 0.03 mol),  $K_2CO_3$  (20.0 g, 0.15 mol) and powdered 4 Å molecular sieves (10 g) in dry butanone (40 ml) was stirred over a 4-7 hours period. A solution of compound **6-1** (4.0 g) was added and the reaction mixture was heated under reflux at 120°C for an additional 18 hours until the reaction was complete (TLC). After filtration of the reaction mixture, the solvent butanone was distilled off and the residue was recrystallized from dichloromethane (10 ml) and ethyl acetate (10 ml) to yield white crystals (2.3 g).

**Mp:** 90 °C

**Yield:** 29 %

**$^1H$  NMR, 400 MHz ( $CDCl_3$ ):**  $\delta$  [ppm] = 3.37 (s, 3 H), 3.55-3.76 (m, 8 H), 3.89 (t, 2 H), 4.14 (t, 2H), 7.18 (d, 2H), 7.88 (d, 2H), 9.88 (s, 1H).

### 6.3.12 Synthesis of (4-(2-(2-(2-methoxyethoxy) ethoxy) ethoxy) phenyl) methanol.<sup>174</sup>



**6-13**

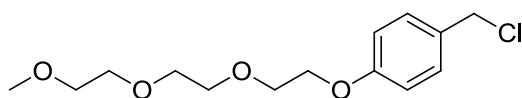
To a mixture of compound **6-12** (8.6 mmol, 2.3 g), anhydrous THF (25 ml), anhydrous methanol (10 ml) and sodium borohydride (0.09 mol, 3.0 g) were added. Sodium were added and the mixture was stirring at r.t for 10 h. The mixture was dissolved in DCM (20 ml) and hydrochloric acid (3 Mol). The organic layer was washed with water (3x) and saturated sodium chloride (1x), and dried over sodium sulphate. Compound **6-13** was purified by column chromatography (ethyl acetate and DCM) (1:10), which yielded a yellow crystal product (1.6 g).

**Mp:** 37-40 °C

**Yield:** 68 %

**<sup>1</sup>H NMR, 400 MHz (CDCl<sub>3</sub>):**  $\delta$  [ppm] = 3.37 (s, 3 H), 3.55-3.76 (m, 8 H), 3.89 (t, 2 H), 4.14 (t, 2H), 4.62 (s, 2H), 6.90 (d, 2H), 7.27 (d, 2H).

### 6.3.13 Synthesis of 1-(chloromethyl)-4-(2-(2-(2-methoxyethoxy)ethoxy)ethoxy) benzene.



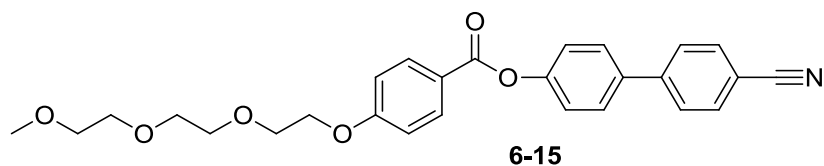
**6-14**

Compound **6-13** (0.35 g) (1.3 mmol) was dissolved in dry toluene (10 ml) under nitrogen; thionyl chloride (0.3 ml, 1.3 mol) was added and the solution heated to 80 °C for 2 h. The thionyl chloride and toluene were distilled off under nitrogen atmosphere and the remaining product was dried further under vacuum, which yielded a light red liquid product (0.2 g).

**Yield:** 65 %

**<sup>1</sup>H NMR, 400 MHz (CDCl<sub>3</sub>):**  $\delta$  [ppm] = 3.37 (s, 3 H), 3.55-3.76 (m, 8 H), 3.89 (t, 2 H), 4.14 (t, 2H), 4.62 (s, 2H), 6.90 (d, 2H), 7.27 (d, 2H).

### 6.3.14 Synthesis of 4'-cyano-[1,1'-biphenyl]-4-yl 4-(2-(2-(2-methoxyethoxy) ethoxy) ethoxy) benzoate



Compound **6-3** (0.26 g, 0.91 mmol), 4, 4'-hydroxy-4'-cyanobiphenyl (0.21 g, 1.10 mmol) and 4-Dimethylaminopyridine (DMAP) (0.01 g, 0.1 mmol) were dissolved in DCM (15 ml) and N,N-dicyclohexylcarbodiimide (DCC) (0.18 g) (0.91 mmol) was added. After stirring for 1 h at room temperature, the reaction mixture was filtered and washed with DCM. After removal of the solvent, compound **6-15** was purified by column chromatography (methanol 2% in DCM). The column chromatography was repeated with by ethyl acetate and hexane (1:1). Recrystallization from ethanol yielded a white crystalline product (0.1 g).

**Mp:** 49 °C

**Yield:** 20 %

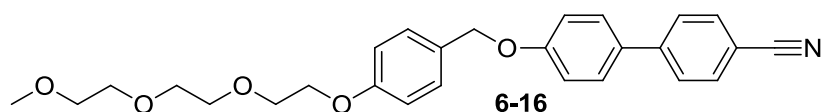
**<sup>1</sup>H NMR, 400 MHz (CDCl<sub>3</sub>):** δ [ppm] = 3.37 (s, 3 H), 3.55-3.76 (m, 8 H), 3.89 (t, 2 H), 4.14 (t, 2H), 7.00 (d, 2H), 7.32 (d, 2H), 7.65 (d, 2H), 7.70 (d, 2H), 7.73 (d, 2H), 8.17 (d, 2H).

**<sup>13</sup>C NMR, 100 MHz (CDCl<sub>3</sub>):** 167.8, 165.2, 148.3, 145.1, 137.6, 132.7, 132.7, 130.9, 130.9, 129.5, 129.5, 127.7, 127.7, 122.1, 122.1, 121.8, 118.6, 114.3, 114.3, 111.5, 71.6, 70.4, 70.4, 70.1, 69.3, 59.3.

**Experimental:** C: 70.27%, H: 5.90%, N: 3.30%.

**Calculated:** C, 69.99; H, 6.13%, N: 3.08%.

### 6.3.15 Synthesis of 4'-((4-(2-(2-(2-methoxyethoxy) ethoxy) ethoxy) benzyl) oxy)-[1,1'-biphenyl]-4-carbonitrile.



A mixture of compound **6-14** (0.36 g, 1.3 mmol),  $K_2CO_3$  (1.0 g, 6.5 mmol) and powdered 4 Å molecular sieves (10 g) in dry butanone (20 ml) was stirred over a 4-7 h. A solution of 4, 4'-hydroxy-4'-cyanobiphenyl (1.43 mmol, 0.3 g) in anhydrous butanone (5 ml) was added and the reaction mixture was heated under reflux at 120°C for an additional 18 hours until the reaction was complete (TLC). After filtration of the reaction mixture, the solvent was distilled off and the residue was purified in an efficient way. Compound **6-16** was dissolved in a mixture of ethyl acetate (5 ml) and hexane (5 ml) (1:1) and treated by ultrasonic cleaner bath for 30 seconds. The white solid product was filtered and yielded (0.17 g).

**Mp:** 62 °C

**Yield:** 25 %

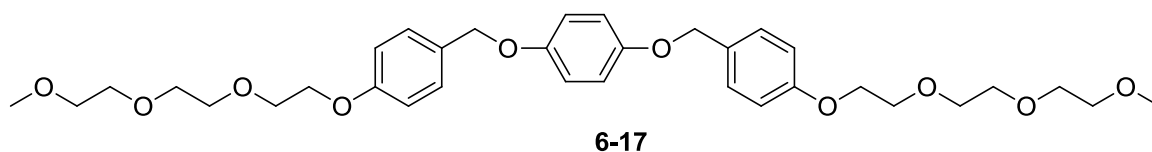
**$^1H$  NMR, 400 MHz ( $CDCl_3$ ):**  $\delta$  [ppm] = 3.37 (s, 3 H), 3.55-3.76 (m, 8 H), 3.89 (t, 2 H), 4.14 (t, 2H), 5.04 (s, 2H), 6.96 (d, 2H), 7.08 (d, 2H), 7.37 (d, 2H), 7.55 (d, 2H), 7.63 (d, 2H), 7.69 (d, 2H).

**$^{13}C$  NMR, 100 MHz ( $CDCl_3$ ):** 158.3, 157.9, 145.1, 133.1, 132.7, 132.7, 130.1, 130.1, 128.9, 128.9, 127.7, 127.7, 118.9, 114.8, 114.8, 114.6, 114.6, 71.6, 70.4, 70.4, 70.1, 69.3, 59.3.

**Experimental :** C: 72.46%, H: 6.53%, N: 3.13%.

**Calculated:** C: 72.07%, H: 6.80%, N: 2.91%.

### 6.3.16 Synthesis of 1,4-bis((4- (2- (2- (2-methoxyethoxy) ethoxy) ethoxy) benzyl) oxy) benzene.



A mixture of compound **6-14** (0.30 g, 1.1 mmol),  $K_2CO_3$  (1.5 g, 0.01 mol) and powdered 4 Å molecular sieves (5 g) in dry butanone (10 ml) was stirred over a 4-7 hours period. A solution of hydroquinone (0.06 g, 0.55 mmol) in anhydrous butanone (5 ml) was added and the reaction mixture was heated under reflux at 120 °C for an additional 18 h until the reaction was complete (TLC). After filtration of the reaction mixture, the solvent (butanone) was distilled off. Compound **6-17** was purified by column chromatography (THF: hexane) (1:1.5) and yielded a yellow oily product (0.17 g).

**Yield:** 48 %

**$^1H$  NMR, 400 MHz ( $CDCl_3$ ):**  $\delta$  [ppm] = 3.37 (s, 6 H), 3.55-3.76 (m, 16 H), 3.89 (t, 4 H), 4.22 (t, 4H), 4.56 (s, 4H), 6.71 (s, 4H), 6.89 (d, 4H), 7.30 (d, 4H).

**$^{13}C$  NMR, 100 MHz ( $CDCl_3$ ):** 158.3, 158.3, 154.0, 154.0, 128.9, 128.9, 128.9, 128.9, 128.3, 128.3, 115.3, 115.3, 115.3, 115.3, 114.6, 114.6, 114.6, 114.6, 71.6, 71.6, 70.8, 70.8, 70.4, 70.4, 70.4, 70.4, 70.1, 70.1, 69.3, 69.3, 59.3, 59.3.

## 7 Hemiphasmidics

A limited number of examples of calamitic mesogens are known consisting of benzoic acid aromatic esters (Gallic acid) with the terminal chains bearing three oligo-ethylenoxy groups in one side. These materials have not been reported and present new challenges in understanding its behaviour. Hemisphasmidic mesogen containing an alkane group attached on the end was designed and synthesised.

Compared to other mesogens which contain a single and/or double oligo-ethylenoxy groups the temperature expectation of nematic phase behaviour in this mesogen were dramatically dropped, low melting points and low transition between phases temperatures. The hemiphasmidic mesogen was designed to be attached to the pentamethyldisiloxane and/or tetramethyldisiloxane or AuNPs.

Compound **7-12** was one of the targets for the research conducted to improve techniques and synthetic procedures in order to obtain room temperature molecules which form LC phase behaviour with water and as thermotropic liquid crystals. However, there were challenges and problems regarding the synthetic procedures and characterisation, these issues will be discussed in this chapter. Two routes were followed in this work. The first one was in the preparation of compound **7-4** and the second one was in the preparation leading to these intermediates (compound **7-11**). The main challenges were low reaction yields in the reactions step, as purification resulted in loss of product. It was observed that the reactions could not be scaled up in order to obtain large quantities of the final mesogen. A simple and efficient purification technique was developed. This chapter is divided into two parts: the first part describes mainly the general procedures behind all experiment conditions carried out to synthesize the target mesogen and the second part focuses characterisations of target molecules with discussion of properties and comparison.

## 7.1 Synthesis discussion

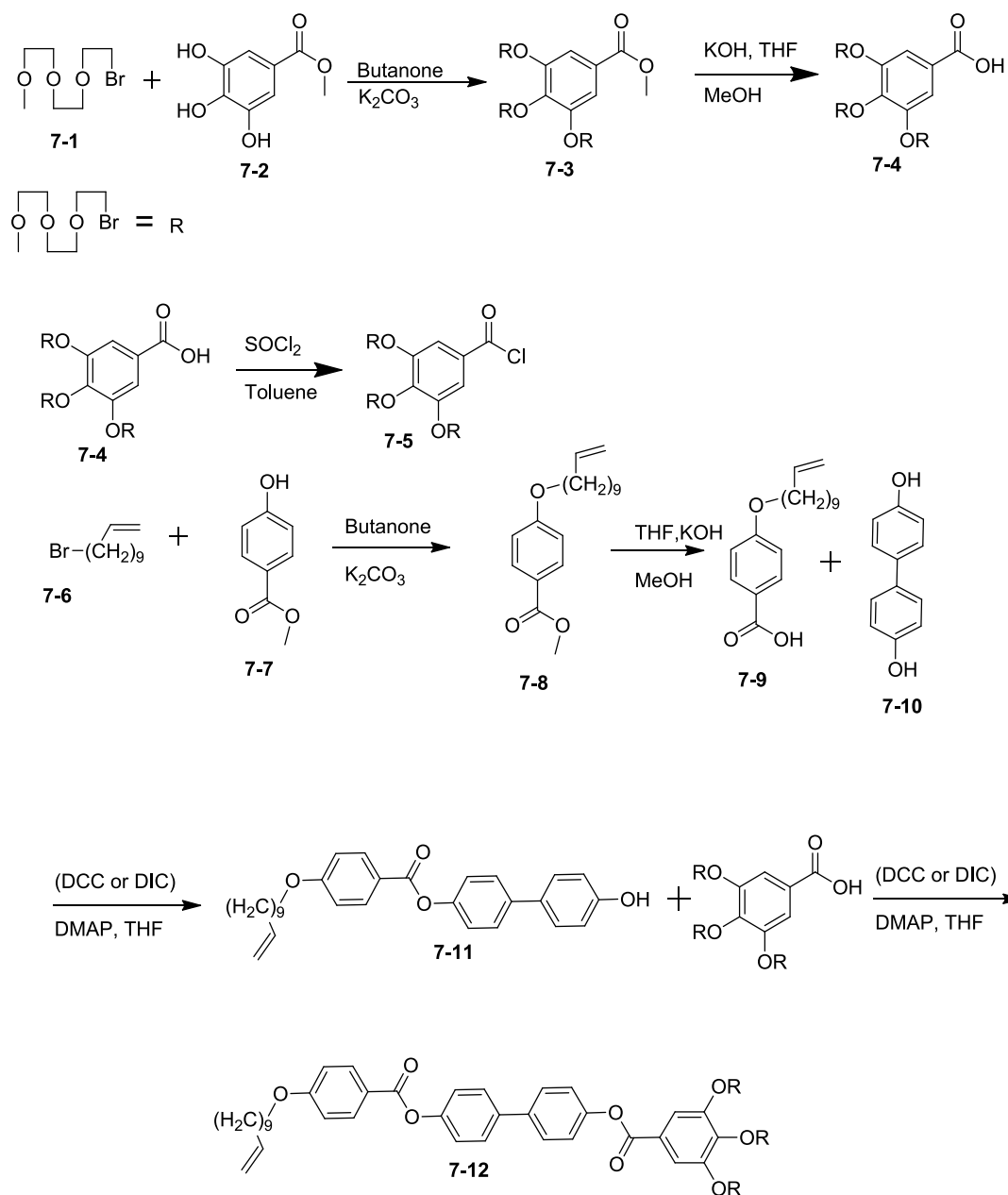


**Figure 7-1:** Scheme for the synthesis of compound **7-12**.

Figure 7-1 shows the classic synthesis method of the target mesogen with oligoethylenoxy groups (compound **7-12**). The first step involved a Williamson ether synthesis reaction of the methyl gallate. Excess of compound **7-1** was added in order to avoid a side product function. However, there was a small by product a partly reacted compound with two chains in 3 and 5 positions. Potassium iodide was used as a catalyst under nitrogen atmosphere and refluxed in dried butanone as a solvent

for 18 hours and  $K_2CO_3$  as a base. The etherification reaction was found to be better in terms of yield; it was found to give 67% yield of the etherified product.<sup>175</sup>

As etherification usually requires heat to reflux to obtain the target, in some cases by-products are formed and decrease the overall yield of the reaction. Moreover, one important challenge was the purification of the materials (compound **7-3**). Column chromatography was used twice and the product was washed with hexane. Perhaps this reduced the yield. Overall the reaction towards a reasonable yield went well, such as the reaction time, the process of reagents addition and the work-up in order to obtain the yield of around 70%.

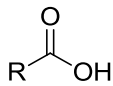
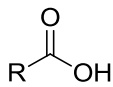
The hydrolysed precursors used to prepare the gallic acid derivatives were challenging to prepare when the methyl group was removed under basic conditions in water from the gallic acid derivatives (compound **7-3**), it was found that the isolation of the free acid (compound **7-4**) was problematic. This is associated with high solubility of compound **7-4** in water. Several approaches were taken. Three different solvents were used in high quantity (to extract and purify) in order to solve this problem. Also, in silica gel column methanol was used and the aqueous phase was subsequently removed. The main issue of acid chloride step was the sensitivity of compound **7-5** towards moisture, so the reaction was performed in dry condition and the yield was high (more than 90%). The synthetic routes for these reactions (etherification and hydrolysis) were involved in most of the desired compounds. These reactions could be improved further to achieve higher yields.

For the preparation of compound **7-11**, a different approach was taken. In order to identify what causes this low yield, the reaction progress was checked and followed by TLC. It was found that the reaction mixture contained significant amounts of disubstituted and starting materials (4, 4-dihydroxybiphenyl) and other by-products. From the previous study, it was noticed that 4, 4-dihydroxybiphenyl tends to form disubstituted rather than monosubstitution product (confirmed by TLC and NMR). All the reaction conditions were evaluated, one at a time and any possible problem was eliminated. This reaction was performed in  $CH_2Cl_2$ , but THF was used as solvent, with slightly lower yield when compared to DCM, even though the polarity of THF is 4.0 (polarity Index<sup>1</sup>) compared to 3.1 (polarity Index<sup>1</sup>) of DCM. Possibly because 4, 4-dihydroxybiphenyl is not soluble in DCM, this might be responsible for the reaction towards single replacement. Also, it was not easy to separate this

material (compound **7-11**) from 4, 4-dihydroxybiphenyl due to the similarity in molecular structure and polarity. New synthetic routes were attempted and the reaction development was followed by TLC. It was assumed that there might be a problem with the acid or with the solvents which were used (Table 7-1).

The reaction was performed with on acid chloride and toluene as a solvent. The reaction was left reacting overnight at 60 °C; the structure of the reaction products could not be identified. The reaction with DCM as a solvent was found to give the best yield, which was around 41%. However, the increasing temperature did not speed up the reactions in all synthetic paths were used. As it was found that the reaction could not be scaled up, a different approach was needed for the final target. It was decided that an alternative synthetic route that can resolve low yield problem was needed in order to move on within the project. This route led to an interesting mesogen which was attached to AuNPs and it will be discussed in the next chapter.

Table 7-1 : The investigation of compound **7-11** under different reaction conditions.

Entry	Acid	Time/hour	Cabodiimide	Solvent	Product
i		18	DCC/DIC	THF	Monomer 25% - 36%
ii		18	DCC/DIC	DCM	Monomer 37% - 41%
iii		18	Pyridine	Toluene	unidentified
iv		18	Et <sub>3</sub> N	Toluene	unidentified

For the preparation of mesogen **7-12**, the issue was that the product was formed in low yield. The reaction mixture was stirred for 18 h and filtered through a plug of Celite® and the filtered mixture further was washed twice with water. The gathered aqueous phases were extracted with diethyl ether five times in order to get the

remaining product from water. Especially as this material showed some solubility in water, the aqueous phases were checked by TLC. The organic layers were gathered and dried over  $\text{Mg}_2\text{SO}_4$ . Purification was carried out by column chromatography; hexane, THF and triethylamine were used. A number of solvents were explored (DCM\hexane), (ethanol/DCM), (ethyl acetate\hexane) and ethanol\THF) for recrystallization. A further complicated sequence of recrystallizations made it possible to purify the desired compound. A suitable, simple and a dry method was required to yield the final mesogens. The approach was esterification which is shown for the synthesis of compound **7-12** method **2**. However, the yield obtained was around 50%, which is similar to method **1**. The reaction mixture where left overnight in a dry atmosphere at 80 °C, washed with DCM and evaporated under the vacuum to obtain the crude product. The purification was carried out by column chromatography using DCM and a few drops of  $\text{Et}_3\text{N}$  as a solvent. A basic solvent such as  $\text{Et}_3\text{N}$  was added in order to prevent the cleavage of the ester bond. Finally, methanol was added to the column to wash down the product which yielded around 50% of product.



## 7.2.1 Liquid crystal and thermal properties

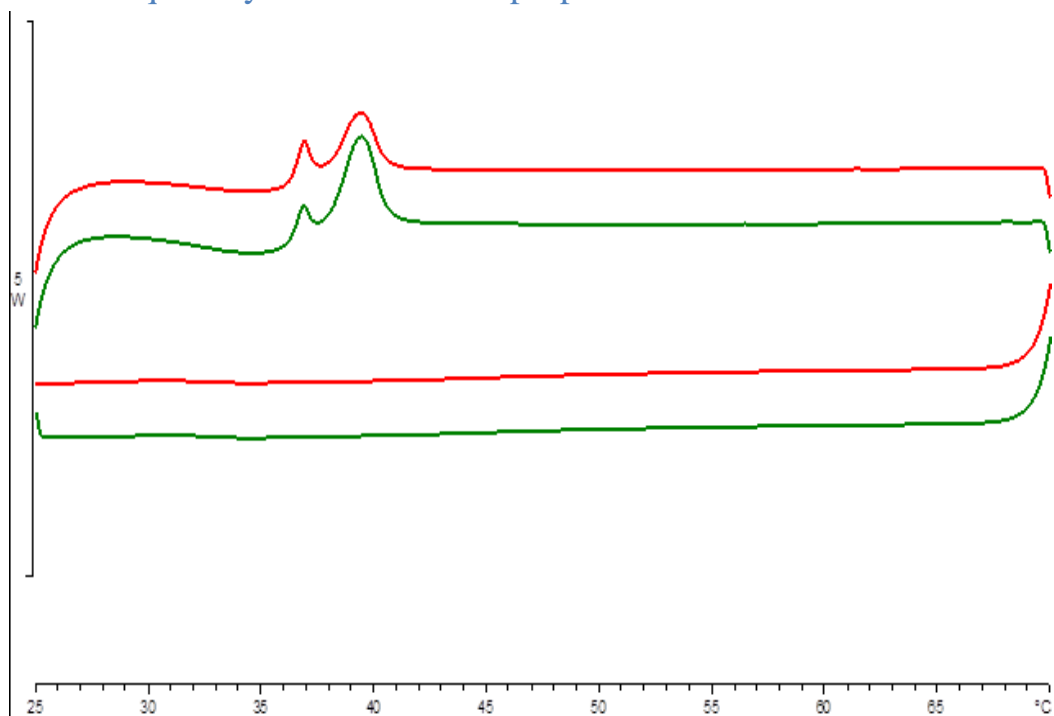


**Figure 7-2:** DSC heating and cooling trace for material **7-12**.

In Fig. 7-2, the DSC heating and cooling trace for the material **7-12** is presented. A full cycle of heating and cooling exhibits a transition from crystalline to isotropic. The onset temperature is 36.3 °C. DSC curves were recorded at 10 °C/ min and it can be seen that compound **7-12** melts to crystalline at around 35 °C, cooling curves no sign of phase transition was observed. The textures obtained by OPM are shown in Fig 7-5, a) crystalline on heating at 30 °C and b) starting to be isotropic (Cr-Iso) at 35 °C. The DSC experiment did not show the existence of clearing point, however it is possible that the clearing point of this material is between 35-40 °C, outside the temperature ranges that could be investigated with the available equipment.

## 7.2.2 MALDI and HPLC

Both MALDI (figure 7-3) and HPLC (figure 7-4) experiments are confirmation of compound **7-12** and present a high level of purity (100%).

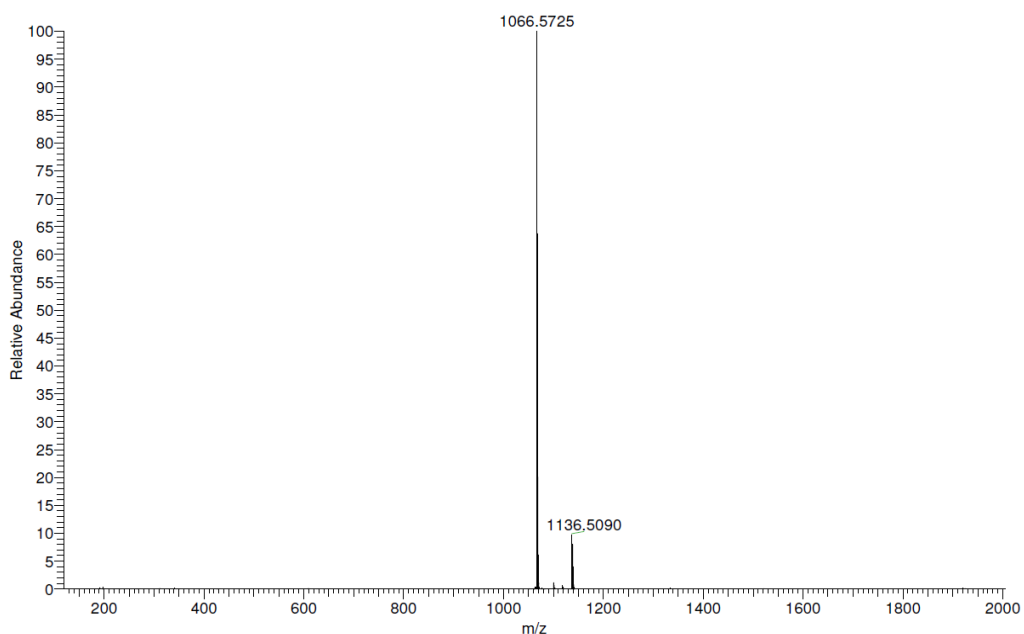
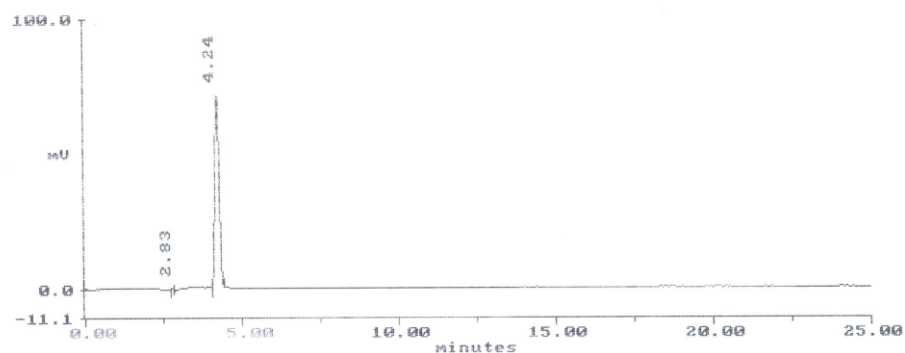


**Figure 7-3:** The MALDI spectrum of compound **7-12**; the main peak 1066.57 represents the  $[M + H_2O]$



Channel 1

Peak Quantitation : AREA  
Calculation Method : AREA%

NO	RT	AREA	area %	BC
2	4.24	488870	100.000	BB

**Figure 7-4:** The hplc trace from compound **7-12**; the main peak 4.24 showing 100% purity.

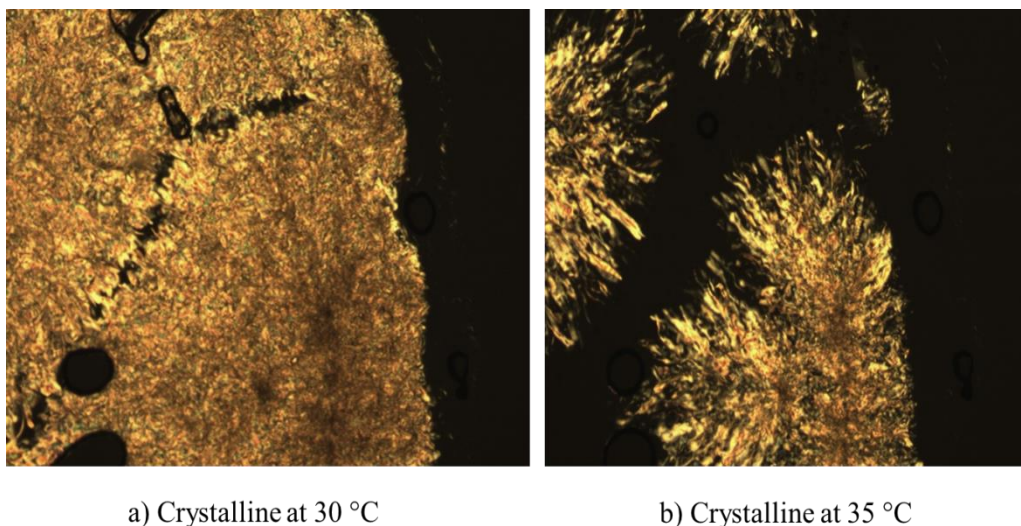


**Figure 7-5:** Micrographs of crystalline phase of compound 7-12.

OPM studies of compound **7-12** were carried out in water (w%/w%). In Fig 7-6 the texture obtained is the formation of schlieren and a marble-like texture at room temperature. Surprisingly, the material did not show any thermotropic mesophase phase itself (figure 7-5). However, with the addition of water it shows a nematic phase at room temperature. The existence of oligo-ethylenoxy chains allows the molecules to have more solubility in water and lowering the transition temperature. Compound **7-12** was prepared in different amounts and dissolved in water (w%/w %) in order to detect and study lyotropic behaviour.

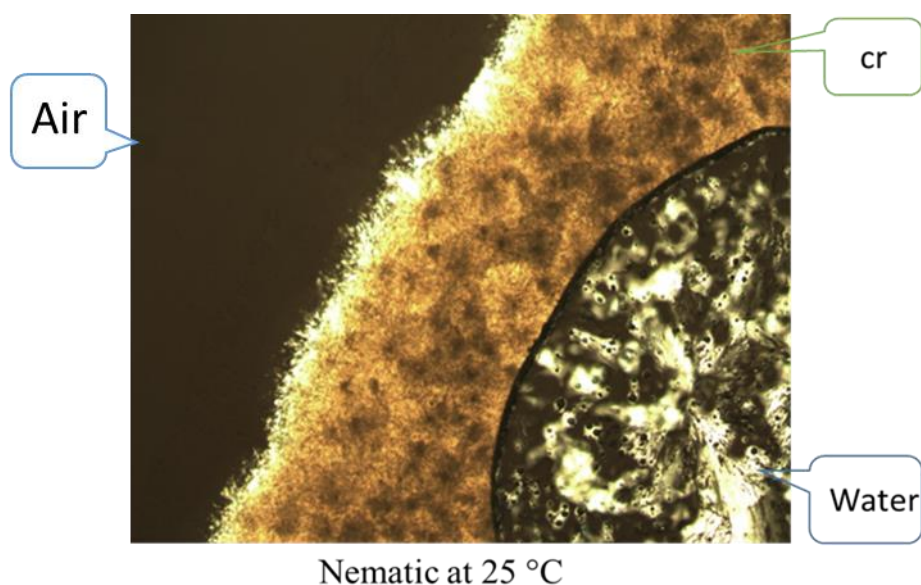


**Figure 7-6:** Micrographs of compound 7-12 with water, contact sample.

The preparation of compound **7-12** and water was as schematically presented in Figure 7-7. Water and material were weighted and placed in a Vortex mixer in order to obtain homogenous sample (Figure 7-7 a). Around 2-5 milligrams of the material was placed on a glass slide (figure 7-7 b). The material was covered by another glass slide in such a way that half of the area was filled with the material and the other half was air interface. The cover slip was on the last third in order to ensure that sample was visible through the Mettler Toledo hot stage. The samples were sealed with Loctite super glue (stable up to 250 °C), in order to prevent evaporation of the water (Figure 7-7 c). The contact samples were studied by OPM up to the crystallisation temperature of water. This is as water condenses on the cover slip and obscures vision in some cases. The sealed samples described below are easy to prepare and convenient for the identification of lyotropic behaviour.

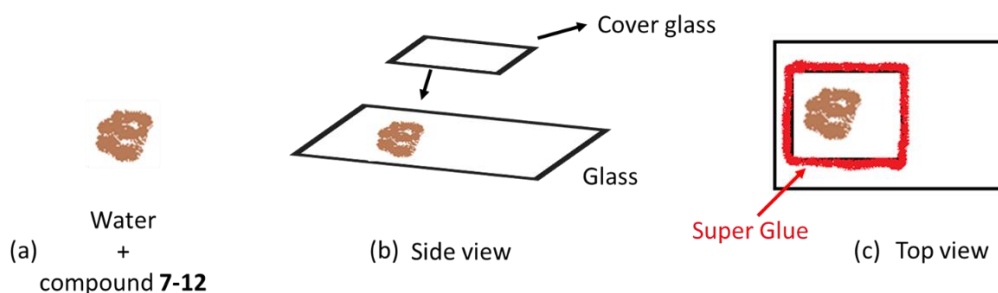


**Figure 7-7:** Schematic of compound **7-12** and water preparation used for detection and study of lyotropic behaviour.

For the studied materials in sealed slides, sequences of new phases were determined by distinctive textures and their changes were observed by OPM. The phase-transition temperatures and transition features were evaluated from OPM. The liquid-crystalline properties of a sealed material under study are summarized in Figure 7-8. These materials showed birefringent OPM textures. Contact and miscibility studies showed couples of a new phase behaviour. It can be seen in Fig 7-8 from (a) to (f) that when the temperature was increased, there were changes in molecular order. This is might due to the high concentration of water in some parts of the sample. In addition, samples were mixed well to ensure that all parts of the sample had the same water concentration (there was some water loss at some point when temperature was raised). The molecular order change has not been detected by DSC as it is difficult to control water evaporation. The LC clearing point was found

to be pronouncedly higher than that observed for pure material, which is around 86 °C.

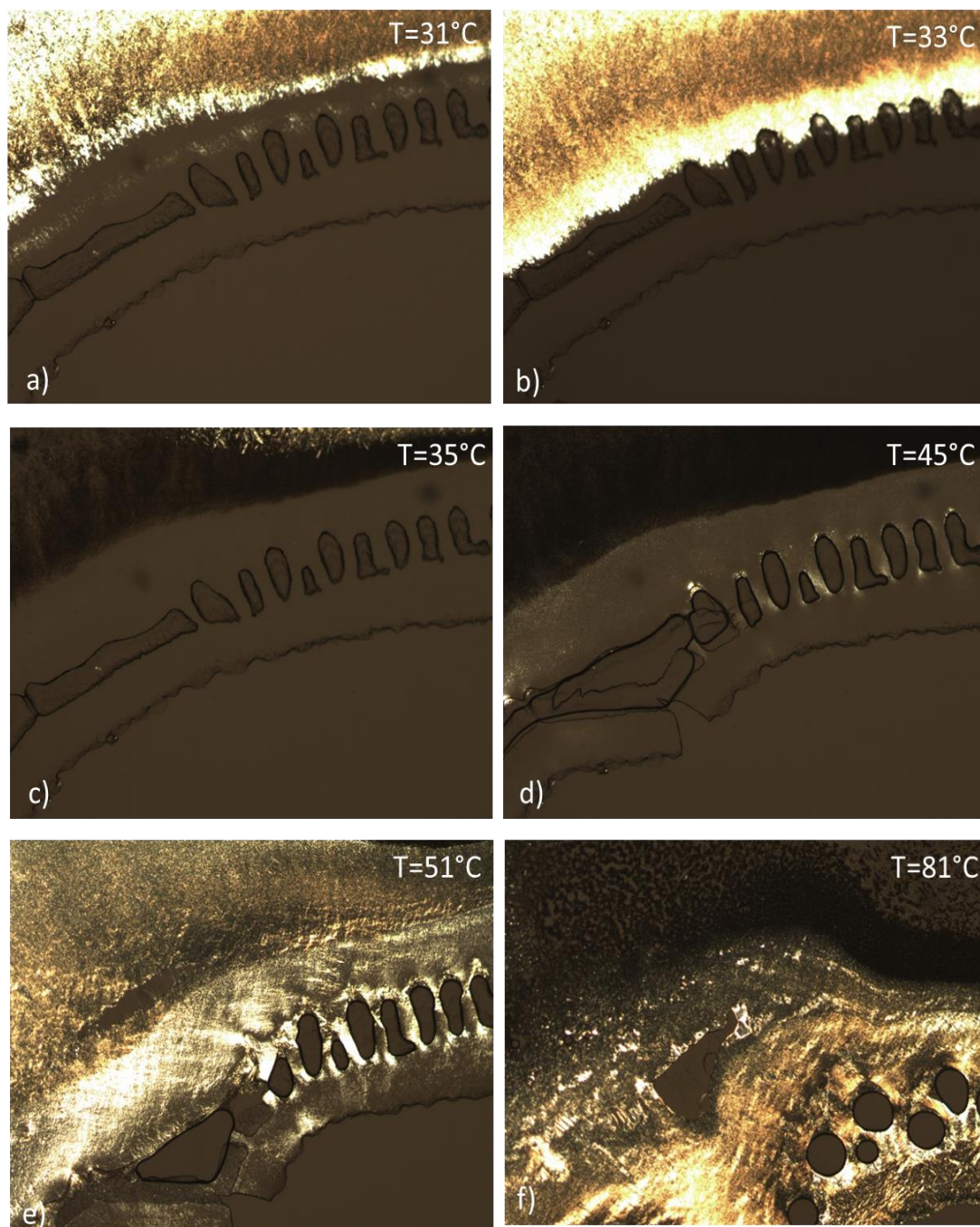


**Figure 7-8:** Microphotographs of the contact sample at different temperature, (a),(b),(c),(d),(e) and (f) were mixtures of 5 wt % compound **7-12** and 95 wt % water.

In figure 7-9 optical images of textures for 16 wt % compound **7-12** and 84 wt % water were taken at different temperature. The sealed samples were studied (Fig 7-9

a and b), both of which can form an unusual class of lyotropic liquid crystals in water. After careful testing of all the contact material, clearly, it shows birefringent striated feature starting at the temperature of 51 °C on heating. The striated texture observed in Fig 7-9 b at 57 °C has some features of and similarities with lamellar phase textures. Water visibly penetrates into the area of material, indicating solubility at this concentration.

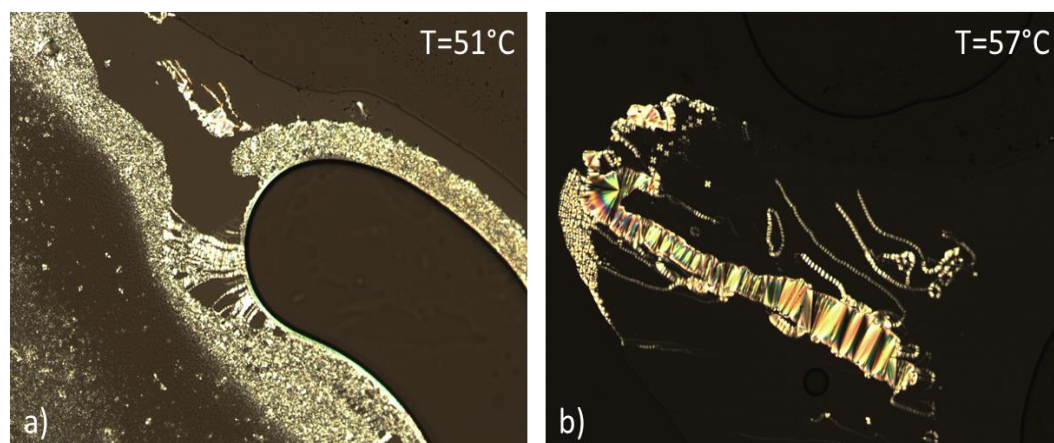


**Figure 7-9:** Optical images of 16 wt % compound **7-12** and 84 wt % water with magnification of 400x (POM).

Quite remarkable observations can be seen, when comparing the optical image in Fig 7-10 (20 wt % compound **7-12** and 80 wt % water) properties with those of lower material concentration in water ( Fig 7-8 and Fig 7-9). The texture in figure 7-8 was obtained at low temperature (25 °C) on cooling, however, this texture was unidentified.

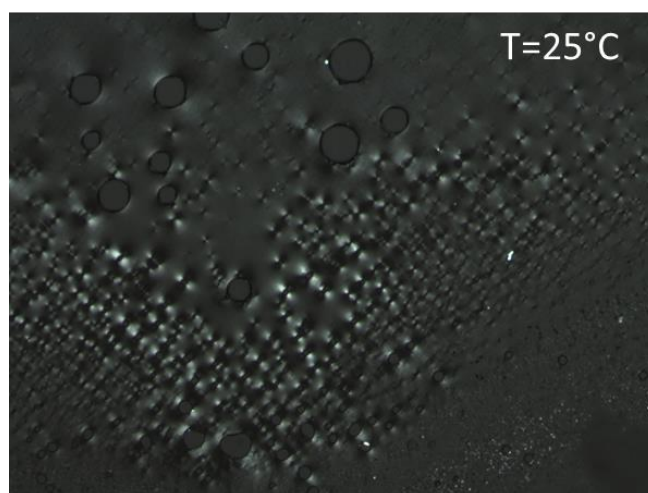


**Figure 7-10:** Optical image of 20 wt % compound **7-12** and 80 wt % water on cooling.

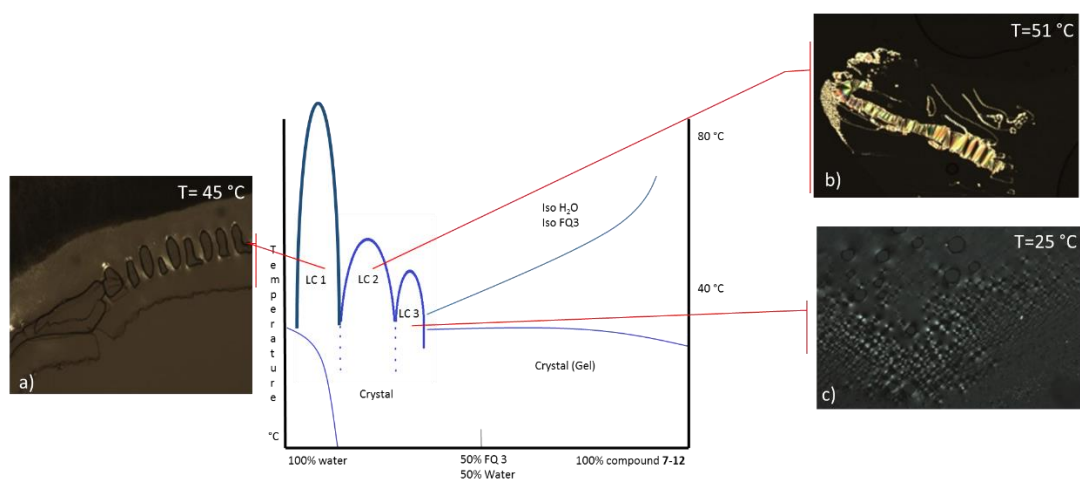


**Figure 7-11:** Sketched provisional phase diagram of compound **7-12** and water.

The sketched provisional phase diagram of compound **7-12** and water is shown above, Its concentration was tested on the OPM textures of a number of discrete mixtures. The key findings are that a number of LC phases are found when adding up to ~20% (w/w) of material to water. The LC phase stability is increased on adding water. At high concentration of water, a cubic LC phase was observed, characterised by sharp edges in droplets. In the contact sample, picture A, Fig 7-11 at 45 °C, this can be seen clearly. For clarity the polarizer and analyser are slightly offset from 90°. Above 84 °C at 95% water concentration the cubic phase transforms into isotropic. Increasing temperature in the cubic phase behaviour was observed by OPM and shown in figure 7-8.

Picture B shows that at higher LC concentration 16% (w/w) material to water, a focal conic type texture is prominently visible suggesting the formation of a lamellar phase at 51 °C. The lamellar phase structure is packed in a hexagonal in between bilayers. In addition, the phase behaviour of this system is viscous and different from those formed with 95% water present. Above 55 °C the lamellar phase transformed to an isotropic state.

Picture C at the highest mesogen concentration shows unspecifically birefringent texture at room temperature term LC3. At higher concentrations a gel phase region was formed. It has been found that the concentration of water influenced the phase behaviour of the system. After a certain amount of concentration up to approximately 78% (w/w), the sample is not homogenous. A gel phase region was observed in the system.

It has been found by Heertje<sup>176</sup> et al. that the lamellar phase is formed above the Krafft temperature, and that the liquid crystalline lamellar phase can transform into the cubic phase when temperature is increased. If the temperature is decreased below the Krafft point, the lamellar phase is turned to a gel. The LC cubic phase exists at temperatures above the lamellar phase. However, systems which contain unsaturated monoglycerides form bicontinuous cubic phases, lamellar phase, and an inverse hexagonal phase.<sup>177</sup> This observation could be relevant for these systems here.

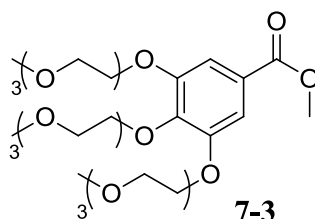
### 7.3 Summary

A new liquid-crystalline material possessing three oligo-ethylenoxy group units, was synthesized and characterised with the aim of looking at a new liquid-crystalline material exhibiting the thermotropic and lyotropic behaviour. Unknown phases were detected in the studied material with the increase or decrease of temperature and water concentration. The properties of this mesogen with water exhibit nematic LC phase behaviour at room temperature. If the transition temperatures of the pure material and the contact sample are compared, a difference of 45 °C in the clearing point can be seen. Lyotropic phase behaviour has been tested and studied for this material by using a contact preparation technique. This systems shows lyotropic behaviour, with a range of mesophase of which not all have been identified. A defect texture observed shows a striated texture which is an indication of lamellar phase. A full phase diagram with water and the identification of all the LC phases is outstanding and planned for the future.

An issue to be addressed in future work is the relatively low overall synthetic yield associated with the preparation of this mesogen.

## 7.4 Experimental procedures

### 7.4.1 Synthesis of methyl 3,4,5 tris(2(2(2methoxyethoxy)ethoxy)ethoxy) benzoate<sup>178</sup>



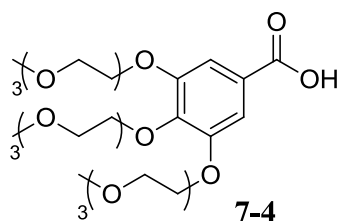
To a solution of methyl gallate (compound **7-2**) (0.1 g, 0.5 mmol) in dry butanone (10 ml) were added  $K_2CO_3$  (1.0 g, 5.0 mmol) and 1-bromo-2-(2-(2-methoxyethoxy)ethoxy)ethane (0.5 g, 2.2 mmol) and heated under reflux for 18 h at  $120^\circ C$  until the reaction was complete (TLC). The reaction mixture was filtered, the filtrate was concentrated and the residue was extracted with DCM. The organic layer was concentrated to give a yellow solid. The solvent butanone and DCM was distilled off and the crude product was purified by column chromatography (silica gel). The first column was in hexane: THF (1:1), the second hexane: THF (4.5:0.5). Finally the product was washed with hexane (to remove the impurity from compound **7-3** as it does not dissolve in hexane) to obtain compound **7-3** and yielded a dense yellow oil product (0.25 g).

**Yield:** 67%

**$^1H$  NMR, 400 MHz ( $CDCl_3$ ):**  $\delta$  [ppm] = 3.30 (s, 9 H), 3.54 (s, 24 H), 3.79 (t, 6 H), 3.89 (s, 3H), 4.31 (t, 6 H), 7.05 (s, 2H).

**$^{13}C$  NMR, 100 MHz ( $CDCl_3$ ):** 165.9, 153.5, 153.5, 142.9, 124.9, 109.4, 109.4, 71.6, 71.6, 71.6, 70.4, 70.4, 70.4, 70.4, 70.4, 70.4, 70.4, 70.1, 70.1, 70.1, 70.0, 70.0, 70.0, 69.6, 69.6, 69.6, 59.3, 59.3, 59.3, 51.5.

#### 7.4.2 Synthesis of 3,4,5-tris(2-(2-(2-methoxyethoxy) ethoxy) ethoxy) benzoic acid



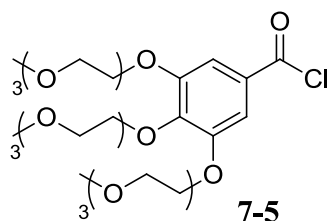
To a solution of compound **7-3** (0.25 g, 0.4 mmol) in methanol (10 ml), water (1.0 ml) and THF (10 ml) was added KOH (0.1 g, 2.0 mol) and heated under reflux for 48 h. The reaction was completed by heating at reflux for 2 h. After acidification with concentrated. HCl (2.0 ml), the residue was extracted with DCM, THF, ethyl acetate and water. To the aqueous layer was added CH<sub>2</sub>Cl<sub>2</sub> (6 x 100 ml). After drying the organic layer over anhydrous Na<sub>2</sub>SO<sub>4</sub> and concentration, the yellow residue was purified by column chromatography (silica gel). The first column of DCM: THF (1:1) eluent purify the desire product from impurity and the column was washed with methanol to obtain the compound **7-4** a dense yellow oil product (0.17 g).

**Yield:** 71%

**<sup>1</sup>H NMR, 400 MHz (CDCl<sub>3</sub>):** δ [ppm] = 3.30 (s, 9 H), 3.54 (s, 24 H), 3.79 (t, 6 H), 4.31 (t, 6 H), 7.05 (s, 2H).

**<sup>13</sup>C NMR, 100 MHz (CDCl<sub>3</sub>):** 165.3, 153.5, 153.5, 143.8, 126.9, 109.9, 109.9, 71.6, 71.6, 71.6, 70.4, 70.4, 70.4, 70.4, 70.4, 70.4, 70.4, 70.1, 70.1, 70.1, 70.0, 70.0, 70.0, 69.6, 69.6, 69.6, 59.3, 59.3, 59.3.

### 7.4.3 Synthesis of 3,4,5-tris(2-(2-(2-methoxyethoxy)ethoxy)ethoxy) benzoyl chloride<sup>179</sup>

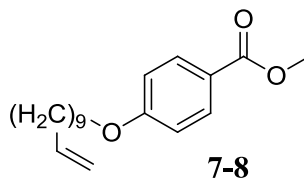


Compound **7-4** (0.02 g, 0.03 mmol) was dissolved in dry toluene (1.0 ml) under nitrogen; thionyl chloride (1.0 ml) was added and the solution heated to 80 °C for 2 h, the reaction being completed after heating for 45 mins at 110 °C . The thionyl chloride and toluene were distilled off under nitrogen atmosphere and the remaining product was dried further under vacuum and yielded a light yellow product (0.019 g).

**Yield:** 90%

**<sup>1</sup>H NMR, 400 MHz (CDCl<sub>3</sub>):**  $\delta$  [ppm] = 3.30 (s, 9 H), 3.54 (s, 24 H), 3.79 (t, 6 H), 4.31 (t, 6 H), 7.15 (s, 2H).

#### 7.4.4 Synthesis of methyl 4-(undec-10-en-1-yloxy) benzoate<sup>180</sup>



A mixture of methyl 4-hydroxy benzoate (compound **7-7**) (30.0 g, 0.02 mmol),  $K_2CO_3$  (138 g, 1.0 mol) and powdered 4 Å molecular sieves (50 g) in dry butanone (200 ml) was stirred over 4-7 h. A was solution of compound **7-6** (46.0 g, 0.2 mol) was added and the reaction mixture heated under reflux at 120°C for an additional 18 h until the reaction was complete (TLC). After filtration of the reaction mixture, the solvent butanone was distilled off and the residue was washed with hexane and recrystallized from ethanol to yield white crystals (30.1 g).

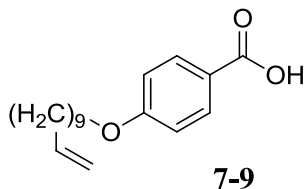
**Mp:** 57 °C

**Yield:** 50%

**<sup>1</sup>H NMR, 400 MHz (CDCl<sub>3</sub>):**  $\delta$  [ppm] = 1.29-2.18 (m, 16 H), 3.89 (s, 3 H), 4.06 (t, 2 H), 5.02-5.07 (m, 2 H), 5.82 (m, 1H), 6.80 (d, 2H) 7.10 (d, 2H).

**<sup>13</sup>C NMR, 100 MHz (CDCl<sub>3</sub>):** 165.9, 163.7, 139.1, 130.5, 130.5, 121.7, 115.7, 114.3, 114.3, 68.7, 51.0, 33.8, 29.3, 29.3, 29.3, 29.3, 29.3, 29.3, 25.8.

#### 7.4.5 Synthesis of 4-(undec-10-en-1-yloxy) benzoic acid<sup>181</sup>



Compound **7-8** (30.6 g, 0.1 mol) was dissolved in THF (60 ml) and methanol (350 ml). A solution of KOH (27 g, 0.5 mol) in water (128 ml) was added. After stirring for 2 days at room temperature, the reaction was completed by heating at reflux for 2 h. The solvents were distilled off and ice/water (250 ml) added. After acidification with conc. HCl (30 ml) the mixture was extracted with CH<sub>2</sub>Cl<sub>2</sub> (6 x 100 ml). After drying the CH<sub>2</sub>Cl<sub>2</sub> phase with MgSO<sub>4</sub> the solvent was distilled off. The mixture was washed with hexane, which yielded off white crystals (21.2 g).

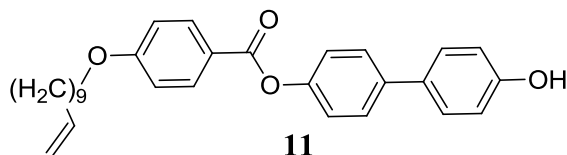
**Mp:** 79-81 °C

**Yield:** 78%

**<sup>1</sup>H NMR, 400 MHz (CDCl<sub>3</sub>):** δ [ppm] = 1.29-2.18 (m, 16 H), 4.06 (t, 2 H), 5.02-5.07 (m, 2 H), 5.82 (m, 1H), 6.80 (d, 2H) 7.20 (d, 2H).

**<sup>13</sup>C NMR, 100 MHz (CDCl<sub>3</sub>):** 165.4, 164.7, 139.0, 130.8, 130.8, 121.9, 115.7, 114.3, 114.3, 68.7, 33.9, 33.8, 29.7, 29.7, 29.6, 29.6, 29.6, 29.6, 25.9.

#### 7.4.6 Synthesis of 4'-hydroxy-[1,1'-biphenyl]-4-yl 4-(undec-10-en-1-yloxy)benzoate



Compound **7-9** (0.1 g, 0.4 mmol), compound **7-10** (0.01 g, 0.5 mmol), and 4-dimethylaminopyridine (DMAP) (0.002 g,  $2 \times 10^{-5}$  mol) were dissolved in DCM (15 ml) and N,N-dicyclohexylcarbodiimide (DCC) (0.1 g, 0.4 mmol) was added. After stirring for 18 h at 80 °C, the reaction mixture was filtered and washed with DCM. After removal of the solvent, compound **7-11** was purified by column chromatography (DCM), recrystallized from ethanol and yielded a white product (0.07 g).

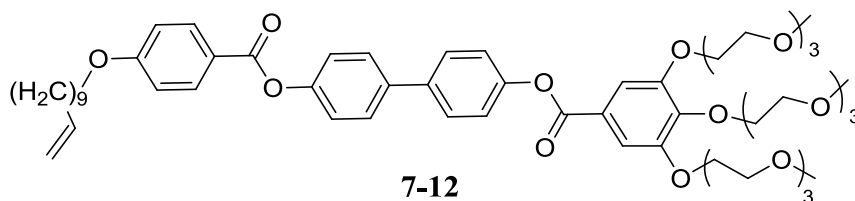
**Mp:** 91 °C.

**Yield:** 41%

**<sup>1</sup>H NMR, 400 MHz (CDCl<sub>3</sub>):**  $\delta$  [ppm] = 1.29-2.18 (m, 16 H), 4.06 (t, 2 H), 5.02-5.07 (m, 2 H), 5.82 (m, 1H), 6.86 (d, 2H) 7.14 (d, 2H), 7.23 (d, 2H) 7.62 (d, 2H), 7.86 (d, 2H) 8.11 (d, 2H).

**<sup>13</sup>C NMR, 100 MHz (CDCl<sub>3</sub>):** 165.2, 164.6, 157.4, 148.3, 139.2, 137.4, 133.4, 130.9, 130.9, 130.4, 130.4, 129.5, 129.5, 122.1, 122.1, 121.6, 116.3, 116.3, 115.7, 114.3, 114.3, 68.7, 33.8, 29.7, 29.7, 29.6, 29.6, 29.6, 29.6, 25.9.

#### 7.4.7 Synthesis of 4'-((4-(undec-10-en-1-yloxy)benzoyl)oxy)-[1,1'-biphenyl]-4-yl 3,4,5-tris(2-(2-(2-methoxyethoxy)ethoxy) ethoxy) benzoate



##### I. Method 1

Compound **7-4** (0.02 g, 0.03 mmol) was dissolved in dry toluene (10 ml) under nitrogen; thionyl chloride (0.01 ml, 0.03 mol) was added and the solution heated to 80 °C for 2 h, the reaction being completed after heating for 45 min at 110 °C. The thionyl chloride and toluene were distilled off under nitrogen atmosphere and the remaining product was dried further under vacuum to obtain compound **7-5**. Pyridine (0.05ml, 0.03 mmol) and a small amount of THF (5.0 ml) were added. A solution of compound **7-11** (0.02 g, 0.03 mmol) in anhydrous THF (10 ml) was added to the residue. This reaction mixture was kept stirring at 70 °C for 18 h.

The reaction mixture was quenched by adding water and extracted with diethyl ether. After removal of the solvent, compound **7-12** was purified by column chromatography (hexane: THF) (4:1) and triethylamine (1.0 ml) was added to the solvent mixture in order to make it more basic. Recrystallization from ethanol yielded a white crystal product (0.016 g) (48%).

##### II. Method 2

Compound **7-11** (0.37 g, 0.9 mmol), compound **7-4** (0.5 g, 0.9 mmol), and 4-dimethylaminopyridine (DMAP) (0.02 g, 0.2 mmol) were dissolved in DCM (50 ml) and N,N-dicyclohexylcarbodiimide (DCC) (0.2 g, 1.0 mol) was added. After stirring for 18 h at 80 °C, the reaction mixture was filtered and washed with DCM. After removal of the solvent, compound **7-11** was purified by column chromatography (DCM with drops of Et<sub>3</sub>N). The column was washed by methanol to obtain the compound **7-12** and yielded a white product (0.41g) (~50%).

**<sup>1</sup>H NMR, 400 MHz (CDCl<sub>3</sub>):** δ [ppm] = 1.29-2.18 (m, 16 H), 3.30 (s, 9 H), 3.54 (s, 24 H), 3.79 (t, 6 H), 4.06 (t, 2 H), 4.31(t, 6 H), 5.02-5.07 (m, 2 H), 5.82 (m, 1H), 7.14 (d, 2H) 7.22-7.32 (d, 6H), 7.86 (d, 4H), 8.11 (d, 2H).

**<sup>13</sup>C NMR, 100 MHz (CDCl<sub>3</sub>):** 165.2, 165.2, 164.2, 153.5, 153.5, 148.2, 148.2, 143.7, 139.0, 137.5, 137.5, 130.8, 130.8, 129.4, 129.4, 129.4, 129.4, 123.1, 121.6, 120.0, 120.0, 120.0, 120.0, 115.6, 114.2, 114.2, 105.6, 105.6, 71.6, 71.6, 71.6, 70.1, 70.1, 70.1, 70.0, 70.0, 70.0, 70.0, 70.0, 70.0, 70.0, 69.8, 69.8, 69.8, 68.7, 59.3, 59.3, 59.3, 33.8, 29.6, 29.6, 29.6, 29.6, 29.6, 29.6, 25.8.

**Experimental :** C: 66.39%, H: 7.69%.

**Calculated:** C: 66.26%, H: 7.78%.

## **8 Liquid crystals attached to pentamethyldisiloxane and AuNPs with alkyl various chain length**

Liquid-crystalline (LC) materials provide a unique opportunities in the field of NP organisation that combine the supramolecular ordering and fluid properties that they possess. They are able to arrange and organise nanoparticles into addressable 2 dimensional and 3 dimensional structures, Liquid-crystalline nanoparticles are an exciting class of new materials with many potential applications. This chapter will focus on the design that describe the preparation, physical properties and characterisation of thermotropic liquid-crystalline materials and liquid-crystalline nanoparticle hybrids (figure 8-1). One of the main aims of this synthesis was to obtain a linear material which exhibits smectic and nematic phases in a wide range of temperatures. These linear materials were designed to be attached laterally to pentamethyldisiloxane and AuNPs attached end-on. For a gold nanoparticle to exhibit a thermotropic liquid-crystalline phase, the basic requirement is coating the AuNPs with a suitable mesogen. This could lead to some interesting properties. Various methods used to synthesise the target mesogen and ligand exchange with AuNPs will be discussed in this chapter.

The main challenges were preparation of thiol mesogens in the intermediate reaction step. This chapter is classified into two major parts: synthesis of target mesogens with lateral thiol will be discussed in the first part. Characterisations of the desired mesogens will be overviewed in the second part. Furthermore, different types of mesogens with various chain length were synthesised and this is also a target.

This chapter will describe the results of our synthetic efforts and of the chemical characterisation of the material itself and with AuNPs. The investigation will overcome properties using optical polarizing microscopy (OPM), nuclear magnetic resonance ( $^1\text{H}$  NMR) and differential scanning calorimetry (DSC), transmission electron microscopy (TEM), thermal gravimetric analysis (TGA ) and UV-Vis spectroscopy (UV).

## 8.1 Synthesis Discussion

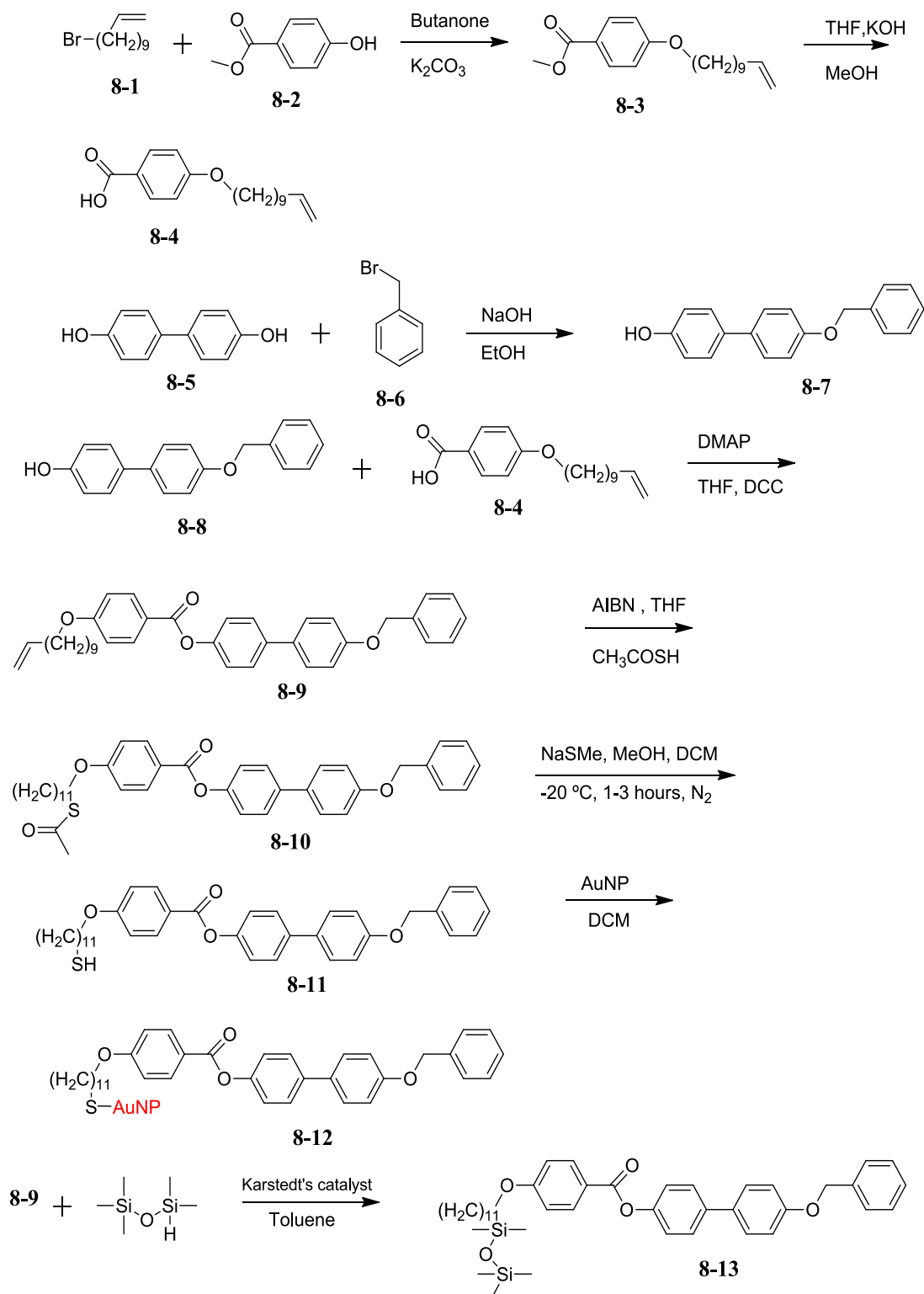
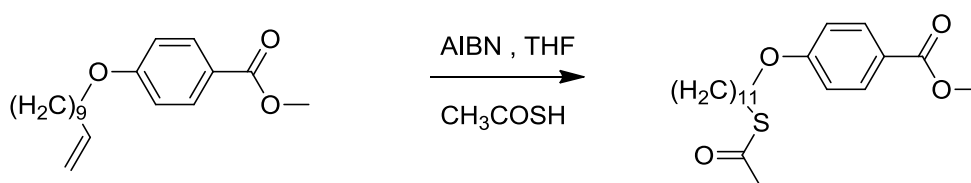


**Figure 8-1:** Scheme of the strategy used to synthesise compounds **8-9**, **8-12** and **8-13**.

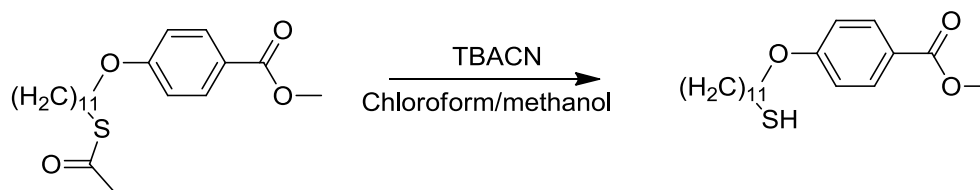
The first step of Fig 8-1 synthesis is a Williamson etherification, which was discussed in chapter 7 and a yield of 50 % was obtained. Preparation of compound **8-7** was easy and recrystallized from EtOH. A filtration was carried out using cold ethanol and processed as quickly as possible in order to not dissolve side product (disubstituted compound). The product was obtained when this condition was followed without problem and yielded white crystals (83%). Compound **8-9** was obtained in a good yield (70%) by esterification and purified by column chromatography (DCM). The synthesis of compound **8-10** was with thioacetic acid in the presence of AIBN and this led to the addition of thioacetyl group to the terminal alkene group. It was purified with DCM and yielded product with a good yield (82%).

Two different procedures were tried for the synthesis of compound **8-11**. The first procedure was to start from compound **8-3** with thioacetic acid in presence of AIBN as shown below. However, none of the first procedures gave the desired product.



The details of the procedure used to prepare methyl 4-((11-(methylsulfinyl)undecyl)oxy) are given below.

- Thioacetic acid (98%, 5.53 ml, 0.08 mol) was introduced to a mixture of compound **8-3** (12.7 g, 0.04 mol) and AIBN (7.0 g, 0.04 mol) in dry THF (100 ml) under nitrogen. This final mixture was heated at 60 °C for 18 hours. The reaction was monitored by TLC until the starting materials disappeared. The solvent was distilled off, and the crude product was filtrated with hexane in order to remove AIBN (AIBN does not dissolve in hexane). Column chromatography was carried out on the residue using ethyl acetate/hexane, 1:2, as an eluent. This yielded white crystal (12.6 g) (78%).
- In order to prepare methyl 4-((11-mercaptoundecyl)oxy)benzoate two methods were used as shown below.



- i. Tetrabutyl ammonium cyanide (0.001 g, 0.002 mmol, 0.1 equiv.) was added to chloroform (5 ml), methyl 4-((11-(methylsulfinyl)undecyl)oxy) (0.017 g, 0.02 mmol, 1.0 equiv.) and methanol (5 ml) under nitrogen. The reaction was stirred at room temperature for 76 h (monitored by TLC). After the completion of the reaction, water (50 ml) and DCM (20 ml) was added. The organic layer was separated and the aqueous layer extracted with DCM (20 ml). The combined organic layers were washed with  $\text{MgSO}_4$ . There was no evidence that the desired product was obtained.
  
- ii. The same conditions as for method (i) were used but with dry solvent (chloroform and methanol). This yielded a white crystal, in a yield of 66%.

Comparing the  $^1\text{H}$  NMR data obtained in figure 8-2, the presence of acetylthio group at 2.52 ppm in spectrum A and the absence of the signal of the acetylthio in spectrum B can be seen. This implies that the target compound was formed.

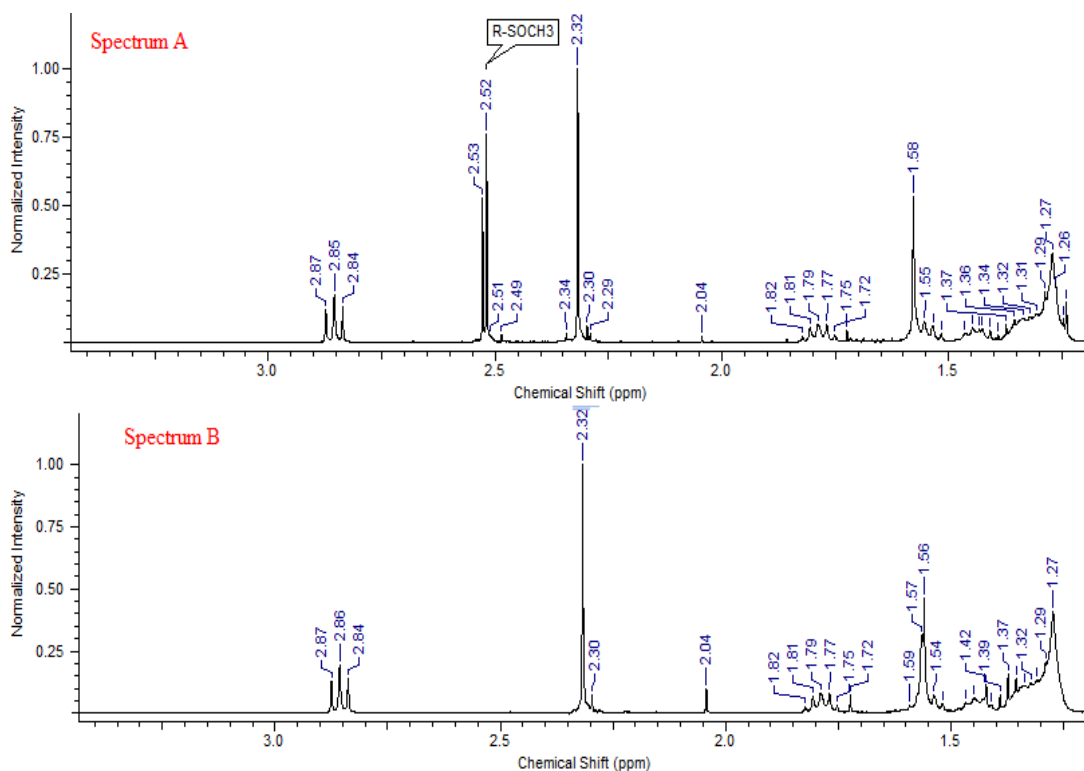
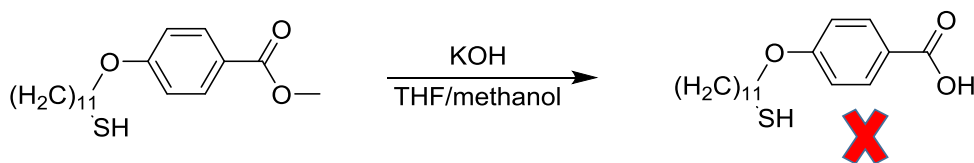
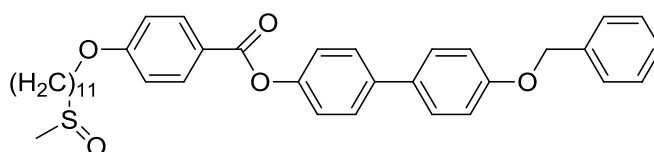


**Figure 8-2:** <sup>1</sup>H NMR spectra of methyl 4-((11-(methylsulfinyl)undecyl)oxy) benzoate (spectrum A) and methyl 4-((11-mercaptoundecyl)oxy) benzoate (spectrum B).

- Hydrolysis was the next step toward the final target. However, the reaction took 76 hours and there was no cleavage of the carbon of the carbonyl group of the ester and the desired product was not obtained. It was noticed that CH<sub>2</sub> protons next to thiol had shifted, which is an indication that a reaction had occurred.



The second procedure started from compound **7-10**. Seven different methods were tried for the synthesis but only one gave the desired product (compound **8-11**) in reasonable yield. There was no indication of product formation in most of the methods explored. The details of the methods are given below.



**8-10**

- i. Tetrabutyl ammonium cyanide (0.01 g, 0.024 mmol, 0.1 equiv.) was added to chloroform (20 ml), compound **8-10** (0.15 g, 0.24 mmol, 1.0 equiv.) and methanol (20 ml) under nitrogen. The reaction was stirred at room temperature for 76 h (monitored by TLC). After the completion of the reaction, water (50 ml) and DCM (50 ml) was added. The organic layer was separated and the aqueous layer extracted with DCM (20 ml). The combined organic layers were washed with MgSO<sub>4</sub>. There was no evidence that the desired product was obtained.
- ii. The same conditions as for method (i) were used but with dry solvents (chloroform and methanol). The <sup>1</sup>HNMR spectrum shows only starting of the ether group material and cannot be recovered. The reaction of the thiol function of the starting material led to an unusable product.
- iii. Compound **8-10** (0.23 g, 0.36 mmol) and hydrogen chloride (conc.) (0.03 ml 0.72 mmol) were measured into 50 ml 3-necked flask and flushed with nitrogen gas. THF (5 ml) and methanol (15 ml) were added to the mixture via a syringe. The solution was stirred for 30 min at room temperature then the temperature was increased by 60 °C for 24 h. After the completion of the reaction, distilled water (50 ml) was added. The organic layer was separated and the aqueous layer extracted with DCM (3 x 50 ml). The combined organic layers were dried over MgSO<sub>4</sub> and concentrated in vacuo. The residue was purified using column chromatography (DCM). No product was formed.
- iv. NaSMe (0.2 g, 2.64 mmol 12.0 equiv.) was dissolved in a minimum amount of methanol, and this solution was added drop-wise into a mixture of compound **8-10** (0.14 mg, 0.22 mmol 1.0 equiv.) dissolved in methanol (10 ml) and THF (5 ml) under nitrogen at 30 °C. The final reaction mixture was

heated at 30 °C for 30 mins, and it was completed by stirring at r.t. for 18 hrs. The whole reaction was monitored by TLC. HCl (0.1 M, 2 ml) and DCM (4 ml) was added, the organic layer was washed with water (4x 4 ml) and brine (3 x 4 ml). The final organic layer was dried over MgSO<sub>4</sub> and solvents distilled off. The crude was filtrated and washed with hexane. Cleavage occurred and the target compound was not formed.

- v. The same conditions as for method (iv) were used but with 5.0 equiv. of NaSMe, Cleavage occurred and the target compound was not formed.
- vi. Similar conditions as for method (iv) were used but with 1.1 equiv. of NaSMe. Cleavage occurred and no product was formed.
- vii. Compound **8-10** (0.35, 0.5 mmol, 1.0 equiv.) was added to DCM (20 ml), NaSMe (0.1 g, 1.1 mmol, 2.0 equiv) and methanol (10 ml) under nitrogen. The reaction was stirred at -20 °C for 30 min and monitored by TLC. After the completion of the reaction (one hour), water (50 ml) and DCM (50 ml) was added. The organic layer was separated and the aqueous layer extracted with DCM (50 ml). The combined organic layers were washed with NaSO<sub>4</sub>. Purification by column chromatography (dichloromethane /hexane, 1:1) yielded a white crystal (0.18 g). (56%). This method was the best found to obtain the target compound.

Compound **8-11** was functionalised to a thiol in order to be attached to Au-NPs. The next step was preparation of the Au-NPs. The method used to prepare compound **8-11** capped gold nanoparticles is the most widely used method, by preparing Au-NPs covered with a capping agent (hexane thiol), then a ligand exchange in the presence of DCM is performed. Reported first by Brust and Schiffrin, it is extensively used for preparing gold nanoparticles capped with a large number of ligands. NPs obtained using the Brust-Schiffrin method are relatively monodispersed, size-controlled and they are stable in the convenient solvent. Figure 8-3 shows that the preparation of < 2 nm coated AuNPs and figure 8-4 is a scheme of facile synthesis of gold monodisperse (3 - 6 nm coated AuNPs).

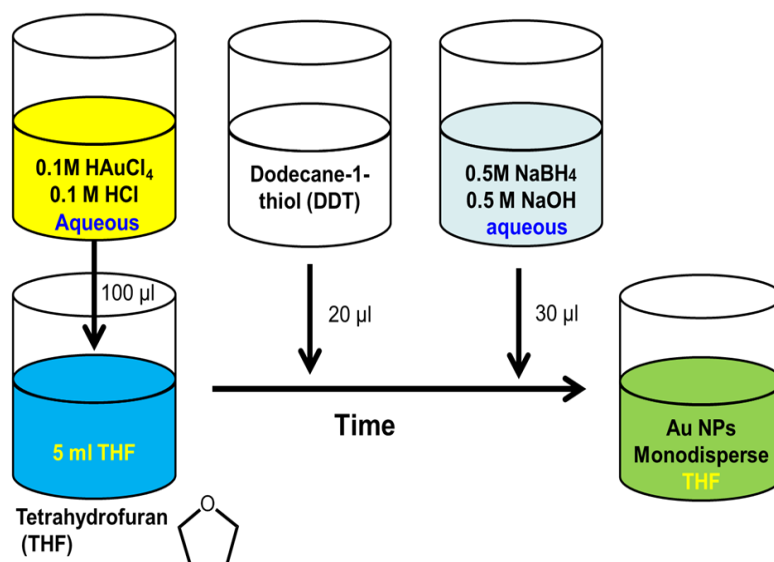
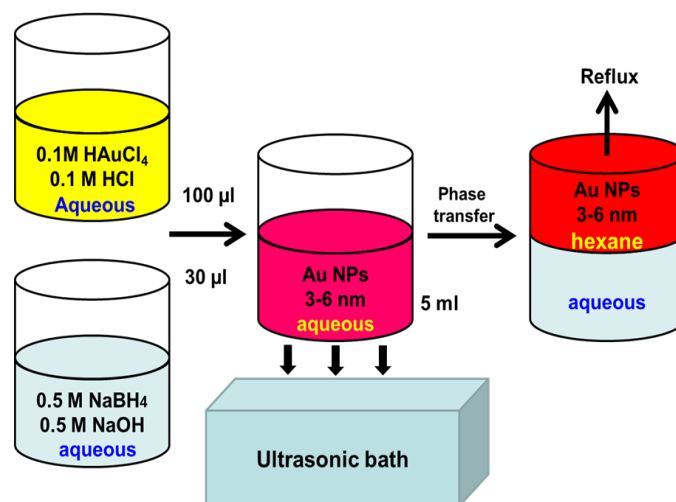


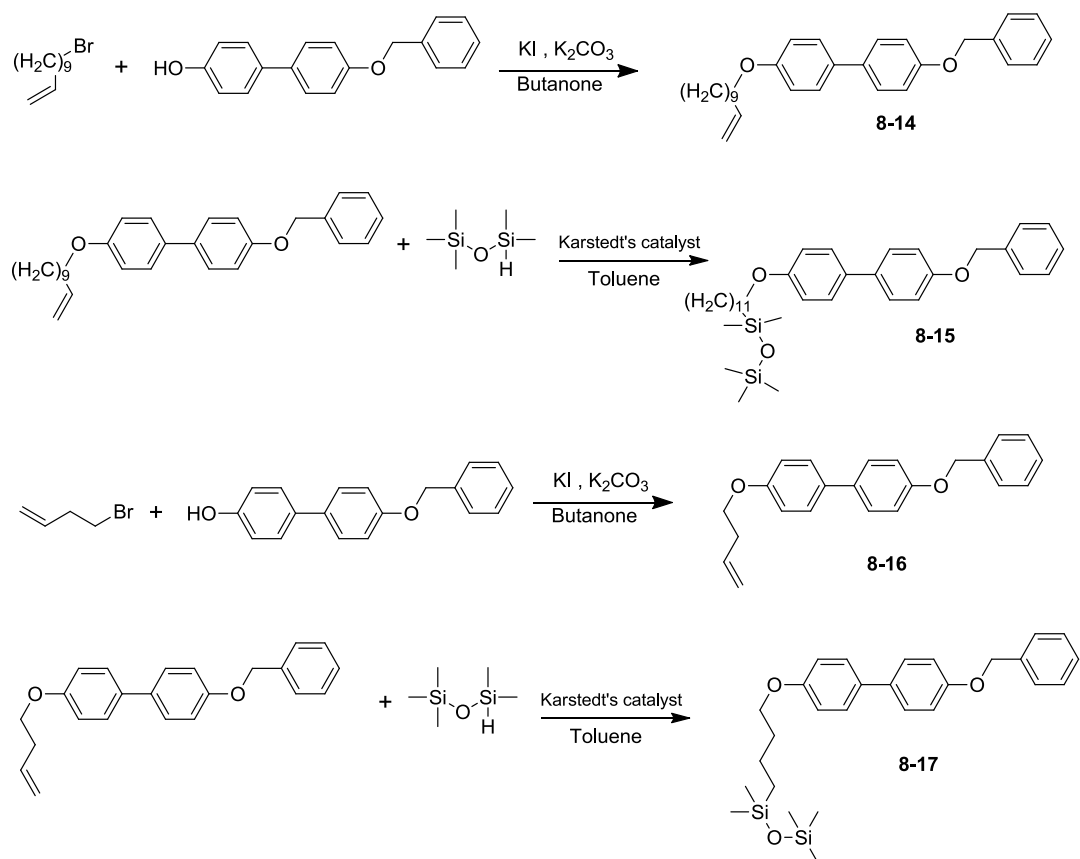
Figure 8-3 : Preparation scheme for < 2 nm coated AuNPs.<sup>182, 183</sup>



**Figure 8-4:** Scheme of facile synthesis of gold monodisperse (3 - 6 nm coated AuNPs).<sup>182, 183</sup>

After preparation of the AuNPs was completed, a thiol mesogen was added and left stirring for five days in the presence of DCM. Purification was straightforward, The solution was the centrifuged for 10 minutes. Free mesogen (as the used mesogen dissolves in ethanol) was removed by pipette. This process was repeated four times in order to remove free mesogen. The black residue was dispersed in hexane and centrifuged. The AuNP LC was then dried in vacuo for 12 hours.

The synthesis and purification of compounds **8-13**, **8-14**, **8-15**, **8-16**, **8-17** was very straightforward as described in the experimental. Thus, the chain lengths were changed in order to compare the properties. The expectation was that compounds attached to pentamethyldisiloxane was going to decrease the clearing point temperature. The results were confirmed by  $^1\text{H}$  NMR spectra by the disappearance of the signals characteristic of terminal alkenes. TLC and  $^1\text{H}$  NMR give information about the purity of the synthesised compounds. The properties of these compounds will be discussed in the next part of this chapter.

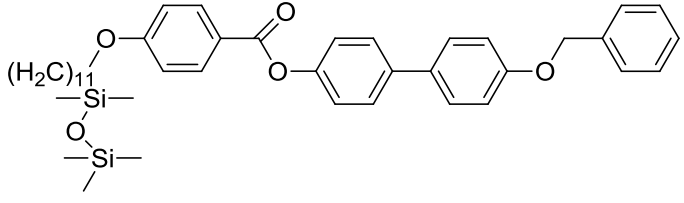
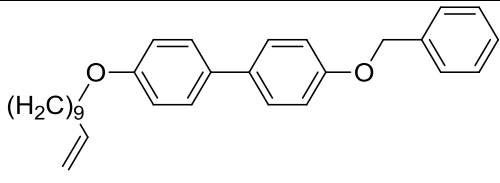
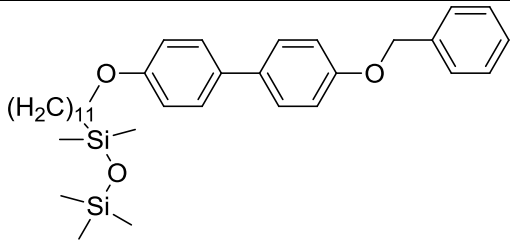
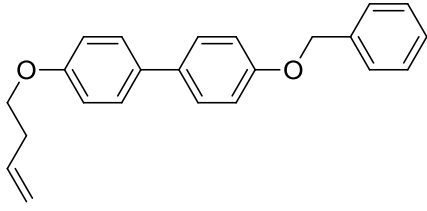
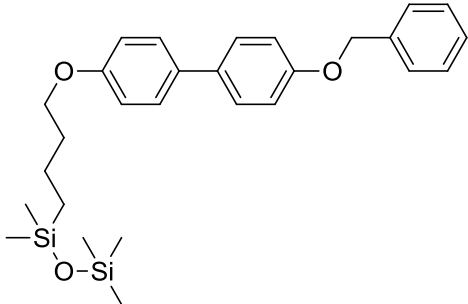


**Figure 8-5:** Scheme of the procedure used to synthesise compounds **8-14**, **8-15**, **8-16** and **8-17**.

The results obtained for compounds **8-14**, **8-15**, **8-16** and **8-17** are shown in figure 8-6 and 8-7. This set of spectra shows the peaks in spectrum A for the alkene group at 5.02 (2 proton) and 5.82 (1 proton) ppm. Additionally, spectrum B in figure 8-6 shows no sign of the alkene group. In figure 8-7 spectrum B, the siloxane group appears at 0.22 ppm, which indicates that compounds **8-15** and **8-17** were formed.

**Table 8-1 :** Table showing series of materials attached to pentamethyldisiloxane., their structures and transitions.

Compound	Structure	Transition (°C )
<b>9</b>		Cr 127 SmA 131 N 173 Iso

13		Cr 194 Iso
14		Cr
15		Cr
16		Cr
17		Cr

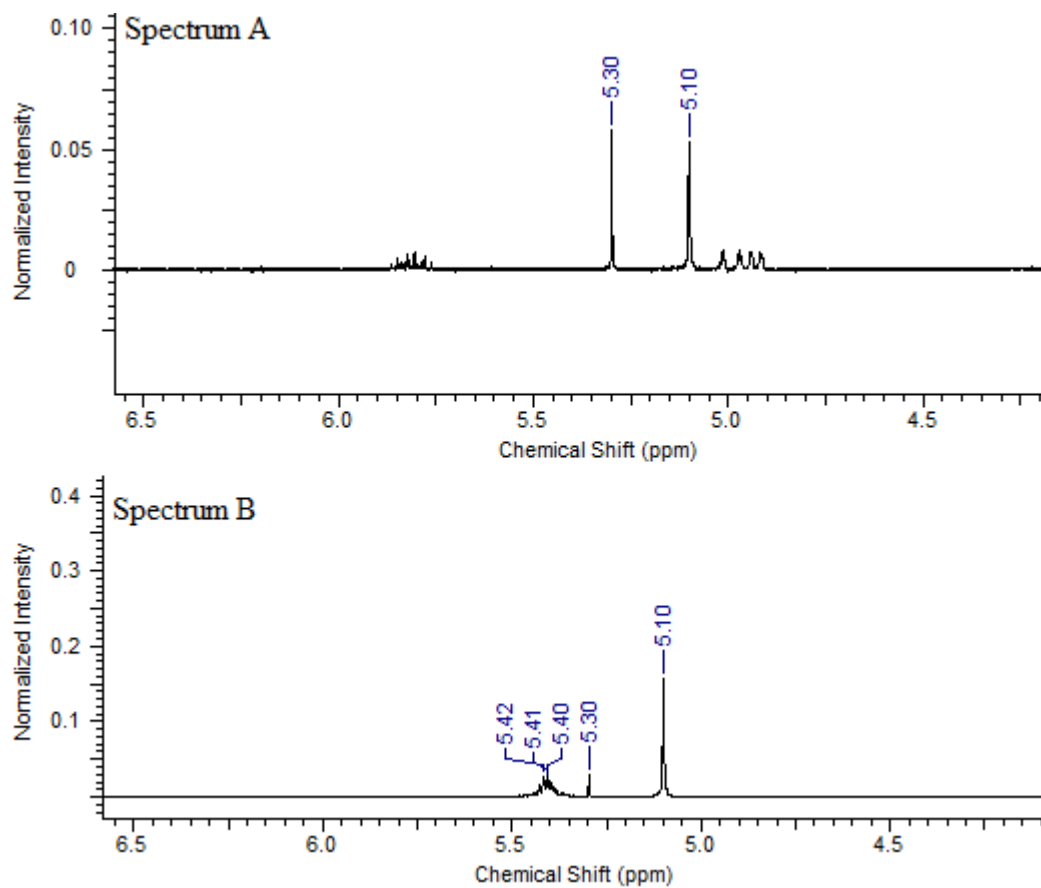


Figure 8-6: <sup>1</sup>H NMR spectra of compound 8-14 (spectrum A) and compound 8-15 (spectrum B).

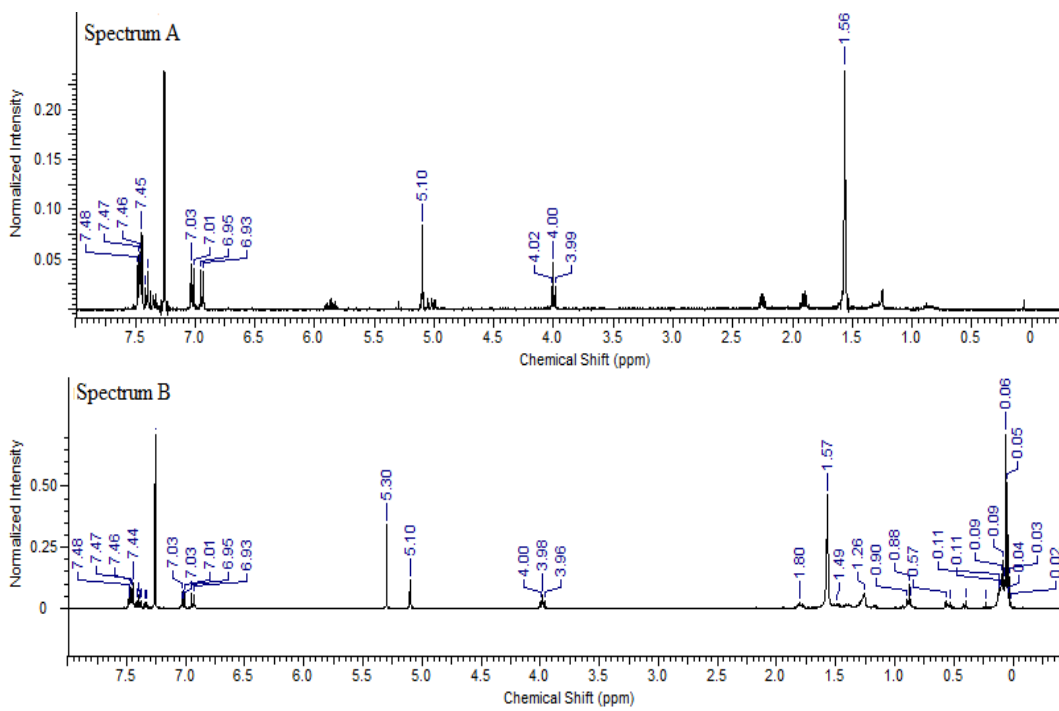
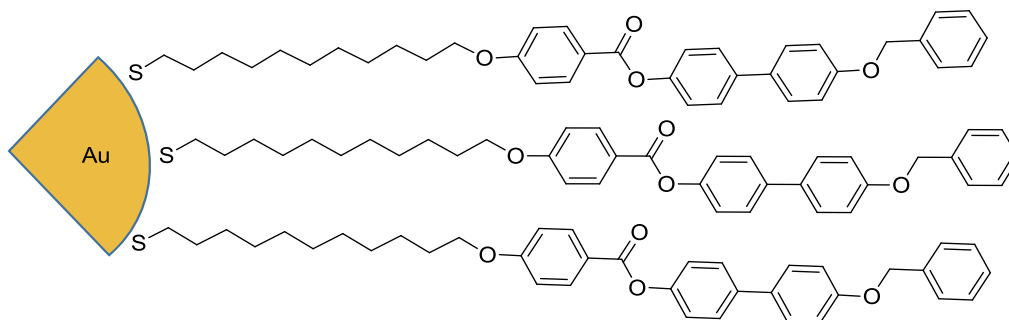


Figure 8-7: <sup>1</sup>H NMR spectra of compound 8-16 (spectrum A) and compound 8-17 (spectrum B).

## 8.2 Discussion of Properties

In this section, discussion will be divided into three parts. The first part will discuss the properties and phase structures of the target mesogen (compound **8-9**). The second discussion will follow the liquid crystalline properties attached to AuNPs (compound **8-12**). The last part will discuss three series of materials attached to pentamethyldisiloxane.



**Figure 8-8:** Schematic representation of AuNPs coated with target mesogen.

## 8.2.1 Liquid crystal and thermal properties of compound 8-9

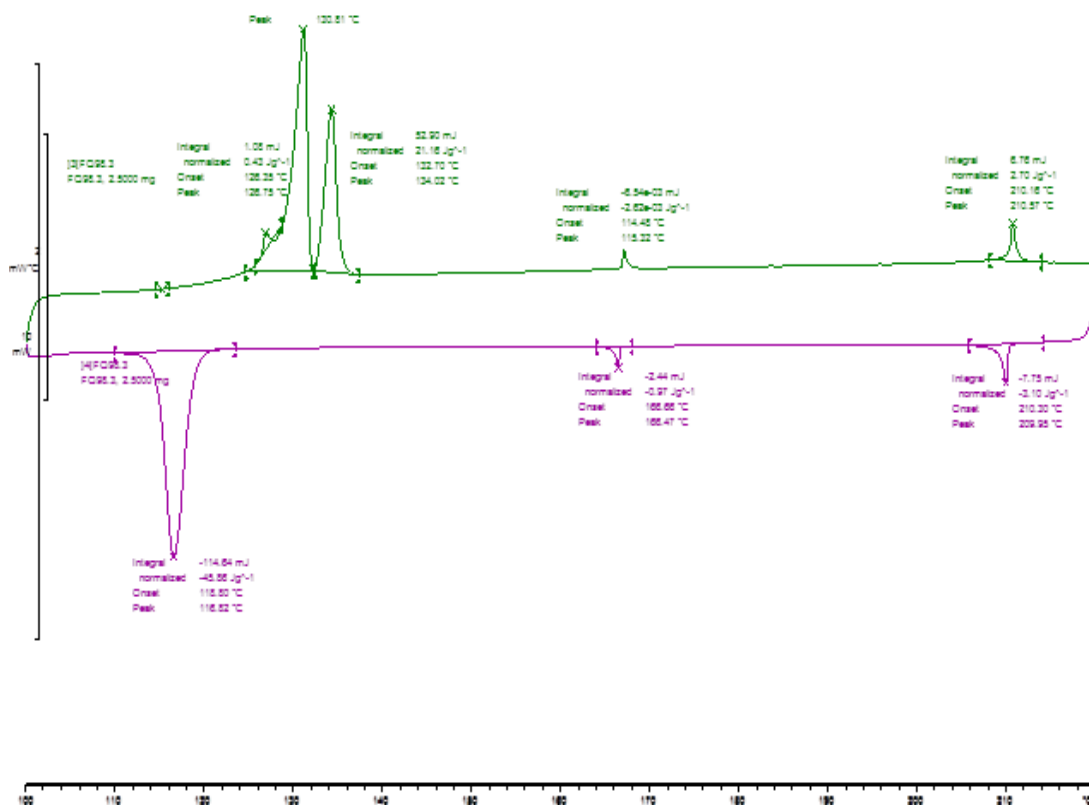


**Figure 8-9:** DSC curves of compound 8-9. Heating / cooling rate is 10°C/min.

The DSC curve heating /cooling were recorded at 10°C /min and it can be observed that compound 8-9 has enantropic liquid crystalline behaviour. The phase transition temperature and associated enthalpies are Cr 127 (42) SmA 131 (21) N 173 (-2.62) Iso (T/°C ( $\Delta H/Jg^{-1}$ )). The polarized optical microscopy carried out on compound 8-9 was interesting. It showed a range of liquid-crystalline phases. The textures obtained by OPM are shown in figure 8-10.



**Figure 8-10:** Textures obtained by OPM for compound 8-9. a) SmA at 157 °C, b) and c) nematic at 177 °C and 178 °C.

## 8.2.2 Liquid crystal attached to AuNPs and thermal properties of compound **8-12**

### 8.2.2.1 NMR study

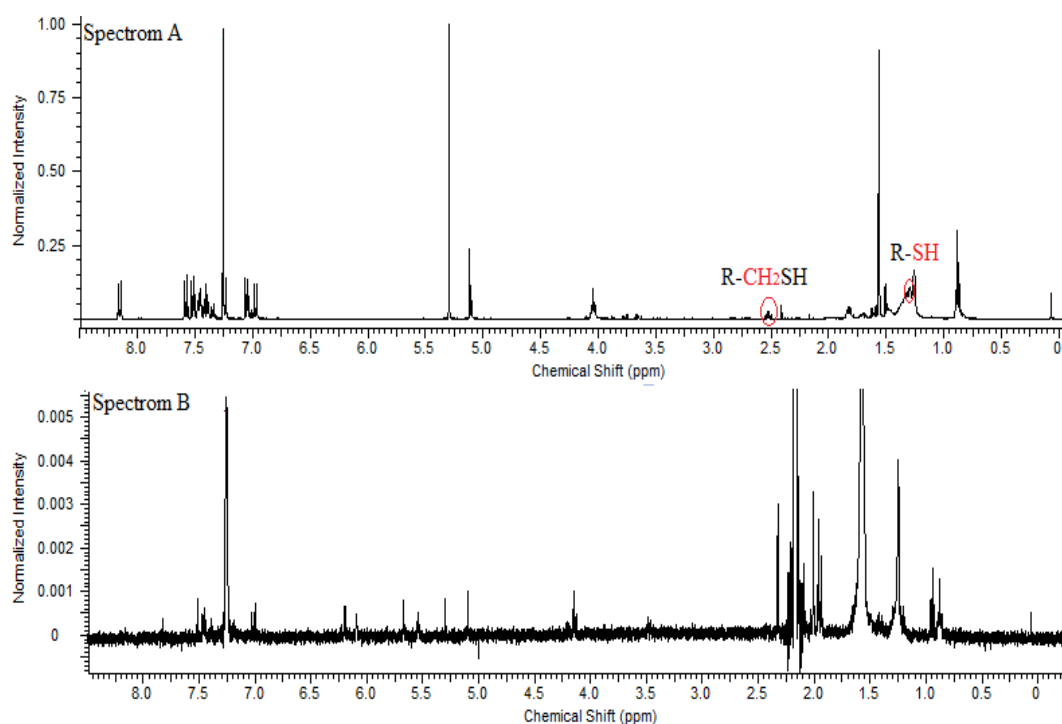
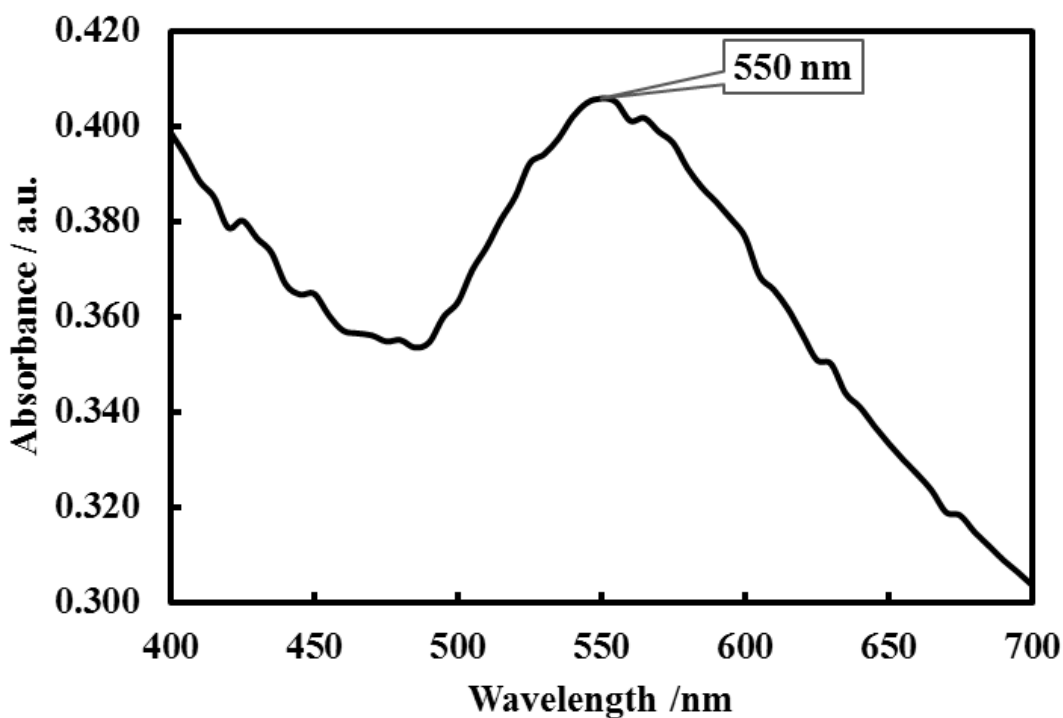


Figure 8-11: <sup>1</sup>H NMR spectra comparison of the free ligand (compound **8-11**) (spectrum A) and mesogen covered gold NPs (compound **8-12**) (spectrum B).

It can be seen that in the <sup>1</sup>H NMR spectra of both materials, spectrum B for compound **8-12** has broader peaks and the peaks are less resolved. This is attributed to the lack of mobility of the organic groups in compound **8-11** bonded to gold nanoparticles. Spectrum A corresponds to the peaks for the free thiol (compound **8-11**).

The spectra peak at  $\delta=2.50$  ppm (R-CH<sub>2</sub>SH) in (B) is broader than in (A), and the peak at  $\delta=1.30$  ppm (-SH) present in the free thiol (A) has disappeared in the AuNP (B). These changes are an indication that the thiol group is chemically attached to the gold cores.

### 8.2.2.2 UV spectroscopy



**Figure 8-12:** UV spectra of compound 8-12.

Fig. 8-12 shows a UV spectrum for compound 8-12 and exhibits an absorption band of high intensity above 550 nm wavelength. The UV spectrum of a free AuNPs has a high intensity absorption at shorter wavelength, 310 nm. The explanation would be that the attachment of the LC mesogens to the AuNPs causes the changes in wavelength absorption.

### 8.2.2.3 NPs parameters calculations (TGA, TEM)

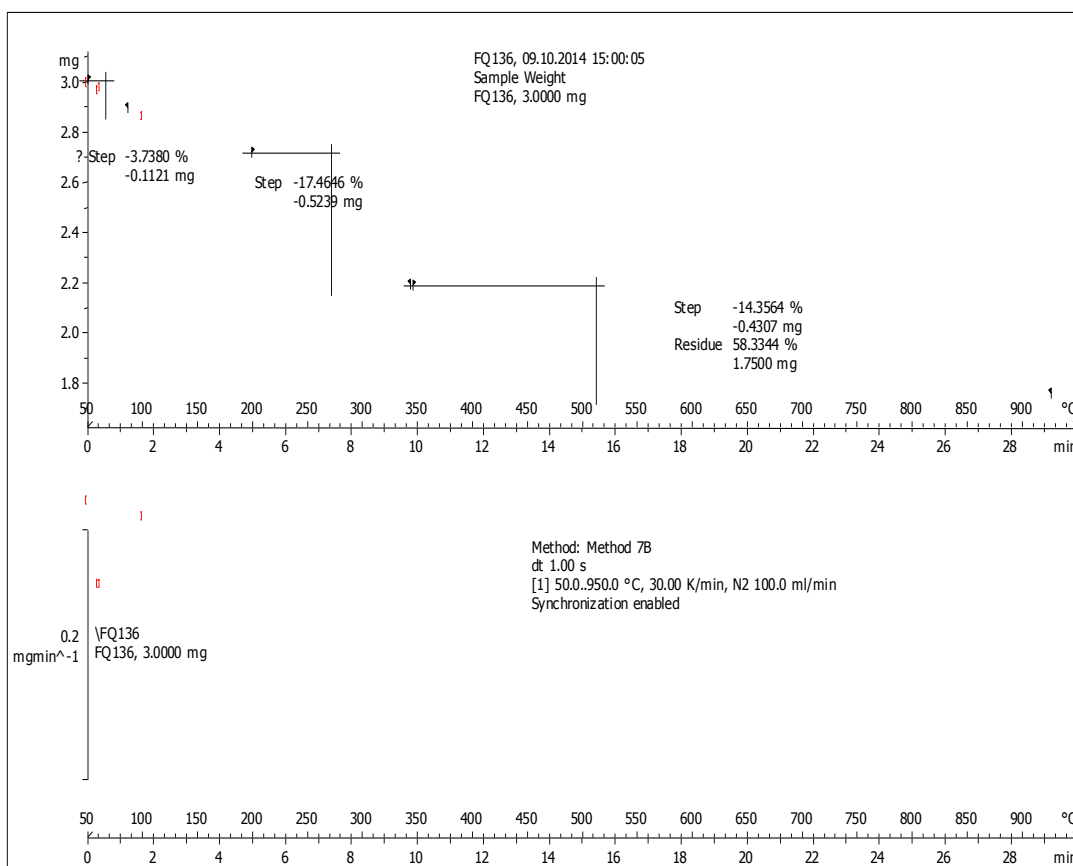


**Figure 8-13:** TGA spectrum of compound 8-12.

The analysis of TGA was performed in air, to ensure that all organic materials were oxidised and removed from the samples in the time set at above 900 °C. The solvent in samples was removed overnight in the oven. As shown in the figure above, the organic material was burned off in two main stages, the first one starting at 70°C and the second one at 290°C. The organic components were completely removed by the time the temperature reached 350 °C. The organic materials were removed in order to identify the percentage between the ligand (compound 8-11) and the metallic core (AuNPs). The organic components account for 42% of the total mass of compound 8-12 and the residual percentage of pure AuNPs is 58%.

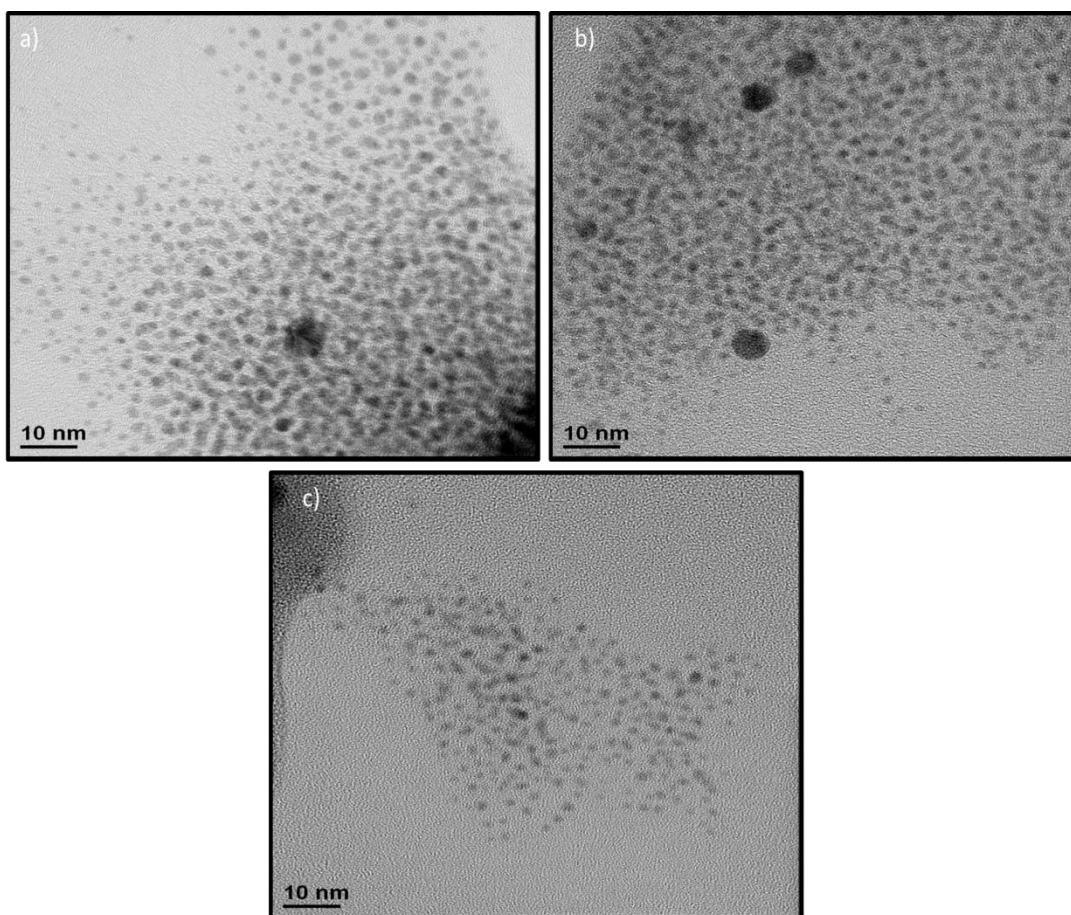


**Figure 8-14:** TEM images of material 8-12.

The sizes of the AuNPs were recorded by using TEM, showing areas of large dark spots (Fig 8-14 a, b) and small size distribution. The larger dark spots in in figure 8-14 (a) and (b) are due to overlapped AuNP or non-dispersed particles. The TEM information and analysis provided information on the size of the AuNPs. The aim was to investigate the size of gold particles and estimate their polydispersity (figure 8-14). The average size of AuNPs as observed on TEM is 2.5 nm. From the TEM images a size variation of  $\pm 0.12$  nm was estimated.

#### 8.2.2.4 Compound 8-12 with liquid crystals properties

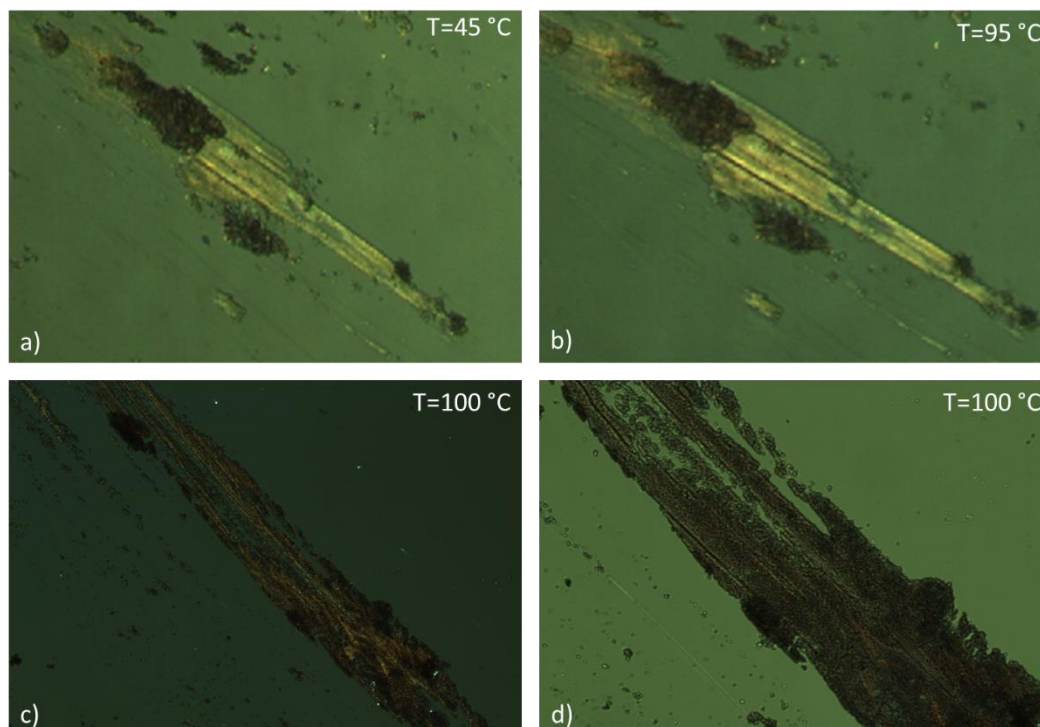


**Figure 8-15:** OPM of compound 8-12 with analyser offset by 10 degrees and maximum gain settings of the camera; images a, b and c were taken with magnification of (x100); image d was taken with magnification of (x500).

It was observed in figure 8-15 by OPM that the AuNPs coupled to the mesogen show liquid crystalline phase behaviour verified by a birefringent area. However due to the high absorption of the gold NPs the birefringence is very weak. In order to enhance the visibility of the birefringent texture, the polarizer was offset by  $10^\circ$  and for photographic recording the setting of the camera were set to maximum gain. This resulted in the greenish colour in Figure 8-15. The LCNPs are visible as a light birefringent region for a very thin sample or in thicker section, areas are dark stripes. It was very difficult to depict correctly the defect texture on the camera recordings. However figure 8-15 a shows a schlieren texture, suggesting the formation of a nematic phase for the mesogens.

### 8.2.2.5 DSC studies of compound 8-12

The DSC shows in the first scan a T<sub>g</sub> and a very abroad melting peak. Due to the material viscosity after the first T<sub>g</sub> the molecular is not fast enough (figure 8-16).

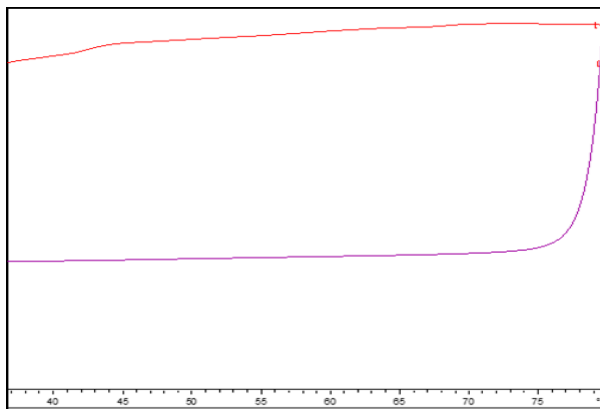


**Figure 8-16:** DSC curves for compound 8-13

### 8.2.3 Liquid crystal and thermal properties of compound **8-13**, **8-14**, **8-15**, **8-16** and **8-17**

In this series the main change is converting double bond to pentamethyldisiloxanyl as well as chain length, as discussed in the synthesis section. Unfortunately, for compounds **8-13**, **8-14**, **8-15**, **8-16** and **8-17**, there was no observation of liquid crystalline phase in both DSC and OPM. It can be observed from the DSC data that the isotropization temperature for compound **8-13** is about 193°C (figure 8-16).

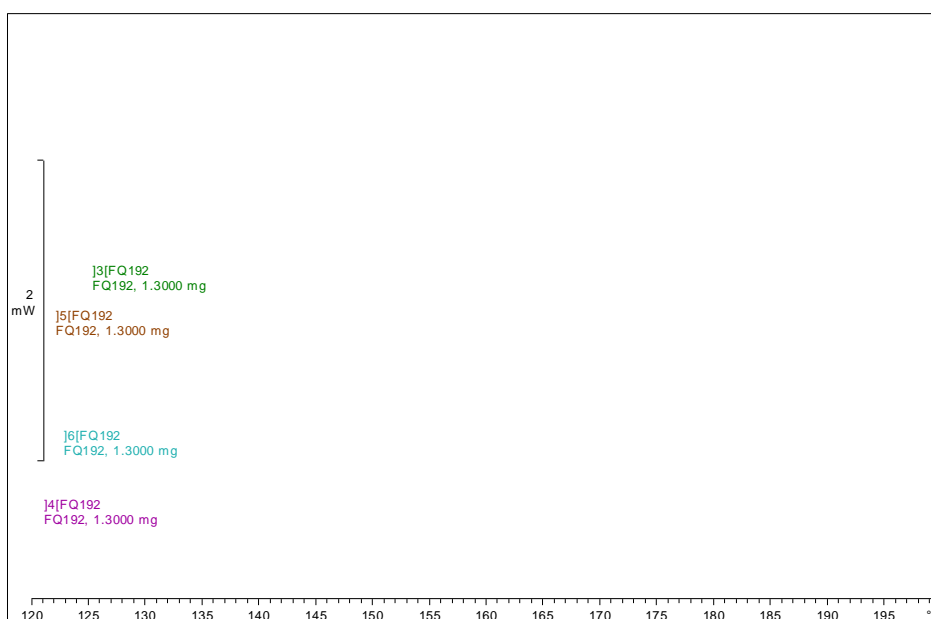


**Figure 8-17** : DSC curves for compound **8-13**.

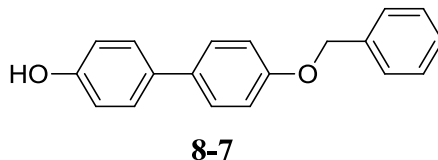
## 9 Summary

The synthesis of the target thiol terminated mesogens synthesis was explored and modified and optimized. The overall achievement of yield was around 55 %. Gold nanoparticles in the 2-3 nm size regime were synthesized and subsequently functionalized with the thiol terminated mesogen. The gold nanoparticles covered by mesogens were characterized by OPM,  $^1\text{H}$  NMR, DSC, TEM, TGA and UV-Vis spectroscopy (UV). The LC AuNPs exhibit thermotropic phase behaviour and shows some birefringent textures in OPM investigations. They are the first Au-LC NPs where the LC groups bear neither lateral nor terminal chains. Although the materials are birefringent, and a schlieren texture could possibly be identified, suggesting nematic phase behaviour. The superstructure of the gold nanoparticles needs to be investigated further.

A range of molecules bearing terminal olefinic groups were attached to pentamethyldisiloxane and investigated in order to have low molecular mass analogues of the LC-Au-NP systems. Surprisingly the phase behaviour of such model systems was quite different from the LC-Au-NPs, indicating that an approach which has useful for the investigation of side-chain LC polymers and LC dendrimers cannot easily transferred to Au-LC-NP nanocomposites.

## 9.1 Experimental procedures

### 9.1.1 Synthesis of 4'-(benzyloxy)-[1,1'-biphenyl]-4-ol<sup>184</sup>

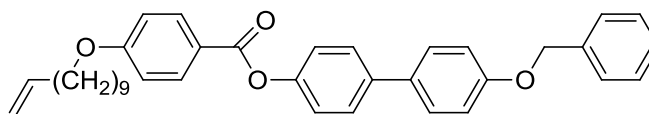


4,4'-Dihydroxybiphenyl (3.72 g, 20 mmol) and sodium hydroxide (0.8 g, 20 mmol) were dissolved in EtOH (100 mL), and the solution was heated to refluxing. The solution turned to dark green. Benzyl bromide (3.42 g, 20 mmol) was added all at once, and the reaction was refluxed for 3-4 h. Once the solution cooled to ambient temperature, it was subsequently acidified with HCl (2 M). The product was collected by filtration, washed with DCM, dried in a vacuum, and recrystallized from a mixture of Et<sub>2</sub>OH (95%)/THF to give a white crystalline powder (4.61 g).

**Yield:** 83%

**<sup>1</sup>H NMR, 400 MHz (CDCl<sub>3</sub>):** δ [ppm] = 5.16 (s, 2 H), 6.86 (d, 2 H), 7.05 (d, 2 H), 7.38-7.47 (m, 5 H), 7.62 (d, 2 H), 7.68 (d, 2 H).

### 9.1.2 Synthesis of 4'-(benzyloxy)-[1,1'-biphenyl]-4-yl 4-(undec-10-en-1-yloxy)benzoate



**8-9**

Compound **8-7** (0.5 g, 0.2 mmol), 4-(undec-10-en-1-yloxy) benzoic acid (0.5 g, 0.2 mmol), and 4-dimethylaminopyridine (DMAP) (0.01 g) (0.1 mmol) were dissolved in THF (50 ml) and N,N-dicyclohexylcarbodiimide (DCC) (0.4 g) (0.2 mmol) was added. After stirring for 18 h at 80 °C, the reaction mixture was filtered and washed with DCM. After removal of the solvent, compound **8-9** was purified by column chromatography (DCM), recrystallized from ethanol and yielded white product (0.66 g).

**Mp:** 130 °C

**Yield:** 70%

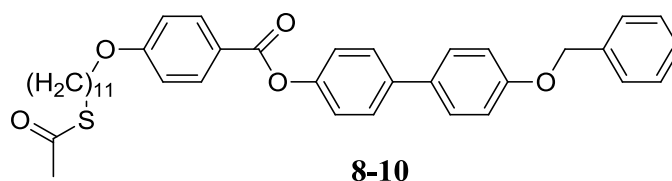
**<sup>1</sup>H NMR 400 MHz (CDCl<sub>3</sub>):** δ [ ppm] = 1.29-2.18 (m, 16 H), 4.06 (t, 2 H), 5.02-5.07 (m, 2 H), 5.16 (s, 2 H), 5.82 (m, 1 H), 7.05 (d, 2 H) 7.14 (d, 2 H), 7.23 (d, 2 H), 7.38-7.47 (m, 5 H), 7.68 (d, 2 H), 7.86 (d, 2 H), 8.11 (d, 2 H).

**<sup>13</sup>C NMR, 100 MHz (CDCl<sub>3</sub>):** 165.1, 164.5, 158.0, 148.1, 139.1, 137.5, 136.7, 133.0, 130.9, 130.9, 130.1, 130.1, 129.5, 129.5, 128.9, 128.9, 127.6, 127.1, 127.1, 122.0, 122.0, 121.6, 115.7, 114.8, 114.8, 114.6, 114.6, 70.7, 68.7, 33.8, 29.7, 29.7, 29.6, 29.6, 29.6, 29.6, 25.9.

**Experimental :** C: 80.99%, H: 7.35%.

**Calculated:** C: 80.78%, H: 7.43%.

### 9.1.3 Synthesis of 4'-(benzyloxy)-[1,1'-biphenyl]-4-yl 4-((11(methylsulfinyl)undecyl)oxy)benzoate



Thioacetic acid (98%, 0.6 ml, 0.8 mmol) was introduced to a mixture of compound **8-9** (0.84 g, 0.5 mmol) and Azobisisobutyronitrile (AIBN) (0.1 g, 0.4 mmol) in dry THF (30 ml) under nitrogen. This mixture was heated at 60 °C for 18 h. The reaction was followed by TLC until the starting materials disappeared. The solvent was distilled off and column chromatography carried out using DCM as an eluent. This yielded a white crystals (0.4 g).

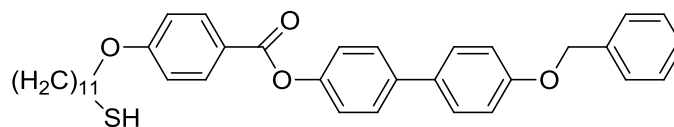
**Mp:** 119 °C

**Yield:** 82%

**<sup>1</sup>H NMR, 400 MHz (CDCl<sub>3</sub>):**  $\delta$  [ ppm] = 1.29-1.93 (m, 18 H), 3.24 (t, 2 H), 3.86 (s, 3 H), 4.06 (t, 2 H), 5.16 (s, 2 H), 7.05 (d, 2 H) 7.14 (d, 2 H), 7.23 (d, 2 H), 7.38-7.47 (m, 5 H), 7.68 (d, 2 H), 7.86 (d, 2 H), 8.11 (d, 2 H).

**<sup>13</sup>C NMR, 100 MHz (CDCl<sub>3</sub>):** 165.1, 164.5, 158.0, 148.1, 139.1, 137.5, 136.7, 133.0, 130.9, 130.9, 130.1, 130.1, 129.5, 129.5, 128.9, 128.9, 127.6, 127.1, 127.1, 122.0, 122.0, 121.6, 115.7, 114.8, 114.8, 114.6, 114.6, 70.7, 68.7, 52.0, 33.3, 29.7, 29.7, 29.6, 29.6, 29.6, 25.9, 25.1.

#### 9.1.4 Synthesis of 4'-(benzyloxy)-[1,1'-biphenyl]-4-yl 4-((11-mercaptoundecyl) oxy) benzoate



**8-11**

Compound **8-10** (0.35, 0.5 mmol, 1.0 equiv.) was added to DCM (20 ml), NaSMe (0.1 g, 1.1 mmol, 2.0 equiv) and methanol (10 ml) under nitrogen. The reaction was stirred at -20 °C for 30 min and monitored by TLC. After the completion of the reaction (one hour), water (50 ml) and DCM (50 ml) was added. The organic layer was separated and the aqueous layer extracted with DCM (50 ml). The combined organic layers were dried with NaSO<sub>4</sub>. Purification by column chromatography (dichloromethane/hexane, 1:1) yielded white crystals (0.18 g).

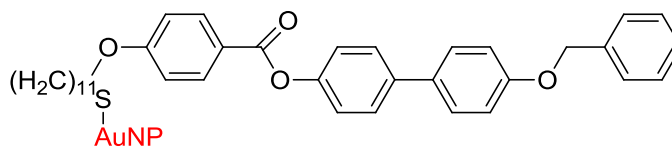
Mp: 123 °C

**Yield:** 54 %

**<sup>1</sup>H NMR, 400 MHz (CDCl<sub>3</sub>):** δ [ ppm] = 1.29-1.76 (m, 19 H), 2.56 (t, 2 H), 4.06 (t, 2 H), 5.16 (s, 2 H), 7.05 (d, 2 H) 7.14 (d, 2 H), 7.23 (d, 2 H), 7.38-7.47 (m, 5 H), 7.68 (d, 2 H), 7.86 (d, 2 H), 8.11 (d, 2 H).

**<sup>13</sup>C NMR, 100 MHz (CDCl<sub>3</sub>):** 165.1, 164.5, 158.0, 148.1, 139.1, 137.5, 136.7, 133.0, 130.9, 130.9, 130.1, 130.1, 129.5, 129.5, 128.9, 128.9, 127.6, 127.1, 127.1, 122.0, 122.0, 121.6, 115.7, 114.8, 114.8, 114.6, 114.6, 70.7, 68.7, 33.3, 29.7, 29.7, 29.7, 29.7, 28.9, 28.2, 25.9, 24.7.

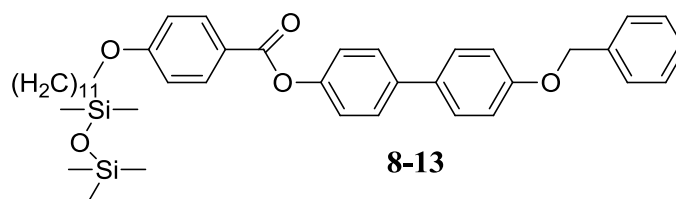
### 9.1.5 Synthesis of ((11-(4-(((4'-(benzyloxy)-[1,1'-biphenyl]-4-yl)oxy)carbonyl) phenoxy) undecyl)thio)gold



**8-12**

To a solution of dodecanethiol capped gold nanoparticles (0.01 g, in freshly distilled 5 ml DCM) was added a solution of the mesogen (compound **8-11**) (0.07 g in 5 ml of DCM) and the mixture was stirred at room temperature for 5 days. Ethanol (12 ml) was added the mixture and briefly sonicated. The solution was then centrifuged at 5000 rpm for 10 minutes and then ethanol removed by pipette. This process was repeated four times in order to remove free mesogen. The black residue was dispersed in hexane and centrifuged. The AuNP LC was then dried in vacuo for 12 hours.

### 9.1.6 Synthesis of 4'-((benzyloxy)-[1,1'-biphenyl]-4-yl 4-(((1,1,3,3,3-pentamethyldisiloxanyl) undecyl)oxy)benzoate



Compound **8-9** (0.001 g; 0.002 mmol) and 2% solution of Karstedt's catalyst (10  $\mu$ l) were dissolved in a solution of dry toluene (20 ml). A solution of 1, 1, 1, 3, 3-pentamethyldisiloxane (0.001 g; 0.005 mmol) in dry toluene (5 ml) was added at room temperature. After the addition was complete, the reaction was left overnight under nitrogen. Purification by column chromatography (dichloromethane/hexane, 3:2) yielded white crystals.

**Mp:** 127 °C

**$^1\text{H NMR}$  400 MHz ( $\text{CDCl}_3$ ):**  $\delta$  [ ppm] = 0.21 (s, 15), 1.29-1.76 (m, 20 H), 4.06 (t, 2 H), 5.16 (s, 2 H), 7.05 (d, 2 H) 7.14 (d, 2 H),), 7.23 (d, 2 H), 7.38-7.47 (m, 5 H), 7.68 (d, 2 H), 7.86 (d, 2 H), 8.11 (d, 2 H).

**$^{13}\text{C NMR}$ , 100 MHz ( $\text{CDCl}_3$ ):** 165.1, 164.5, 158.0, 148.1, 139.1, 137.5, 136.7, 133.0, 130.9, 130.9, 130.1, 130.1, 129.5, 129.5, 128.9, 128.9, 127.6, 127.1, 127.1, 122.0, 122.0, 121.6, 115.7, 114.8, 114.8, 114.6, 114.6, 70.7, 68.7, 34.7, 29.5, 29.5, 29.5, 29.5, 29.5, 29.2, 25.9, 23.8, 20.0, 6.2, 6.2, 5.6, 5.6, 5.6.

## 10 Overall summary

A number of mesogenic systems were investigated which have in common that the central aromatic group was rod shaped. The length of this group was varied. The groups flanking the aromatic centre were varied ranging from two ethylenoxy chains at both ends, one hydrocarbon chain at one terminus and three ethylenoxy chains, and at the other end, only a hydrocarbon chain at one terminus. Additionally an example was attached to specially prepared gold nanoparticles. The chemical synthesis of a number of these systems was explored systematically and optimized.

The materials were characterized chemically and the liquid crystalline phase behaviour was determined by OPM, DSC and for selected samples by XRD. Additionally the materials containing ethylenoxy groups were investigated for their lyotropic liquid crystalline properties in mixtures with water and schematic phase diagrams were proposed.

One of the most interesting systems is a material bearing two tri-ethylenoxy chains at the end of a mesogenic groups consisting of three aromatic rings linked by two ester groups. It shows a nematic phase of the NcybC type identified by DSC, OPM and XRD studies. Additionally this material forms in water at temperatures above 45.7 °C a nematic phase.

A hemiphasmidic system possessing a three oligo-ethylenoxy group unit and a hydrocarbon chain at the other end of an aromatic unit consisting of four aromatic rings, was found to show nematic LC phase behaviour at room temperature in conjunction with water. Additionally OPM data indicates the formation of additional LC phases which need to be investigated further in more detail, though one of the phases was identified as lamellar based on the OPM textures.

The synthesized gold nanoparticles sized in the 2-3 nm regime covered by mesogens were characterized by OPM, <sup>1</sup>H NMR, DSC, TEM, TGA and UV-Vis spectroscopy. The LC-Au-NPs exhibit thermotropic phase behaviour and show some birefringent textures in OPM investigations indicating mesomorphic assembly. They are the first Au-LC NPs where the LC groups bear neither lateral nor terminal alkyl chains.

Their simpler and optimized architecture, when compared to current systems reported in the literature paves the way to Au-LC-NP nano-composites which can be accessed by less organic synthetic steps than current materials and this opens the way to easier access to technological applications.

## 11 Outlook

For rod shaped mesogens bearing ethylenoxy groups at both ends of the central aromatic groups, the effect of the lengthening the ethylenoxy chains should be explored systematically both as neat substances and in mixtures with water.

For the hemispharmidic systems, the phase structures of the water based LC phases should be investigated further. Future synthetic effort could focus on the length of the aromatic core to promote thermotropic LC phase behaviour and the length of the ethylenoxy chains.

For the AuNP based system, the investigation of phase structures of the nanocomposite system is underway and this work could be extended further by exploring systematically the impact of the number of mesogenic groups in Au-LC NP systems on the mesomorphic phase behaviour.

## 12 References

- 1 R. C. Desai and R. Kapral., '*Dynamics of Self-Organized and Self-Assembled Structures*', Cambridge University Press, 2009.
- 2 P. Schiller, *Crystal Research and Technology*, 1996, **31**, 54.
- 3 S. Singh, '*Liquid Crystals Fundamentals*', Word Scientific Publishing, 2001.
- 4 S. Singh, *Phys. Rep.*, 1996, **277**, 283.
- 5 D. Erdmann, in '*Twenty years of Liquid Crystals Research at Merck*', Kontakte (Darmstadt), 1988.
- 6 S. J. Klosowicz and J. Zmija, *Opt. Eng.*, 1995, **34**, 3440.
- 7 P. J. Collings and M. Hird, '*Introduction to liquid crystals chemistry and physics*', Taylor & Francis, 1997.
- 8 I. W. Stewart, '*The Static and Dynamic Continuum Theory of Liquid Crystals*', Taylor & Francis, 2004.
- 9 D. Lacey, in '*Topics in Nanotechnology*', 2009.
- 10 I. W. Hamley, '*Introduction to Soft Matter-Polymers, Colloids, Amphiphiles and Liquid Crystals*', Wiley, 2000.
- 11 M. Baron, *Pure Appl. Chem.*, 2001, **73**, 845.
- 12 I. W. Stewart, '*The Static and Dynamic Continuum Theory of Liquid Crystals*', Taylor & Francis, 2004.
- 13 E. B. Priestley, P. J. Wojtowicz, and S. Ping, '*Introduction to liquid crystals*', 1974.
- 14 I. Dierking, '*Textures of Liquid Crystals*', 2003.
- 15 C. K. Ober, J. I. Jin, and R. W. Lenz, *Adv. Polym. Sci.*, 1984, **59**, 103.
- 16 M. Laus, A. S. Angeloni, A. Spagna, G. Galli, and E. Chiellini, *J. Mater. Chem.*, 1994, **4**, 437.
- 17 I.-C. Khoo, in '*Liquid Crystal Optics and Electro-Optics*', 2006.
- 18 P. J. Collings and M. Hird, '*Introduction to Liquid Crystals Chemistry and Physics*', Taylor & Francis, 1997.
- 19 I. C. Khoo, '*Liquid Crystals*', John Wiley & Sons, 2007.
- 20 In website of '*Virtual Textbook Polymer Liquid Crystals*', 2010.
- 21 In website of '*Encapsulation of Macromolecules*', 2011.
- 22 In website of '*Micelles*', 2011.

- 23 in website of '*Lipids and Membranes*', 2011.
- 24 J. Rego, J. Harvey, A. MacKinnon, and E. Gatzdula, *Liq. Crys.*, 2010, **37**, 37.
- 25 T. Kreer, M. H. Müser, K. Binder, and J. Klein, *Langmuir*, 2001, **17**, 7804.
- 26 In website of '*LiquidCrystal-MesogenOrder*', 2011.
- 27 P. Yeh and C. Gu, '*Optics of Liquid Crystal Displays*', Wiley Publishing, 2009.
- 28 L. J. Yu and A. Saupe, *Phys. Rev. Lett.*, 1980, **45**, 1000.
- 29 F. Hessel and H. Finkelmann, *Polym. Bull.*, 1986, **15**, 349.
- 30 F. Hessel, R.-P. Herr, and H. Finkelmann, *Die Makromolekulare Chemie*, 1987, **188**, 1597.
- 31 H. F. Leube and H. Finkelmann, *Die Makromolekulare Chemie*, 1990, **191**, 2707.
- 32 H. F. Leube and H. Finkelmann, *Die Makromolekulare Chemie*, 1991, **192**, 1317.
- 33 K. Merkel, A. Kocot, J. K. Vij, R. Korlacki, G. H. Mehl, and T. Meyer, *Phys. Rev. Lett.*, 2004, **93**, 237801.
- 34 L. A. Madsen, T. J. Dingemans, M. Nakata, and E. T. Samulski, *Phys. Rev. Lett.*, 2004, **92**, 145505.
- 35 P. K. Karahaliou, P. H. J. Kouwer, T. Meyer, G. H. Mehl, and D. J. Photinos, *Soft Matter*, 2007, **3**, 857.
- 36 O. Francescangeli, M. Laus, and G. Galli, *Phys. Rev. E*, 1997, **55**, 481.
- 37 O. Francescangeli and E. T. Samulski, *Soft Matter*, 2010, **6**, 2413.
- 38 P. H. J. Kouwer, S. J. Picken, and G. H. Mehl, *J. Mater. Chem.*, 2007, **17**, 4196.
- 39 G. Ungar, V. Percec, and M. Zuber, *Macromolecules*, 1992, **25**, 75.
- 40 M. W. Schroder, S. Diele, G. Pelzl, U. Dunemann, H. Kresse, and W. Weissflog, *J. Mater. Chem.*, 2003, **13**, 1877.
- 41 M. Šepelj, A. Lesac, U. Baumeister, S. Diele, D. W. Bruce, and Z. Hameršak, *Chem. Mater.*, 2006, **18**, 2050.
- 42 V. P. Panov, M. Nagaraj, J. K. Vij, Y. P. Panarin, A. Kohlmeier, M. G. Tamba, R. A. Lewis, and G. H. Mehl, *Phys. Rev. Lett.*, 2010, **105**, 167801.
- 43 A. Zep, S. Aya, K. Aihara, K. Ema, D. Pocięcha, K. Madrak, P. Bernatowicz, H. Takezoe, and E. Gorecka, *J. Mater. Chem.*, 2013, **1**, 46.

- 44 E. B. Priestley, P. J. Wojtowicz, and S. Ping, *'Introduction to Liquid Crystals'*, 1974.
- 45 I. W. Stewart, *'The Static and Dynamic Continuum Theory of Liquid Crystals'*, Taylor & Francis, 2004.
- 46 E. B. Priestley, P. J. Wojtowicz, and S. Ping, *'Introduction to liquid crystals'*, 1974.
- 47 in website of 'Cholesterinisch.png', 2011.
- 48 S. S. Funarit and M. C. Holmes, *J. Phys. Chem*, 1994, **98**, 3015.
- 49 In website of 'Lyotropic', 2011.
- 50 P. O. Quist, H. Halle, and F. I., *J. Chem. Phys.*, 1991, **95**, 6946.
- 51 H. Kunieda, A. Y. Yamaguchia, K. Ozawa, and M. Suzuki, *Langmuir*, 1999, **325**, 243.
- 52 In website of '*Crystallization of cyclosporin A in lyotropic reverse hexagonal liquid crystals*', 2011.
- 53 P. Alexandridis, U. Olsson, and B. Lindman, *Phy. Chem.*, 1998, **14**, 2627.
- 54 In website of '*Micellar cubic*', 2011.
- 55 in website of '*Ribbon Phase in a Two-Phase Shear Flow*', 2011.
- 56 in website of '*Lyotropic Liquid Crystals*', 2011.
- 57 S. M. Wochenschr, *Mol Cryst Liq Cryst Lett* 1980, **110**, 179.
- 58 J. Pepys and A. W. Frankland, '*Disodium cromoglycate in allergic airway disease*', 1970.
- 59 N. H. Hartshorne and G. D. Woodard, *Mol Cryst Liq Cryst Lett*, 1973, **23**, 68.
- 60 J. E. Lydon, *Mol Cryst Liq Cryst Lett*, 1980, **64**, 19
- 61 Y. W. Hui and M. M. Labes, *J. Phys. Chem* 1986, **90**, 4064
- 62 D. Goldfarb, Z. Luz, N. Spielberg, and H. Zimmermann, *Mol Cryst Liq Cryst Lett*, 1984, **124**, 225
- 63 H. Lee and M. M. Labes, *Mol Cryst Liq Cryst*, 1982, **84**, 57.
- 64 T. K. Attwood and J. E. Lydon, *Mol Cryst Liq Cryst*, 1984, **108**, 57.
- 65 G. J. T. Tiddy, D. L. Mateer, A. P. Ormerod, W. J. Harrison, and D. J. Edwards, *Langmuir*, 1995, **11**, 3.
- 66 W. J. Harrison, D. L. Mateer, and G. J. T. Tiddy, *J. Phys. Chem*, 1996, **100**, 21.
- 67 J. Lydon, *Current Opinion in Colloid & Interface Science*, 1998, **3**, 458.

- 68 P. F. Gordon and P. Gregory, '*Organic Chemistry in Colour*', Springer Verlag 1983.
- 69 J. E. Lydon, *J. Curr. Opin*, 2004, **8**, 480.
- 70 D. Demus, J. W. Goodby, G. W. Gray, H. W. Spiess, V. Vill, *Handbook of liquid crystal*, Wiley-VCH, 1998.
- 71 J. E. Lydon, *J. Curr. Opin* 1998, **3**, 458.
- 72 J. E. Lydon, *J. Curr. Opin*, 2004, **8**, 480.
- 73 J. E. Lydon, *J. Curr. Opin*, 2007, **16**, 13.
- 74 J. E. Lydon, *J. Mater. Chem.*, 2010, **20**, 10071.
- 75 D. Goldfarb, M. E. Moseley, M. M. Labes, and Z. Luz, *J. Chem. Phys* 1982, **89**, 119.
- 76 P.J. Collings, A. J. Dickinson, and E. C. Smith., *Liq Cryst*, 2010, **37**, 701.
- 77 J. E. Lydon, *J. Mater. Chem*, 2010, **20**, 10099.
- 78 J. E. Lydon, *J. Mater. Chem*, 2010, **20**, 10073.
- 79 J. N. Israelachvili, D. J. Mitchell, and B. W. Ninham, *J Chem Soc Faraday Trans*, 1976, **72**, 68.
- 80 J. N. Israelachvili and R. M. Pashley, '*Intermolecular and Surface Forces*', 1991.
- 81 P. K. Maiti, Y. Lansac, M. A. Glaser, and N. A. Clark, *Liq Cryst*, 2002, **29**, 26.
- 82 R. G. Edwards, J. R. Henderson, and R. L. Pinning, *Mol. Phys*, 1995, **6**, 93.
- 83 N. Boden, R. J. Bushby, Y. Liu Q, and O. R. Lozman, *J. Mater. Chem.*, 2001, **11**, 7.
- 84 N. Boden, R. J. Bushby, Y. Liu Q, and O. R. Lozman, in '*Designing better columnar mesophases*', York, 2001.
- 85 V. E. Maizlish, G. P. Shaposhnikov, O. V. Balakireva, M. A. Zharnikova, I. G. Abramov, S. A. Ivanovskii, and A. V. Smirnov, *Russ. J. Gen. Chem.*, 2004, **74**, 787.
- 86 B. Donnio, *Curr. Opin. Colloid In.*, 2002, **7**, 371.
- 87 C. Ruslim, M. Hashimoto, D. Matsunaga, T. Tamaki, and K. Ichimura, *J. Mater. Chem* 2003, **19**, 91.
- 88 Y. A. Natishin, H. Liu, T. Schneider, V. Nazarenko, R. Vasyuta, S. V. Shiyankovskii, and O. D. Lavrentovitch, *Phys. Rev. E* 2005, **72**, 041711.
- 89 D. Perahia, E. J. Watchel, and Z. Luz, *Liq. Cryst*, 1991, **9**, 479.

- 90 V. A. Bykov, G. Sharimanov, M. G. Mrevlishvili, T. D. Mdzinarashvili, N. O. Metreveli, and G. R. Kakabadze, *Mol. Mat.*, 1992, **1**, 73.
- 91 N. Usol'tseva, *Mol. Cryst. Liq. Cryst.*, 1996, **288**, 201.
- 92 C. Hahn, I. Spring, C. Thunig, G. Platz, and A. Wokaun, *Langmuir*, 1998, **14**, 8.
- 93 K. Ichimura, T. Fujiwara, M. Momose, and D. Matsunaga, *J. Mater. Chem* 2002, **12**, 3380.
- 94 Y. A. Natishin, H. Liu, T. Schneider, V. Nazarenko, R. Vasyuta, S. V. Shiyonovskii, and O. D. Lavrentovitch, *Phys. Rev. E*, 2005, **72**, 041711.
- 95 J. E. Lydon, *Curr. Opin Colloid In.*, 2004, **8**, 482.
- 96 J. M. C. Jonathan and M. May, *Opt. Commun* 1979, **28**, 30.
- 97 J. E. Lydon, *Curr. Opin. Colloid In.*, 2004, **8**, 483.
- 98 D. Matsunaga, T. Tamaki, and K. Ichimura, *J. Mater. Chem*, 2003, **13**, 60+.
- 99 D. Matsunaga, T. Tamaki, and K. Ichimura, *J Mater Chem* 2003, **13**, 64.
- 100 K. Ichimura, T. Fujiwara, M. Momose, and D. Matsunaga, *J Mater Chem*, 2002, **12**, 3386.
- 101 I. K. Iverson, S. M. Casey, W. Seo, and S. W. Tam-Chang, *Langmuir* 2002, **18**, 3510.
- 102 I. K. Iverson, S. M. Casey, W. Seo, S. W. Tam-Chang, and B. A. Pindzola, *Langmuir*, 2002, **18**, 6.
- 103 D. Matsunaga, T. Tamaki, H. Akiyama, and K. Ichimura, *Adv. Mater.*, 2002, **14**, 1477.
- 104 S. Remizow, A. Krivoschchepov, V. Nazarov, and A. Grodsky, *Mol. Mater.*, 2001, **14**, 90.
- 105 I. K. Iverson and S. W. Tam-Chang, *J. Am. Chem. Soc.*, 1999, **121**, 5801.
- 106 T. Schneider and O. D. Lavrentovich, *Langmuir* 2000, **16**, 5227.
- 107 T. Sergan, T. Schneider, J. Kelly, and O. D. Lavrentovich, *Liq Cryst*, 2000, **27**, 567.
- 108 J. E. Lydon, *J. Mater. Chem*, 2010, **20**, 10080.
- 109 G. Seifert, *Cryst. Res. Technol.*, 1994, **29**, 956.
- 110 G.-T. Wei and F.-K. Liu, *J. Chromatogr. A*, 1999, **836**, 253.
- 111 T. K. Sau and A. L. Rogach, *Adv. Mater.*, 2010, **22**, 1781.
- 112 B. Wiley, Y. Sun, and Y. Xia, *Acc. Chem. Res.*, 2007, **40**, 1067.

- 113 T. S. Ahmadi, Z. L. Wang, T. C. Green, A. Henglein, and M. A. El-Sayed, *Science*, 1996, **272**, 1924.
- 114 H.-G. Liao, L. Cui, S. Whitelam, and H. Zheng, *Science*, 2012, **336**, 1011.
- 115 L. -S. Li, J. Hu, W. Yang, and A. P. Alivisatos, *Nano Lett.*, 2001, **1**, 349.
- 116 C. Pribenszky, L. Lin, Y. Du, E. Losonczi, A. Dinnyes, and G. Vajta, *Reprod. Domestic Anim.*, 2012, **47**, 197.
- 117 G. H. Chan, J. Zhao, E. M. Hicks, G. C. Schatz, and R. P. Van Duyne, *Nano Lett.*, 2007, **7**, 1947.
- 118 X. Peng, L. Manna, W. Yang, J. Wickham, E. Scher, A. Kadavanich, and A. P. Alivisatos, *Nature*, 2000, **404**, 59.
- 119 Y. Isomura, T. Narushima, H. Kawasaki, T. Yonezawa, and Y. Obara, *Chem. Commun.*, 2012, **48**, 3784.
- 120 A. Tao, P. Sinsermsuksakul, and P. Yang, *Angew. Chem. Int. Edit.*, 2006, **45**, 4597.
- 121 M. R. Knecht and R. M. Crooks, *New J. Chem.*, 2007, **31**, 1349.
- 122 A. P. Alivisatos, *Science*, 1996, **271**, 933.
- 123 C. Gautier and T. Bürgi, *ChemPhysChem*, 2009, **10**, 483.
- 124 T. Yonezawa, S.-y. Onoue, and N. Kimizuka, *Langmuir*, 2000, **16**, 5218.
- 125 G. Schmid and B. Corain, *Eur. J. Inorg. Chem.*, 2003, **2003**, 3081.
- 126 G. Hodes, *Adv. Mater.*, 2007, **19**, 1307.
- 127 M.-C. Daniel and D. Astruc, *Chem. Rev.*, 2003, **104**, 293.
- 128 Z. W. Pan, Z. R. Dai, and Z. L. Wang, *Science*, 2001, **291**, 1947.
- 129 S. A. Claridge, A. W. Castleman, S. N. Khanna, C. B. Murray, A. Sen, and P. S. Weiss, *ACS Nano.*, 2009, **3**, 244.
- 130 K. Naka and Y. Chujo, '*Nanohybridization of Organic-Inorganic Materials, Advances in Materials Research*', 2009
- 131 P. Reiss, E. Couderc, J. De Girolamo, and A. Pron, *Nanoscale*, 2011, **3**, 446.
- 132 J. Tian, J. Jin, F. Zheng, and H. Zhao, *Langmuir*, 2010, **26**, 8762.
- 133 H. Fan, K. Yang, D. M. Boye, T. Sigmon, K. J. Malloy, H. Xu, G. P. López, and C. J. Brinker, *Science*, 2004, **304**, 567.
- 134 D. Weller and A. Moser, *Magnetics, IEEE Transactions on*, 1999, **35**, 4423.
- 135 J. Boudon, '*Dendrimer-Based Gold Nanoparticles: Syntheses, Characterization and Organization*', University of Neuchatel, 2009.
- 136 D. Thompson, *Gold Bull.*, 2007, **40**, 267.

- 137 D. V. Leff, P. C. Ohara, J. R. Heath, and W. M. Gelbart, *J. Phys. Chem.*, 1995, **99**, 7036.
- 138 K. Kim, H. B. Lee, J. W. Lee, H. K. Park, and K. S. Shin, *Langmuir*, 2008, **24**, 7178.
- 139 V. Maheshwari, J. Kane, and R. F. Saraf, *Adv. Mater.*, 2008, **20**, 284.
- 140 O. P. Khatri, K. Murase, and H. Sugimura, *Langmuir*, 2008, **24**, 3787.
- 141 J. A. Jordan-Hore, C. C. C. Johansson, M. Gulias, E. M. Beck, and M. J. Gaunt, *J. Am. Chem. Soc.*, 2008, **130**, 16184.
- 142 M.-C. Daniel and D. Astruc, *Chem. Rev.*, 2004, **104**, 293.
- 143 G. Schmid, V. Maihack, F. Lantermann, and S. Peschel, *J. Chem. Soc., Dalton Trans.*, 1996, 589.
- 144 N. Toshima, *Macromolecular Symposia*, 2003, **204**, 219.
- 145 S. K. Ghosh and T. Pal, *Chem. Rev.*, 2007, **107**, 4797.
- 146 M. Brust and C. J. Kiely, *Colloids and Surfaces A: Physicochemical and Engineering Aspects*, 2002, **202**, 175.
- 147 J. C. Love, L. A. Estroff, J. K. Kriebel, R. G. Nuzzo, and G. M. Whitesides, *Chemical Reviews*, 2005, **105**, 1103.
- 148 G. Schmid, '*Nanoparticles: From Theory to Application*', 2005.
- 149 M.-C. Bowman, T. E. Ballard, C. J. Ackerson, D. L. Feldheim, D. M. Margolis, and C. Melander, *J. Am. Chem. Soc.*, 2008, **130**, 6896.
- 150 C. J. Murphy, A. M. Gole, J. W. Stone, P. N. Sisco, A. M. Alkilany, E. C. Goldsmith, and S. C. Baxter, *Acc. Chem. Res.*, 2008, **41**, 1721.
- 151 T. W. Odom and C. L. Nehl, *ACS Nano*, 2008, **2**, 612.
- 152 R. A. Sperling, P. Rivera Gil, F. Zhang, M. Zanella, and W. J. Parak, *Chem. Soc. Rev.*, 2008, **37**, 1896.
- 153 L. Duchesne, D. Gentili, M. Comes-Franchini, and D. G. Fernig, *Langmuir*, 2008, **24**, 13572.
- 154 J. Zhao, A. O. Pinchuk, J. M. McMahon, S. Li, L. K. Ausman, A. L. Atkinson, and G. C. Schatz, *Acc. Chem. Res.*, 2008, **41**, 1710.
- 155 E. Boisselier and D. Astruc, *Chem. Soc. Rev.*, 2009, **38**, 1759.
- 156 I. Freestone, N. Meeks, M. Sax, and C. Higgitt, *Gold Bull.*, 2007, **40**, 270.
- 157 L. N. Lewis, *Chem. Rev.*, 1993, **93**, 2693.
- 158 A. N. Shipway, E. Katz, and I. Willner, *ChemPhysChem*, 2000, **1**, 18.

- 159 M. J. Hostetler, J. E. Wingate, C.-J. Zhong, J. E. Harris, R. W. Vachet, M. R. Clark, J. D. Londono, S. J. Green, J. J. Stokes, G. D. Wignall, G. L. Glish, M. D. Porter, N. D. Evans, and R. W. Murray, *Langmuir*, 1998, **14**, 17.
- 160 M. Faraday, *Philosophical Transactions of the Royal Society of London*, 1857, **147**, 145.
- 161 M. Yoshimura, *Advanced Infocomm Technology (ICAIT), 2013 6th International Conference on*, 2013, p. 67.
- 162 In [www.micro.magnet.fsu.edu/primer/java/interference/index.html](http://www.micro.magnet.fsu.edu/primer/java/interference/index.html), 2011.
- 163 In '[http://www.hitachi-hitec-science.com/en/products/thermal/tec\\_descriptions/dsc.html](http://www.hitachi-hitec-science.com/en/products/thermal/tec_descriptions/dsc.html)', 2014.
- 164 In [http://www.hk-phy.org/atomic\\_world/tem/tem02\\_e.html](http://www.hk-phy.org/atomic_world/tem/tem02_e.html)' 2014.
- 165 In '<http://www.buzzle.com/articles/light-microscope-vs-electron-microscope.html>', 2014.
- 166 In '<http://pharmaxchange.info/press/2011/12/ultraviolet-visible-uv-vis-spectroscopy-principle/>', 2011.
- 167 In '<http://www.olympusmicro.com/primer/techniques/polarized/polmicroalignment.html>', 2012.
- 168 T. W. Brockmann and J. M. Tour, *Journal of the American Chemical Society*, 1995, **117**, 4437-4447.
- 169 S. Kohmoto, E. Mori and K. Kishikawa, *Journal of the American Chemical Society*, 2007, **129**, 13364-13365.
- 170 Y. M. Lee, M. E. Moon, V. Vajpayee, V. D. Filimonov and K.-W. Chi, *Tetrahedron*, 2010, **66**, 7418-7422.
- 171 B. M. Rosen, D. A. Wilson, C. J. Wilson, M. Peterca, B. C. Won, C. Huang, L. R. Lipski, X. Zeng, G. Ungar, P. A. Heiney and V. Percec, *Journal of the American Chemical Society*, 2009, **131**, 17500-17521.
- 172 K. Ishihara, M. Kubota, H. Kurihara and H. Yamamoto, *The Journal of Organic Chemistry*, 1996, **61**, 4560-4567.
- 173 J. M. McFarland and M. B. Francis, *Journal of the American Chemical Society*, 2005, **127**, 13490-13491.
- 174 Y. Hizume, K. Tashiro, R. Charvet, Y. Yamamoto, A. Saeki, S. Seki and T. Aida, *Journal of the American Chemical Society*, 2010, **132**, 6628-6629.
- 175 M. G. Tay, Z. Ngaini, N. M. Sarih, S. W. Foo and M. H. Tiong.

176. I. Heertje, E. C. Roijers, and H. Hendrickx, *Food Science and Technology-Lebensmittel-Wissenschaft & Technologie*, 1998, **31**, 387.
- 177 R. Mezzenga, C. Meyer, C. Servais, A. I. Romoscanu, L. Sagalowicz, and R. C. Hayward, *Langmuir*, 2004, **21**, 3322.
- 178 L.-G. Wang, T.-G. Zhan, X. Zhao, X.-K. Jiang and Z.-T. Li, *Tetrahedron*, 2012, **68**, 5303-5310.
- 179 M. R. Molla, A. Das and S. Ghosh, *Chemical Communications*, 2011, **47**, 8934-8936.
180. V. M. Marx, H. Girgis, P. A. Heiney and T. Hegmann, *Journal of Materials Chemistry*, 2008, **18**, 2983-2994.
- 181 G. S. Lee, Y.-J. Lee, S. Y. Choi, Y. S. Park and K. B. Yoon, *Journal of the American Chemical Society*, 2000, **122**, 12151-12157.
- 182 M. N. Martin, J. I. Basham, P. Chando, and S.-K. Eah, *Langmuir*, 2010, **26**, 7410.
- 183 B. L. V. Prasad, S. I. Stoeva, C. M. Sorensen, and K. J. Klabunde, *Langmuir*, 2002, **18**, 7515.
- 184 J. D. Revell and A. Ganesan, *Organic Letters*, 2002, **4**, 3071-3073.